PB81-147340

Transport and Transformation of Sulfur Oxides through the Tennessee Valley Region

Tennessee Valley Authority
Chattanooga

Prepared for

Environmental Protection Agency
Washington, DC

Jun 80

U.S. Department of Commerce
National Technical Information Service
NTIS

TECHNICAL REPORT DATA

(Please read Instructions on the reverse before completing)

1. REPORT NO. EPA-600/7-80-126	2.	3. RECIPIENT'S ACCESSION NO. PB81 147340
4. TITLE AND SUBTITLE TRANSPORT AND TRANSFORMATION OF SULFUR OXIDES THROUGH THE TENNESSEE VALLEY REGION		5. REPORT DATE June 1980
		6. PERFORMING ORGANIZATION CODE
7. AUTHOR(S) T. L. Crawford and L. M. Reisinger		8. PERFORMING ORGANIZATION REPORT NO. N581
9. PERFORMING ORGANIZATION NAME AND ADDRESS Office of Natural Resources Tennessee Valley Authority Muscle Shoals, AL 35660		10. PROGRAM ELEMENT NO. 1NE-832
		11. CONTRACT/GRANT NO. IAG-D9-E721 81 BDL
12. SPONSORING AGENCY NAME AND ADDRESS U.S. Environmental Protection Agency Office of Research & Development Office of Energy, Minerals & Industry Washington, D.C. 20460		13. TYPE OF REPORT AND PERIOD COVERED Milestone
		14. SPONSORING AGENCY CODE EPA-ORD

15. SUPPLEMENTARY NOTES

This project is part of the EPA-planned and coordinated Federal Interagency Energy/Environment R&D Program.

16. ABSTRACT

This report is directed to scientists interested in the long-range atmospheric transport and transformation of sulfur compounds.

Statistical and climatological analyses of historical data and the results of two long-range transport studies are presented. The two long-range atmospheric transport field studies were conducted over a 300-km^2 area of the southern United States centered on the Tennessee Valley region The first study was conducted during the spring of 1976, and the second was conducted during the summer of 1977. The field study region contains seven large coal-fired power plants and one large city.

Results indicate that the predominant flow and mass transport direction is from the southwest to the northeast. Also, aerometric measurements obtained by aircraft and ground sampling compared favorably with results obtained with an analytical transport-transformation model developed for this study. Results indicate that, during prevailing southwesterly airflow, large sulfur influxes are present. These influxes, which are at the same order of magnitude as the Tennessee Valley regional emission fluxes, can only partly be explained by upwind anthropogenic sources. Natural source emissions are hypothesized to account for about half of this sulfur influx.

17. KEY WORDS AND DOCUMENT ANALYSIS

a. DESCRIPTORS	b. IDENTIFIERS/OPEN ENDED TERMS	c. COSATI Field/Group
Earth Atmosphere	Transport Processes Charac..Meas. & Monit.	6F 8A 8F 8H 10A 10B 7B 7C 13B

18. DISTRIBUTION STATEMENT Release to public	19. SECURITY CLASS *(This Report)* Unclassified	21. NO. OF PAGES 152
	20. SECURITY CLASS *(This page)* Unclassified	22. PRICE

EPA Form 2220-1 (9-73)

United States
Environmental Protection
Agency

Office of Environmental Engineering
and Technology
Washington DC 20460

EPA-600/7-80-126
June 1980

Research and Development

PB81-147340

EPA

Transport and Transformation of Sulfur Oxides Through the Tennessee Valley Region

Interagency Energy/Environment R&D Program Report

use this Copy

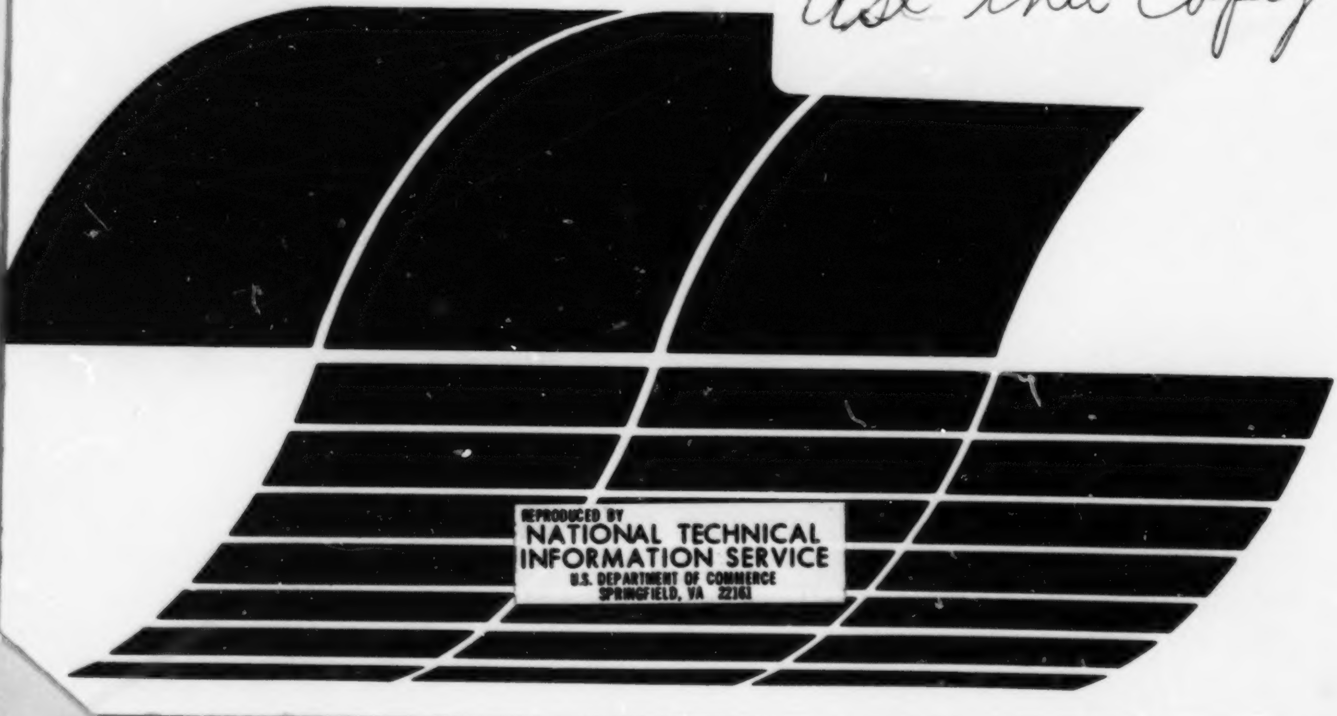

REPRODUCED BY
NATIONAL TECHNICAL
INFORMATION SERVICE
U.S. DEPARTMENT OF COMMERCE
SPRINGFIELD, VA 22161

RESEARCH REPORTING SERIES

Research reports of the Office of Research and Development, U.S. Environmental Protection Agency, have been grouped into nine series. These nine broad categories were established to facilitate further development and application of environmental technology. Elimination of traditional grouping was consciously planned to foster technology transfer and a maximum interface in related fields. The nine series are:

1. Environmental Health Effects Research
2. Environmental Protection Technology
3. Ecological Research
4. Environmental Monitoring
5. Socioeconomic Environmental Studies
6. Scientific and Technical Assessment Reports (STAR)
7. Interagency Energy-Environment Research and Development
8. "Special" Reports
9. Miscellaneous Reports

This report has been assigned to the INTERAGENCY ENERGY-ENVIRONMENT RESEARCH AND DEVELOPMENT series. Reports in this series result from the effort funded under the 17-agency Federal Energy/Environment Research and Development Program. These studies relate to EPA's mission to protect the public health and welfare from adverse effects of pollutants associated with energy systems. The goal of the Program is to assure the rapid development of domestic energy supplies in an environmentally-compatible manner by providing the necessary environmental data and control technology. Investigations include analyses of the transport of energy-related pollutants and their health and ecological effects; assessments of, and development of, control technologies for energy systems; and integrated assessments of a wide range of energy-related environmental issues.

This document is available to the public through the National Technical Information Service, Springfield, Virginia 22161.

EPA-600/7-80-126

JUNE 1980

TRANSPORT AND TRANSFORMATION OF SULFUR OXIDES THROUGH THE TENNESSEE VALLEY REGION

by

Timothy L. Crawford and Lawrence M. Reisinger
Office of Natural Resources
Tennessee Valley Authority
Muscle Shoals, AL 35660

Interagency Agreement No. EPA-IAG-D9-E721
Project No. 81-BDL
Program Element No. 1NE-832

Project Officer

C. W. Hall
U.S. Environmental Protection Agency
401 M Street
Washington, DC 20460

Prepared for

OFFICE OF ENERGY, MINERALS, AND INDUSTRY
OFFICE OF RESEARCH AND DEVELOPMENT
U.S. ENVIRONMENTAL PROTECTION AGENCY
WASHINGTON, DC 20460

DISCLAIMER

This report was prepared by the Tennessee Valley Authority and has been reviewed by the Office of Energy, Minerals, and Industry, U.S. Environmental Protection Agency, and approved for publication. Approval does not signify that the contents necessarily reflect the views and policies of the Tennessee Valley Authority or the U.S. Environmental Protection Agency, nor does mention of trade names or commercial products constitute endorsement or recommendation for use.

TVA is an equal opportunity employer, and is committed to ensuring that the benefits of programs receiving TVA financial assistance are available to all eligible persons regardless of race, color, national origin, handicap, or age.

ABSTRACT

This report is directed to scientists interested in the long-range atmospheric transport and transformation of sulfur compounds.

Statistical and climatological analyses of historical data and the results of two long-range transport studies are presented. The two long-range atmospheric transport field studies were conducted over a 300-km^2 area of the southern United States centered on the Tennessee Valley region. The first study was conducted during the spring of 1976, and the second was conducted during the summer of 1977. The field study region contains seven large coal-fired power plants and one large city.

Results indicate that the predominant flow and mass transport direction is from the southwest to the northeast. Also, aerometric measurements obtained by aircraft and ground sampling compared favorably with results obtained with an analytical transport-transformation model developed for this study. Results indicate that, during prevailing southwesterly airflow, large gaseous sulfur influxes are present. These influxes, which are of the same order of magnitude as the Tennessee Valley regional emission fluxes, can only partly be explained by upwind anthropogenic sources. Natural source emissions are hypothesized to account for about half of this sulfur influx.

This report was submitted by the Tennessee Valley Authority, Office of Natural Resources, in partial fulfillment of Energy Accomplishment Plan 81 BDL under terms of Interagency Agreement EPA-IAG-D9-E721 with the Environmental Protection Agency. Work was completed as of June 1979.

EXECUTIVE SUMMARY

The objective of the Tennessee Regional Atmospheric Transport Study (TREATS) is to develop an understanding of the characteristics and mechanisms affecting regional pollutant levels and interregional transport of primary and secondary sulfur pollutants. This report not only addresses the measurement and modeling of the transport and transformation of sulfur species, but also looks at climatological variations of aerometric and meteorological parameters and emission rates as they impact the Tennessee Valley region. Other pollutant species are dealt with primarily as they relate to the formation of fine particulate sulfates.* Principal ingredients of this analysis are the results from two long-range transport field studies conducted during the spring of 1976 and the summer of 1977. These studies are among the first ever conducted in the United States over distance scales of hundreds of kilometers.

During these studies, aerometric and meteorological measurements defined airmass pollution levels and interregional pollutant mass transport as airmasses entered, passed through, and left the Valley. These unique measurements have led to several significant findings.

In presenting these findings, two important terms, concentration and flux, are used to describe pollutant levels within airmasses. Concentration is simply the mass or amount of pollutant per unit volume of air, typically reported as micrograms per cubic meter ($\mu g\ m^{-3}$), whereas flux is a less frequently used term that describes the rate of pollutant mass transport through a horizontal or vertical area and is reported in micrograms per square meter per second ($\mu g\ m^{-2}\ s^{-1}$). As typically expressed in this report, flux is obtained by multiplying the concentration by the wind speed. This parameter is important in describing the movement of pollutants.

Many different sampling and analytical techniques were used to determine relationships between and among the various parameters measured. One of the more significant findings from these analyses describes the horizontal and vertical diurnal variations of various pollutants. In particular, multiple aircraft traverses at various altitudes and at widely separate locations within the Valley indicate that significant pollutant variations often occur in the horizontal and vertical during the night and early morning. However, by midday, the gradients are significantly reduced, except near the ground, where sulfate data obtained from high-volume samplers indicate that ambient air concentrations average twice the airmass concentrations as measured by aircraft flights near ground level. Additional research is needed to determine whether this is a sampling artifact or a real phenomenon.

---

*Prominent among the "sulfates" are sulfuric acid, ammonium bisulfate, and ammonium sulfate. Within this report, the terms, sulfate, particulate sulfate and $SO_4^=$ are synonymous and are defined as the traditional water soluble fraction of the total filterable particulate analyzed and expressed as micrograms of sulfate per cubic meter of sampled air.

Another interesting analysis involves aircraft sampling of the same airmass as it enters the Tennessee Valley region and again as it leaves (known as Lagrangian sampling). Analyses of measurements made on five such days compared very well with an analytical model developed to simulate the transport and transformation processes. By using the model simulations on six non-Lagrangian days together with the five measurement days, some unexpected and interesting results were obtained. These results need additional confirmation due to limits of the present data set. One result shows that for the days with both inflow and outflow measurements, the change in flux as the airmass passed over the region was negligible.

When flow was from the south, sulfate flux, from inflow to outflow, increased; however, sulfate concentrations were low at both boundaries. Again, model estimates indicate that the region was a minor contributor to this increase (only 12 percent); the remaining 88 percent increase in sulfates resulted from conversion of gaseous sulfur compounds already in the air before the airmass entered the region. An attempt to identify the significant source region(s) that might be contributing to this large inflow flux resulted in the conclusion that upwind anthropogenic sources account for only about half of the gaseous sulfur flux, whereas biogenic sources (i.e., wetland areas in and around the Gulf Coast States) could, in theory, account for the other half. However, available data are insufficient to accurately quantify this biogenic source hypothesis.

One reason that our findings are significant is that this southwesterly flow direction is the principal transport avenue over not only the Tennessee Valley region but the entire United States east of the Mississippi River. Also, this flow direction is frequently associated with summertime high air pollution episodes over the eastern United States.

This study also indicates that, when wind speeds are light, TVA is a principal source of pollution in the Tennessee Valley region.

CONTENTS

Page

Abstract . . . iii
Executive Summary . . . v
List of Figures . . . ix
List of Tables . . . xi
Acknowledgments . . . xii
Nomenclature . . . xiii

1. Introduction . . . 1
Background . . . 1
Scope of Research . . . 2
2. Conclusions and Recommendations . . . 4
Conclusions . . . 4
Recommendations . . . 5
3. Materials and Methods . . . 7
Characterization of the Region . . . 7
Physical characterization . . . 7
Emissions characterization . . . 9
Meteorological characterization . . . 12
Synoptic weather patterns . . . 12
Trajectory data . . . 13
Sampling platforms . . . 15
Meteorological measurements and support . . . 23
Sampling procedures . . . 23
1976 study . . . 25
1977 study . . . 25
Analytical methods . . . 26
Continuous gas analyzers . . . 26
Low-volume filters . . . 27
High-volume filters . . . 27
Transformation-transport model . . . 29
Model development . . . 29
Analytical model . . . 29
Simple box model . . . 32
Eulerian model . . . 33
Model analysis . . . 34
4. Results and Discussion . . . 38
Sulfate Concentration and Flux Climatology . . . 38
Seasonal concentration variations . . . 38
Regional sulfate flux rose . . . 42
Flux calculations . . . 48
Estimating concentration and flux . . . 48
Estimating U, H_R, and H_S . . . 51
Estimating SO_x and NO_4^+ concentrations . . . 51
Estimating NO_3^- and O_3 concentrations . . . 51
Flux measurement criteria . . . 54
Tabular summary of flux calculations . . . 58

Page

Eulerian space and time variations 58
    Eulerian space variations 58
        Horizontal variations 61
        Vertical variations 66
    Eulerian time variations 72
Lagrangian flux analysis 72
    Field results 73
    Model results 77
    Upwind sources 81

References 82

Appendixes

A. Synoptic Weather Typing A-1
B. Tabulation of TREATS 1976 and 1977 aircraft field study data B-1
C. Altitude correction, Meloy model SH202 and SA285 sulfur analyzer C-1
D. Tabulation of TREATS 1976 and 1977 high-volume field study data D-1
E. Inversion heights and average wind velocities for Lagrangian and Eulerian days E-1
F. Synoptic meteorological summaries for Lagrangian and Eulerian days F-1

LIST OF FIGURES

Figure Page

1 Physiographic divisions of the TREATS study region. . . 8
2 Annual average SO_2 emission density map 10
3 Locations and emissions of major point sources 11
4 Favored 24-h airmass source regions for Nashville, Tennessee 14
5 Percent occurrence of airmass movement out of the Tennessee Valley region (1972). 16
6 deHavilland Beaver U6-A airplane 17
7 Airplane instrument layout 18
8 U6-A instrument package 19
9 Bell 47A helicopter 21
10 Helicopter instrument layout. 22
11 Location and type of meteorological measurements . . . 24
12 Region used in the development of the long-range transport model 30
13 Schematic of the box model 32
14 Comparison of Lagrangian and Eulerian boundary conditions and solution domains. 33
15 Predicted variation in SO_2 and $SO_4^=$ concentrations as a function of transport time 35
16 Effect of variation in model parameters on predicted response after 24 h of transport 36
17 Regional air quality trend stations 39
18 Monthly variations of TVA's SO_2 emissions and regional sulfate concentrations, 1974-1977 40
19 Giles County sulfate concentration ($\mu g\ m^{-3}$) vs the average concentration of Cumberland, Gallatin, and Giles 43
20 Annual frequency distributions of wind speed, wind direction, sulfate concentration, and sulfate flux for Nashville, Tennessee 44
21 Seasonal frequency distributions of Nashville sulfate flux ($\mu g\ m^{-2}\ s^{-1}$) 45
22 Relative frequency distributions 46
23 Schematic of typical flux calculation procedure 50
24 Typical early morning sulfur profiles 52
25 Typical midday sulfur profiles 53
26 Typical early morning and midday normalized ozone profiles 55
27 Typical early-morning nitrate profiles 56
28 Airmass transport distance vs. inflow-to-outflow sampling distance 57
29 Temporal variation of sulfate 62
30 Temporal variation of ammonium 63
31 Temporal variation of normalized total sulfur 64
32 Temporal variation of nitrate 65
33 Comparison of ground-level to upper-air sulfate concentrations 69

Figure Page

34 Giles County sulfate concentration vs. Colbert 70
35 Comparison of inflow to outflow sulfate flux 74
36 Comparison of inflow to outflow total sulfur flux . . 75
37 Inflow to outflow concentrations and mole ratio changes 76
38 Observed vs predicted outflow total sulfur (X 10^2) and sulfate concentration 78
39 Relative change in total sulfur flux across the TREATS field study region 79
40 Sulfate flux change across the TREATS field study region 80

LIST OF TABLES

Table Page

1 Airplane Instrument Package, Beaver U6-A 15
2 Helicopter Instrument Package, Bell 47A 20
3 Accuracy of Analytical Methods, 37-mm Millipore Filters 28
4 Percent Variation in Model Response Resulting from a ±50 Percent Change in a Single Parameter 34
5 Median Sulfate Flux and Concentration Values Regardless of Sector 47
6 Summary of Lagrangian and Eulerian Measurements 59
7 Inflow-Outflow Concentrations (μg m^{-3}) by Flow Direction 61
8 High-Volume Concentrations (μg m^{-3}) by Flow Direction 66
9 Comparison of Ground-Level and Upper-Air Sulfate Concentrations 68
10 Suspended Sulfate Correlation Matrix 71
11 Sulfate Speciation 73

LIST OF ABBREVIATIONS AND SYMBOLS

B	--width of the region, m
b	--subscript indicator of pollutant concentration above inversion, $\mu g\ m^{-3}$
C_i	--concentration, $\mu g\ m^{-3}$
H	--height of the capping inversion, m
i	--indicator of SO_2 ($i = 1$) or $SO_4^=$ ($i = 2$)
j	--indicator used with box formulation
k	--first-order transformation rate constant for SO_2 to $SO_4^=$, s^{-1}
k_1	-- $-k$, s^{-1}
k_2	--$3k/2$, s^{-1}
K_x, K_y, K_z	--diffusivities along the principal axes, $m^2\ s^{-1}$
Q	--point-source SO_2 emission rate, $\mu g\ s^{-1}$
t	--time, s
t_a	--age of airmass passing the outflow plane, s
t*	--time at which the relative $SO_4^=$ concentration is maximum, s
U, V, W	--mean wind speed components along the principal axes, $m\ s^{-1}$
v_i	--deposition velocity, $m\ s^{-1}$
x, y, z	--distances along the principal axes, m

Note: Subscript or superscript zero (0) indicates an initial value.

ACKNOWLEDGMENTS

This work was primarily funded by the Federal Interagency Energy/Environment Research and Development Program administered through the Environmental Protection Agency under contract number EPA-IAG-DG-E721. The support of this agency is gratefully acknowledged, as is the advice and guidance of the Project Officer, C. W. Hall. However, without additional funding by the Regional Air Quality Management Program of the Tennessee Valley Authority and without the use of TVA's extensive facilities, this work would not have been possible.

We wish to especially express our appreciation to Dr. Herbert Jones, The TVA Project Director and Drs. James F. Meagher and Leonard Stockburger of the Air Quality Research Section for their logistic and design assistance before and during the two field studies and for their thought-provoking input during data analysis. Also, we wish to express our appreciation to William J. Parkhurst, Air Quality Monitoring Section, for his input to the seasonal concentrations variations subsection; to Malcolm C. Babb, Applied Research Staff, for his assistance in generating plots; and to Hollis E. Lindley, Computer Applications Staff, for his assistance in processing data. Finally, we wish to express our appreciation to Elizabeth M. Bailey of the Air Quality Research Section for serving as instrument operator during the 1977 study.

SECTION 1

INTRODUCTION

The Tennessee Valley Authority (TVA) has long been concerned about regional transport and transformation of atmospheric sulfur species (Gartrell et al. 1963). The primary reason for this concern is that TVA operates 12 large coal-fired power plants within the southeastern United States, which constitute a major source of sulfur dioxide (SO_2), the precursor to sulfates ($SO_4^=$).

In 1975, a program to study the regional atmospheric transport of coal-fired power plant emissions, the Tennessee Regional Atmospheric Transport Study (TREATS), was initiated by TVA as part of the Federal Interagency Energy/Environmental Research and Development program being administered through the Environmental Protection Agency. The primary objective of the TREATS research is to develop an understanding of the characteristics and mechanisms affecting regional pollutant levels and interregional transport of primary and secondary sulfur pollutants. With respect to this objective, the impacts of TVA emissions on the TREATS study region and downwind regions are of primary concern.

BACKGROUND

Historically, when evaluating the impact of power plant emissions, the region of concern was generally the immediate vicinity (within 20 km) of the power plant in question, and the pollutants of concern were mainly particulates and SO_2. In most scientific work relating to atmospheric transport of pollutants, little or no attention was given to the intermediate (20 to 100 km) or regional (beyond 100 km) transport of pollutants. Recently, however, emphasis has been placed on the evaluation of intermediate and regional transport of power plant emissions. Emphasis on the intermediate transport was changed abruptly by the December 1974 publication of the Prevention of Significant Deterioration (PSD) regulations (Federal Register 1978). Emphasis on the regional transport of pollutants was changed by the gradually evolving regional sulfate transport-transformation theory. This theory implies that remote primary SO_2 emissions (preferentially from power plants with tall stacks) are transformed to secondary particulate sulfates and transported over long distances. Within the last 10 years, interest in regional transport has steadily increased, as indicated by numerous international publications (e.g., Bolin et al. 1971; Eliassen and Saltbones 1974; Smith and Jeffrey 1975; Bolin and Pearson 1975; Altshuller 1976; Wilson et al. 1977; and Wilson 1978).

During the same period, researchers have been compiling an ever-growing list of adverse effects that result from exposure of the human population, biota, and materials to atmospheric sulfate particulate. In particular, acid sulfate particulates have been implicated in the health damage formerly attributed to SO_2 (EPA 1974a; Hausknecht and Ziskind 1975). Other adverse environmental effects of atmospheric sulfates include acidic deposition (wet and dry), with related adverse effects on the ecology of lakes, rivers, soils, and forests (Braekke 1976), and corrosion of materials (Yocom and Grappone 1976). More recently, visibility reduction has also been related to increases in atmospheric $SO_4^=$ levels (Trijonus and Kung 1978). Reduction in visibility and possible harmful health effects are of special concern for aerosols in the 0.1- to 1-μm size range. Sulfates are one of the more important contributors to atmospheric aerosols in this size range.

The problem with controlling sulfates is that they are predominantly secondary pollutants transported to the receptor from usually unknown source regions, and little is known about the transport-transformation phenomenon. Even so, EPA is expected to promulgate National Ambient Air Quality Standards for fine particulates, which are mostly sulfates, within one to two years (Rowe et al. 1978). The promulgation of fine particulate air quality standards is expected to pose difficult problems for emission control and siting strategies for future fossil-fired power plants--possibly more difficult than those for PSD. The transformation and long-range transport of sulfates from unknown sources make the problem of equity in sulfate control strategies particularly acute. Thus, development of a physically realistic regional transport-transformation modeling technology is an essential link in the development of an equitable control strategy.

Development of a regional-scale modeling technology will require submodels for gas-to-particulate conversion processes and various removal processes. Also, detailed information on the time-dependent regional emissions and diffusion and transport wind fields will be required to drive the model.

Highly accurate models are expected to be complicated because of the possible nonlinear dependence of sulfate production on the source strength of SO_2. Another potential problem is the dependence of the gas-to-particulate reaction on other trace atmospheric constituents (e.g., OH radicals, cloud water pH, O_3, and NH_3). Also, the question of biogenic (natural) sources of sulfur compounds is now an open area of research, and active efforts are underway to understand it.

SCOPE OF THE RESEARCH

This report addresses not only the measurement and modeling of the transport and transformation of sulfur species, but also the climatological variations of aerometric and meteorological parameters, emission rates, and their interrelationships. Other pollutant species are dealt with primarily as they relate to the formation of particulate sulfates. Prominent among the "sulfates" are sulfuric acid, ammonium bisulfate, and ammonium sulfate. Within this report, the terms sulfate, particulate sulfate, and $SO_4^=$ are synonyms and are defined as the traditional water-soluble fraction of the total filterable particulate analyzed and are expressed as micrograms of $SO_4^=$ per cubic meter of sampled air.

This report describes the results of the first three years of studies into long-range transport of secondary sulfate pollutants. Results from two discrete field studies that characterize long-range transport and transformation into, within, and out of the Tennessee Valley region, along with several other "paper" studies, are reported. Although the results are politically and scientifically significant, the limited resources require that they be considered only indicative and not conclusive.

SECTION 2

CONCLUSIONS AND RECOMMENDATIONS

Our conclusions and recommendations are based on a limited number of data collected during two long-range transport field studies conducted in the Tennessee Valley region. Therefore, these findings, although significant and in some cases totally unexpected, should be viewed as preliminary and requiring confirmation by further research.

CONCLUSIONS

1. Although TVA and other power plants account for 90 percent of the regional anthropogenic sulfur emissions, aircraft flux measurements indicated that, during southwesterly flow, these emissions are of the same magnitude as those advected into the region. Therefore, with respect to interregional sulfur transport, TVA emissions contribute about half of the outflow sulfur burden. However, during light wind or calm conditions, TVA is the principal contributor to regional pollutant levels. Within the Valley such episode conditions are more frequent than in the northeastern United States, but less severe with respect to pollutant levels.

2. During transport from the southwest, only about 40 percent of the measured sulfate influx can be explained by upwind anthropogenic sources. The balance appears to be due to biogenic sulfur emissions from the Gulf of Mexico and the extensive wetland areas of the southeastern United States.

3. Eleven Lagrangian measurement days--four with inflow and outflow measurements of both total sulfur and $SO_4^=$-- indicate that during southwesterly flow, no significant change occurred across the Tennessee Valley region in total sulfur flux or concentration. Although the sulfate flux increased by a factor of two from inflow to outflow, the actual concentrations were low--5.4 $\mu g/m^3$ at the outflow boundary. Also, model estimates of the percentage of sulfate flux attributable to regional emissions are small (around 10 percent).

4. The 24-h airmass movement across the Tennessee Valley area frequently originates in a broad band from southern Alabama, Mississippi, and central Louisiana (the wetland areas of the Gulf Coast). These airmasses typically exit the Tennessee Valley, heading toward the northeastern part of the United States.

5. Highest sulfate fluxes occur with southwesterly flow, whereas highest sulfate concentrations occur with northeasterly flow. Also, daily variation in sulfate and ammonium concentrations are greater for northeasterly flow than for southwesterly flow.

6. Nitrate concentrations show an opposite trend to the direction-dependent concentration variations of sulfate and ammonium (i.e., higher concentrations for southwesterly flow).

7. Model calculations (which did not consider wet deposition) indicated that airborne SO_2 decays exponentially with transport time. Its half-life of about 16 h results from the nearly equal effects of removal by dry deposition and transformation to $SO_4^=$. The decay rate is only a mild function of mixing height. The model also predicts that $SO_4^=$, aside from the initial presence of $SO_4^=$ concentrations, increases, reaching a maximum after about three days of transport, after which it decays almost exponentially. Model calculations indicate that $SO_4^=$ is most sensitive to changes in the transformation rate of SO_2 to $SO_4^=$. It is relatively insensitive to changes in mixing height or deposition rates. Comparison with data has shown that the model gives reasonable results for a transport time of about 10 h.

8. Ground-level, high-volume measured $SO_4^=$ concentrations indicated that ambient air concentrations were higher than those of aircraft by a factor of two. This finding, which is contrary to accepted dispersion theory and measurements, may represent an artifact of the high-volume sampling technique.

9. Substantial vertical pollutant gradients often exist under stable conditions (radiation inversions), especially during the early morning (and night). However, these gradients often dissipate by midday.

10. Total sulfur (mostly SO_2) concentration measurements showed a trend toward lower values from morning to afternoon; however, the other pollutants analyzed (i.e., $SO_4^=$, NH_4^+, and NO_3^-) showed no such trend. This disparity could have resulted from differences in photochemistry and deposition velocities.

Although this research has allowed us to learn much about the characteristics and mechanisms of long-range atmospheric transport of sulfur pollutants, it also has raised several significant questions. The more significant questions and recommended actions for answering them are presented below.

RECOMMENDATIONS

1. Is the observed large total sulfur influx from the southwest correct in magnitude, in speculated origin (i.e., biogenic), and is it persistent in time? If so, then the TVA and national emission reduction efforts may be limited in their potential to reduce the sulfate, visibility, and acidic deposition problems in the eastern United States. We strongly recommend that the origin and magnitude be substantiated with a spring or summer aircraft study over this region. If the speculation is confirmed, then additional studies will be required to define its persistence in other seasons.

2. Equitable regional control strategies relating to regional and interregional formation and transport of sulfate pollutants--the major contributors to adverse health effects, visibility reduction, and acidic deposition--will be particularly difficult. TVA emissions have been and will continue to be looked at closely since they are the principle sources of regional pollution in the Tennessee Valley and are occasionally transported toward the northeastern United States. Evaluation of control strategies (e.g., NAAQS, PSD, visibility degradation, cost-benefit) is essential for both regional industrial siting and interregional transport. However, these evaluations are nearly impossible because no realistic regional transport-transformation models relating remote emissions to regional air quality exist. Therefore, we recommend that the TREATS program be expanded and redirected to (1) collect additional data for submodel development and model validation, (2) modify or develop a regional scale transport-transformation model, and (3) validate the model.

3. In the next few years TVA will spend about 6 billion dollars to remove 40 percent of its regional emissions. Considering the magnitude of this initial control technology expenditure and the likelihood of future expenditures, we recommend that the subsequent extent of regional and interregional air quality improvement and benefits be established.

SECTION 3

MATERIALS AND METHODS

CHARACTERIZATION OF THE STUDY REGION

Because the TREATS program is focusing attention on the geographical region encompassing the Tennessee Valley, unique regional characteristics that will influence results must be considered. Physical, emission, and meteorological characteristics are important.

Physical Characterization

The solid rectangle of Figure 1 outlines the Tennessee Regional Atmospheric Transport Study region. The outer map border defines the emissions inventory region, and the inner dashed box encompasses the area in which field studies were carried out. The model region (solid rectangular box) consists of parts of Illinois, Indiana, Kentucky, North Carolina, South Carolina, Georgia, Alabama, Mississippi, Arkansas, Missouri, and nearly all of Tennessee. Across this region, there are six primary physiographic features. From east to west, they include the (1) Appalachian Mountains, (2) valley and ridge subregion, (3) Cumberland Plateau, (4) Highland Rim, (5) Central Basin, and (6) Mississippi Embayment.

The Appalachian Mountain chain is comprised of folded and faulted igneous and metamorphic rock. The characteristics of these types of rocks make them particularly susceptible to the effects of acidic precipitation. The Appalachians, which are very sparsely populated, contain few anthropogenic pollution sources.

The valley and ridge subregion is characterized by northeasterly-trending narrow parallel ridges and slightly wider intervening valleys. Two large population centers, Knoxville and Chattanooga, and five TVA coal-fired plants are found within this subregion. The topology and meteorology of this subregion result in persistent up-valley, down-valley winds. Under stable conditions, pollution tends to be trapped and channeled in the valleys.

The Cumberland Plateau consists of a northeasterly-trending belt of highlands bounded by abrupt escarpments. An unusual feature of this region is the Sequatchie Valley. One TVA coal-fired power plant is found in this subregion. The local pollution transport problems encountered in this region are similar to those in the valley and ridge region.

The Highland Rim consists of a rim or bench of highlands surrounding the Nashville Basin. Three TVA coal-fired power plants are found in this region. Because of the low terrain relief, pollution does not become entrapped by physiographic restraints. The Highland Rim supports one of the most fertile agricultural regions within the southeastern United States.

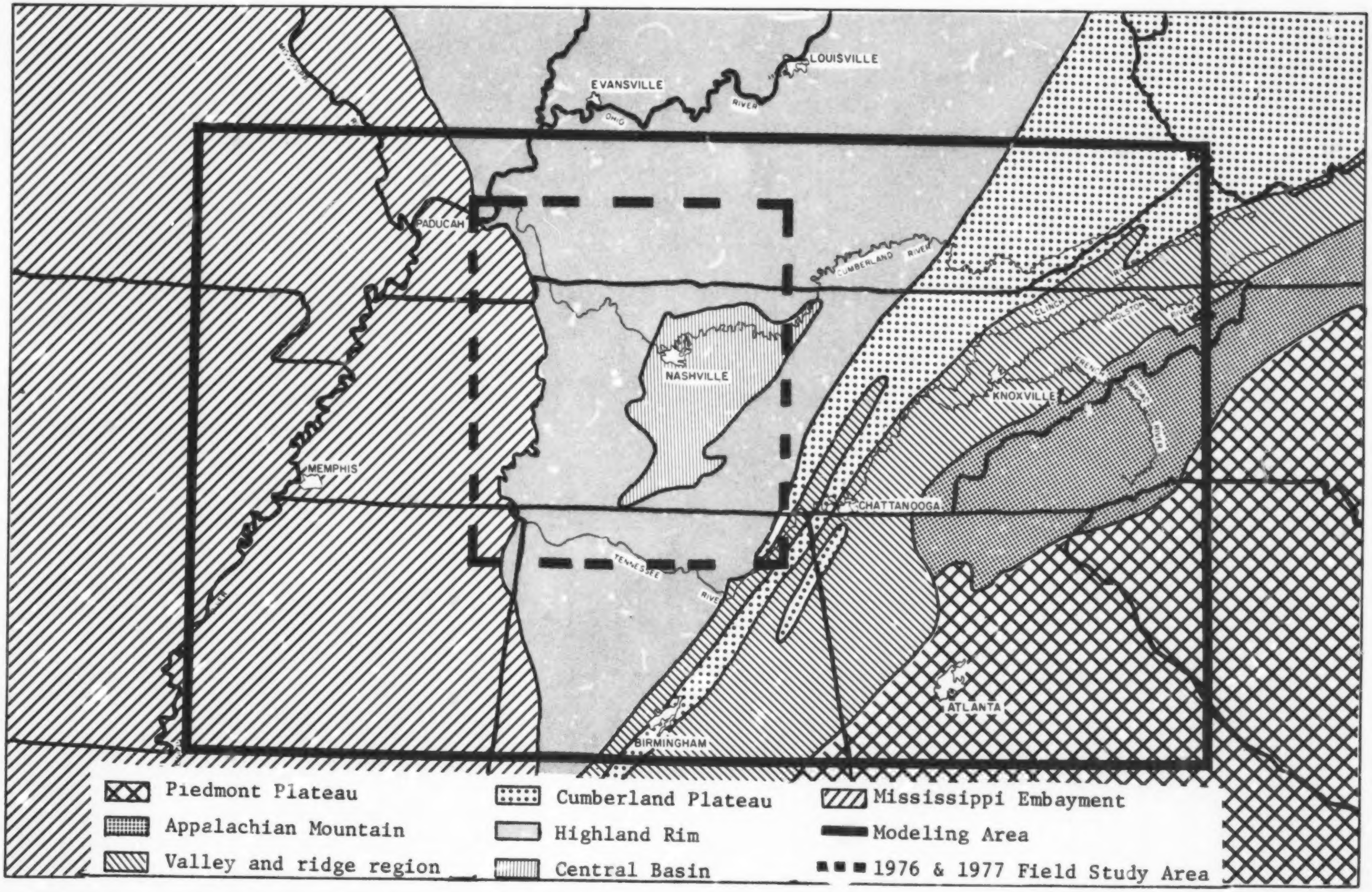
MISSISSIPPI
EVANSVILLE
OHIO
RIVER
LOUISVILLE
PADUCAH
CUMBERLAND RIVER
NASHVILLE
MEMPHIS
CLINCH
HOLSTON
RIVER
KNOXVILLE
FRENCH BROAD RIVER
CHATTANOOGA
TENNESSEE RIVER
ATLANTA
BIRMINGHAM
Piedmont Plateau
Appalachian Mountain
Valley and ridge region
Cumberland Plateau
Highland Rim
Central Basin
Mississippi Embayment
Modeling Area
1976 & 1977 Field Study Area

Figure 1. Physiographic division of the TREATS study regions.

The Central Basin is an oval, northeasterly-trending depression developed within the Highland Rim. One large urban center, Nashville, and one TVA coal-fired power plant are found within this region.

The Mississippi Embayment is characterized by its low relief and by the absence of consolidated rock outcroppings. One large urban center, Memphis, and two TVA steam plants are located within this region.

Some of the physiographic subregions within the Tennessee Valley exhibit topography capable of entrapping and channeling air pollutants. For example, during the summer months, warm, moist tropical air is frequently channeled from southwest to northeast between the Appalachian Mountains and stationary cold fronts to the north (Smith and Niemann 1977). Most parts of the regions are heavily forested, with biota ranging from subarctic coniferous forest biome to deciduous forest biome. Due to humid conditions and a dense forest canopy, pollutant removal by dry deposition should be greater than in many other regions of the United States. The variety of topographical regimes and substrates has, of course, resulted in a variety of edaphic biotic communities.

Emissions Characterization

An essential ingredient for any regional atmospheric transport study or modeling effort is an up-to-date emissions inventory. For this reason, a detailed inventory has been compiled for the TREATS region (Reisinger and Sharma 1977).

The annual average weight of anthropogenic SO_2 emissions for the map area shown in Figure 1 is large--about 15,000 metric tons per day. On a per-unit-area basis, this emission is nearly equivalent to the national average; however, on a per-capita basis, it is about four times the national average. This high emission results from a moderate population density combined with a regional energy supply system, which depends strongly on regional high-sulfur coal. Figure 2 places the regional sulfur emissions in perspective with the rest of the nation. Some 75 percent of the SO_2 emissions occur east of the Mississippi River, with the highest emission density occurring near the Ohio River Valley (Ohio, Pennsylvania, and Indiana).

Nearly 90 percent of the regional emissions result from 33 major coal-fired power plants, which are irregularly scattered over the entire region. Figure 3 illustrates the locations and relative magnitude of SO_2 emissions for the power plants. TVA's 12 coal-fired power plants account for one third of all sulfur emissions. By 1983 various SO_2 control technologies will reduce TVA regional emissions by 40 percent.

Figure 3 shows that many of the larger power plants are geographically grouped along the Ohio and Tennessee river valleys. This can lead to one of several "source intensification" corridors, depending on the synoptic meteorology (Smith and Niemann 1977). Such corridors become significant when the airmass transport direction and the corridor direction coincide. When this happens, emission rates per unit area (along these corridors) increase significantly.

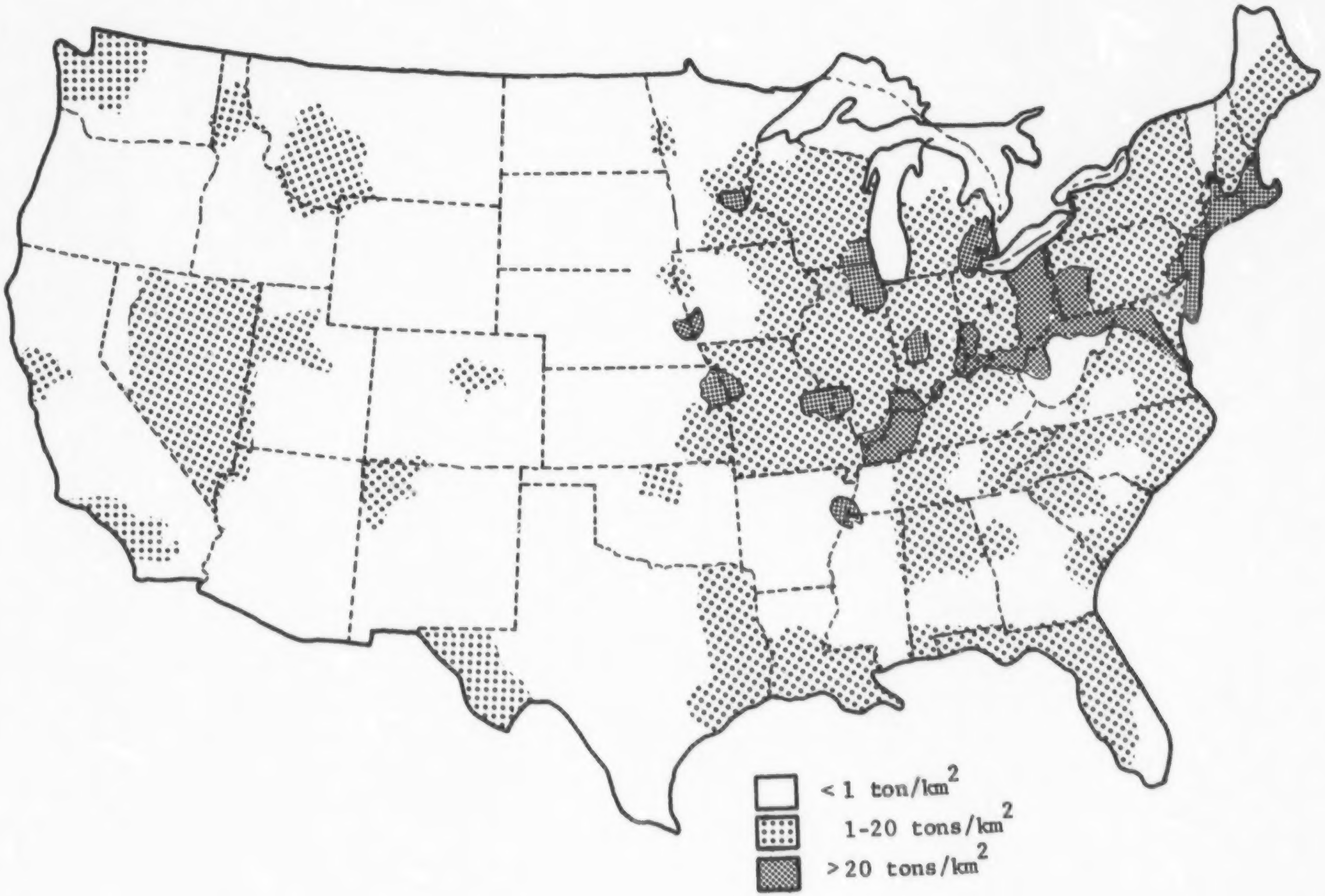
< 1 ton/km^2
1-20 tons/km^2
> 20 tons/km^2

Figure 2. Annual average SO_2 emission density map.

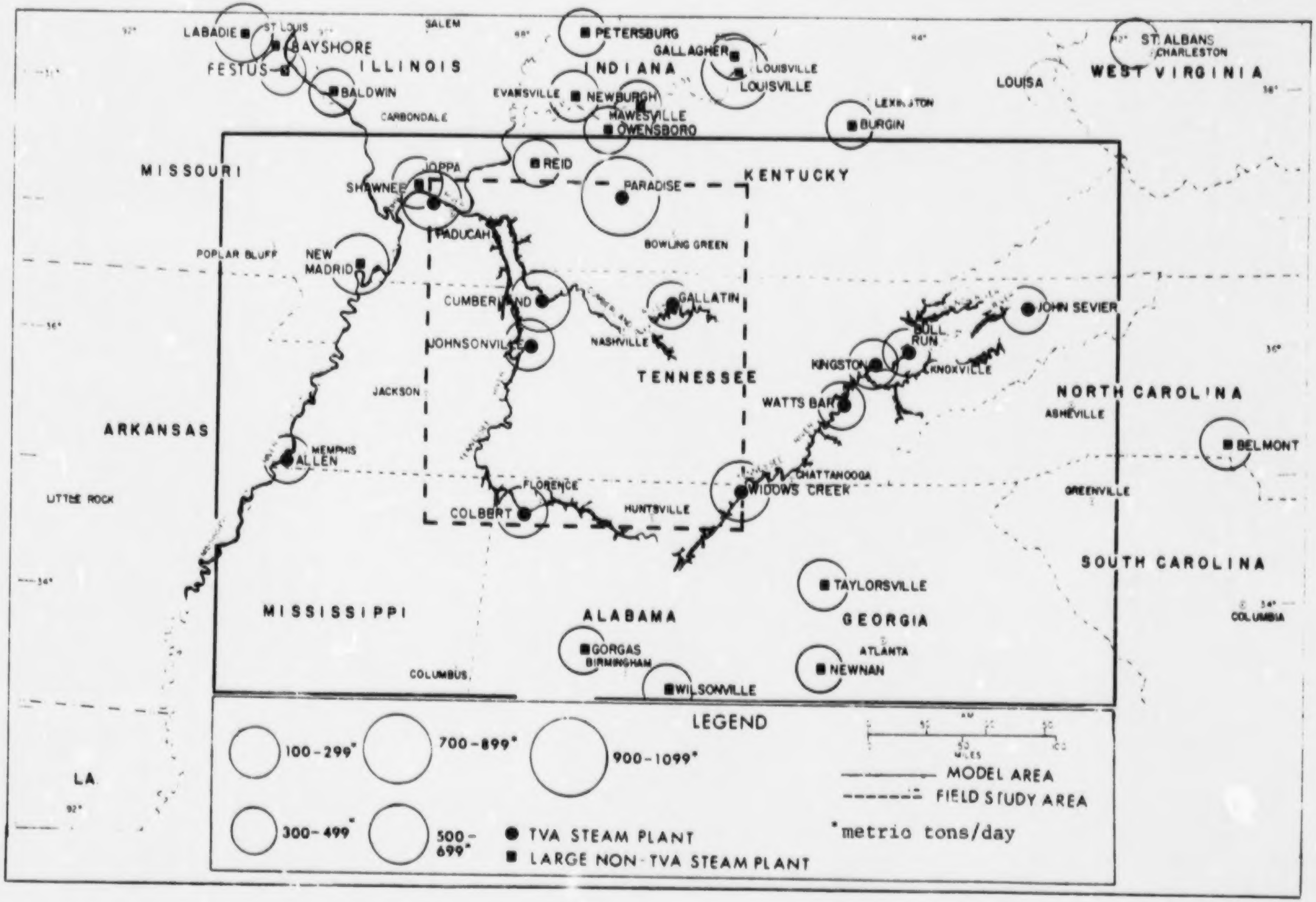
LABADIE
ST LOUIS
BAYSHORE
FESTUS
ILLINOIS
BALDWIN
SALEM
CARBONDALE
PETERSBURG
INDIANA
EVANSVILLE
NEWBURGH
HAWESVILLE
OWENSBORO
GALLAGHER
LOUISVILLE
LOUISVILLE
LEXINGTON
BURGIN
LOUISA
ST. ALBANS
CHARLESTON
WEST VIRGINIA
MISSOURI
JOPPA
SHAWNEE
PADUCAH
REID
PARADISE
KENTUCKY
BOWLING GREEN
POPLAR BLUFF
NEW MADRID
CUMBERLAND
JOHNSONVILLE
GALLATIN
NASHVILLE
TENNESSEE
JACKSON
ARKANSAS
MEMPHIS
ALLEN
LITTLE ROCK
FLORENCE
COLBERT
HUNTSVILLE
JOHN SEVIER
BULL RUN
KINGSTON
KNOXVILLE
WATTS BAR
CHATTANOOGA
WIDOWS CREEK
NORTH CAROLINA
ASHEVILLE
BELMONT
GREENVILLE
SOUTH CAROLINA
COLUMBIA
MISSISSIPPI
ALABAMA
GORGAS
BIRMINGHAM
WILSONVILLE
COLUMBUS
TAYLORSVILLE
GEORGIA
ATLANTA
NEWNAN
LA
92°
36°
34°
LEGEND
100-299*
700-899*
900-1099*
300-499*
500-699*
● TVA STEAM PLANT
■ LARGE NON-TVA STEAM PLANT
KM
MILES
MODEL AREA
FIELD STUDY AREA
*metric tons/day

Figure 3. Locations and SO_2 emissions of major point sources.

An example of a source intensification corridor is evident in the locations of the TVA Colbert, Johnsonville, Cumberland, and Paradise Steam Plants. These plants form a curved corridor oriented from the south to the northeast through middle Tennessee and southern Kentucky. Actual documentation of such a source intensification event along this corridor was found during the recent Sulfur Transport and Transformation in the Environment (STATE) Tennessee Plume Study (Private communication with W. E. Wilson, Environmental Protection Agency, Research Triangle Park, North Carolina, 1978).

Major population centers within the map area include Nashville, Knoxville, Chattanooga, and Memphis, Tennessee; Birmingham, Alabama; Atlanta, Georgia; and the area along the Ohio River from Evansville, Indiana, to Louisville, Kentucky. Historical meteorologic records indicate that average airmass trajectories emanating from this map area have maximum frequency toward the NNE, with a second maximum toward the ESE. Thus, cities such as Chattanooga and Knoxville, Tennessee, and Louisville, Kentucky, are downwind of potentially high emission density corridors.

The Cumberland, Paradise, Widows Creek, and Shawnee Steam Plants are the largest TVA coal-fired plants. These plants, together with TVA's Gallatin, Colbert, and Johnsonville Steam Plants, are base-load plants and are all within the field study area sampled during the 1976 and 1977 studies. The average sulfur content of the coal burned in these plants, most of which comes from the southern Appalachian area, is 3.4 percent.

Meteorological Characterization

In the following subsection, the climatological analyses of significant meteorological variables in and around the Tennessee Valley region are described. Specifically, analyses of seasonal and annual variations in synoptic weather patterns and airmass trajectory analyses are presented.

Synoptic Weather Patterns--

In an effort to objectively quantify the significant meteorological variables that impact the Tennessee Valley region, a quasi-objective weather typing scheme has been devised. This scheme classifies five basic weather parameters identifiable on National Weather Service (NWS) daily weather maps. The area of interest is defined within a 500-nautical-mile (nmi) radius from Nashville, Tennessee. Daily weather maps were tabulated every sixth day from November 5, 1973, through October 28, 1977. Although meteorological cycles are known to exist, we felt that integrating the data base over four years would eliminate this bias. In doing this, a total of over 235 data points were generated for each of the five parameters. These five parameters describe (1) the predominant frontal systems and associated pressure centers; (2) the distance (range) of the most significant pressure center from Nashville, Tennessee; (3) the direction from Nashville, Tennessee (degrees from true north) of this pressure center; (4) the airmass type (e.g., maritime tropical, continental polar); and (5) the relative frequency of measurable precipitation (≥0.01 in.). These parameters are further divided into categories. These categories and their annual and seasonal distributions are presented in Appendix A.

All five parameters have significant departures from the mean during summer, the peak sulfate season for eastern North America. These departures are all correlated with the strong influence of the Bermuda high on weather patterns in the southeastern United States, especially during the summertime. This influence results in reduced wind flow; moist, warm air advection; and poor ventilation, which often leads to air pollution episodes, not only in the southeast but over the entire eastern United States.

Further work that substantiates the significance of the Bermuda high's ability to produce elevated air pollution potential is presented by Korshover (1976). He describes the most significant stagnation, or poor ventilation, areas within the eastern United States on both an annual and seasonal basis. For the high air pollution seasons of summer and fall, his analysis shows that the most intense areas of stagnation are located in an arc from West Virginia southward to central Georgia. The average distance and location of this stagnation arc relative to the TREATS field study region correspond well with the directional and distance analysis for the high-pressure centers listed in Appendix A. This pressure orientation produces an annual airflow toward the northeastern United States and leads to significantly reduced transport during the summer and autumn months. Examples of this flow pattern producing high sulfate pollution levels two to three times as high as the annual average are the TREATS 1977 field study days of late June and early July. However, significant departures in this typical high pollution flow regime can occur (Reisinger and Crawford 1979).

Trajectory Data--

Twice daily NWS 24-h surface and 850-mb back-trajectories for Nashville, Tennessee, were analyzed for a 3-year period (1976-1978) to define significant flow directions into the Tennessee Valley region. Also, for a 1-year period (1972), 850-mb (~1500 m MSL) trajectory data were analyzed for 14 cities surrounding the Tennessee Valley region to describe the movement of airmasses out of the region.

Annual contour analyses of favored origination locations for 24-h back-trajectories are presented in Figure 4. The numbers shown are the occurrences for the period of record, 1976-1978. These analyses were obtained by plotting the frequency of occurrence of 24-h back-trajectories by 1-degree latitude-longitude boxes. The data show that on an annual basis most trajectories originate in a sector from southern Alabama through northwestern Tennessee. Seasonally, the winter pattern is quite similar to the annual frequency pattern, whereas the spring pattern is diffuse with numerous trajectories from the north and east. However, the summer pattern indicates a more compact distribution, with 24-h trajectory origins frequently occurring from west Tennessee. Fall trajectories, like the spring trajectories, show a diffuse source region, with significant maxima around the Ohio River Valley and eastern Tennessee.

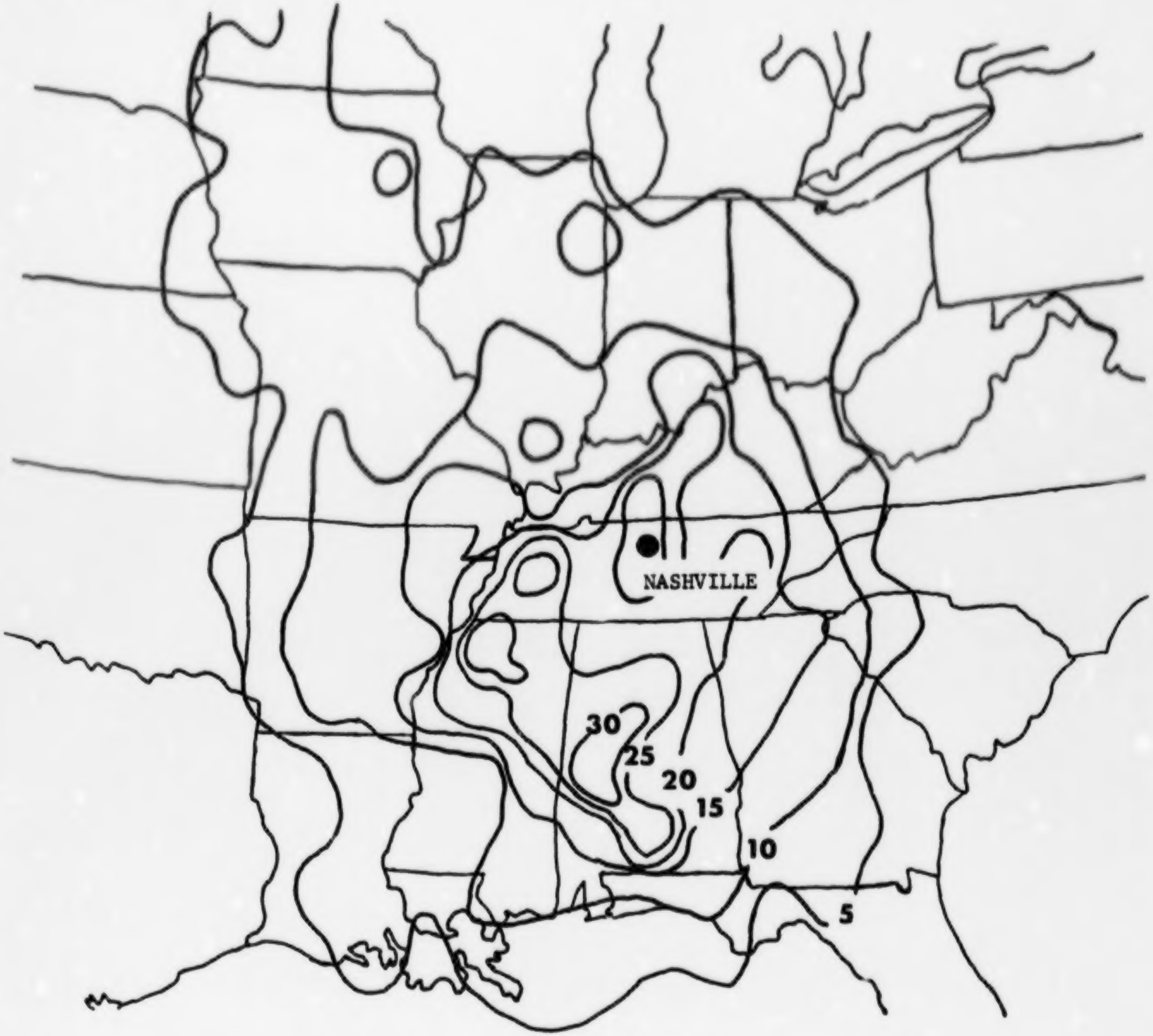
NASHVILLE
30
25
20
15
10
5

Figure 4. Favored 24-h airmass source regions for Nashville, Tennessee.

The frequency of occurrence of trajectories originating within a model area (defined by 38°N, 91°W, 33°N, and 82°W) and passing over eight cities surrounding the area is shown in Figure 5. This model area roughly defines the area within which TVA has coal-fired power plants. From this figure, one can see that trajectories originating within this area rarely affect regions to the south or west, whereas frequent airmass movement occurs toward the north through east.

SAMPLING PLATFORMS

Two aircraft were used for the airborne sampling experiments. A deHavilland Beaver (U6-A)--a single-engine, fixed-wing craft--was used in both the 1976 and 1977 regional transport studies, and a Bell 47A helicopter was also used during the 1977 study. The instruments installed aboard the airplane are described in Table 1.

TABLE 1. AIRPLANE INSTRUMENT PACKAGE, BEAVER U6-A

Parameter	Detector	Instrument	Study
Total sulfur	Flame photometric	Meloy Labs SH202	1976, 1977
Total hydrocarbons	Flame ionization	Meloy Labs SH202	1976, 1977
Ozone	Chemiluminescence ($O_3 + C_2H_4$)	McMillan 1100	1976
NO, NO_x	Chemiluminescence ($O_3 + NO$)	Thermo Electron 14D	1976, 1977
b_{scat}	Integrating nephelometer	Meteorological Research	1977
Temperature	Thermistor	Custom	1976, 1977
Dewpoint	Chilled mirror	Cambridge 137-C3	1976, 1977
	Filter collection system		
$SO_4^=$, NO_3^-, NH_4^+	37 m Millipore filters (Fluoropore)	See text	1976, 1977

Power for the continuous monitors was provided by the aircraft electrical system through two 1-kW Topaz inverters. The output from the instruments was applied to Hewlett-Packard 7100B, dual-channel, strip chart recorders.

The airplane, instrument layout, and instrument package are shown in Figures 6, 7, and 8. The dual-line sampling probe was constructed from two 0.635-cm-OD stainless steel tubes that extended 1.2 m above the fuselage. This arrangement allowed for separate sampling streams for

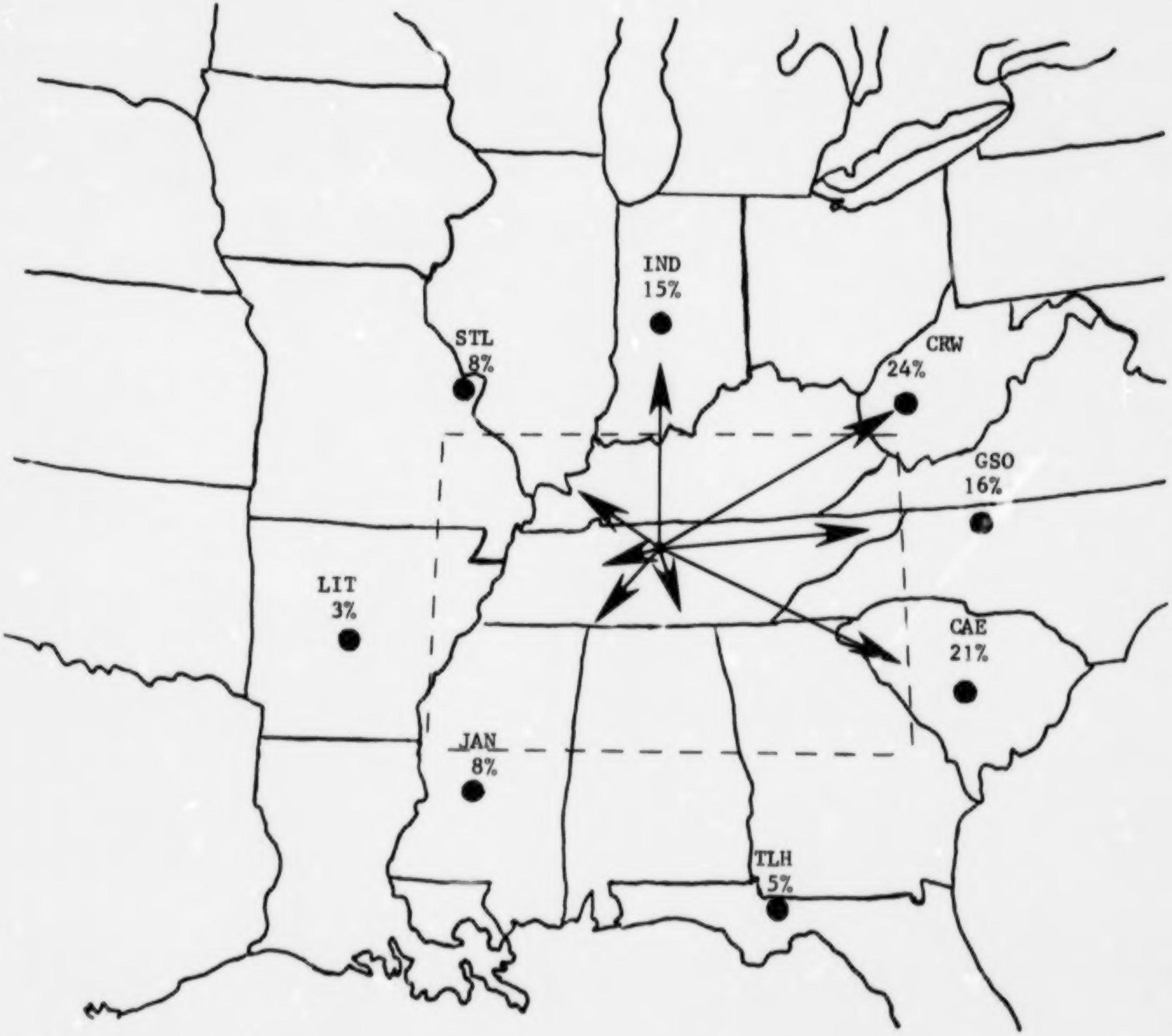
IND
15%
STL
8%
CRW
24%
GSO
16%
LIT
3%
CAE
21%
JAN
8%
TLH
5%

Figure 5. Percent occurrence of airmass movement out of the Tennessee Valley region (1972).

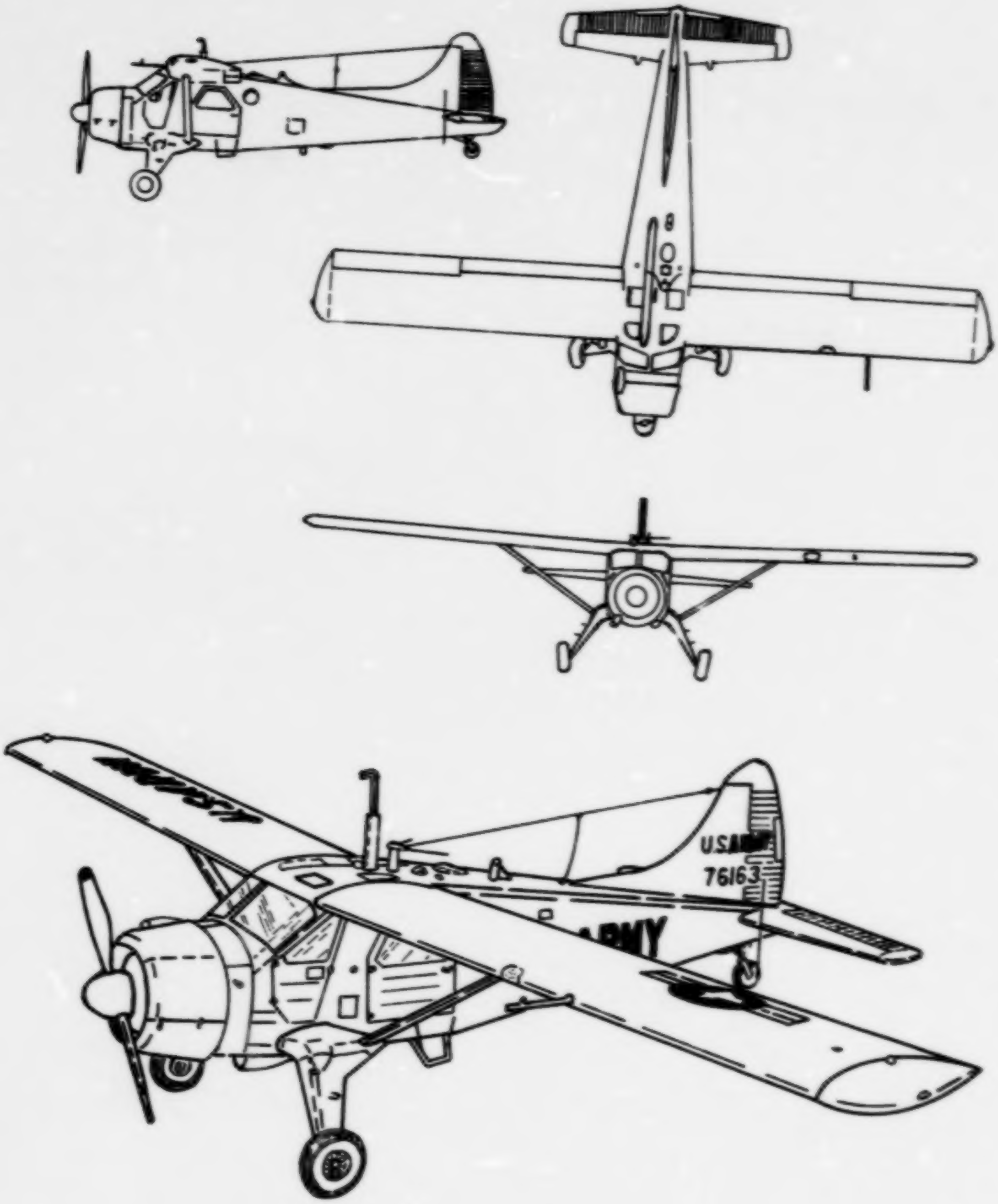

Figure 6. deHavilland Beaver U6-A airplane.

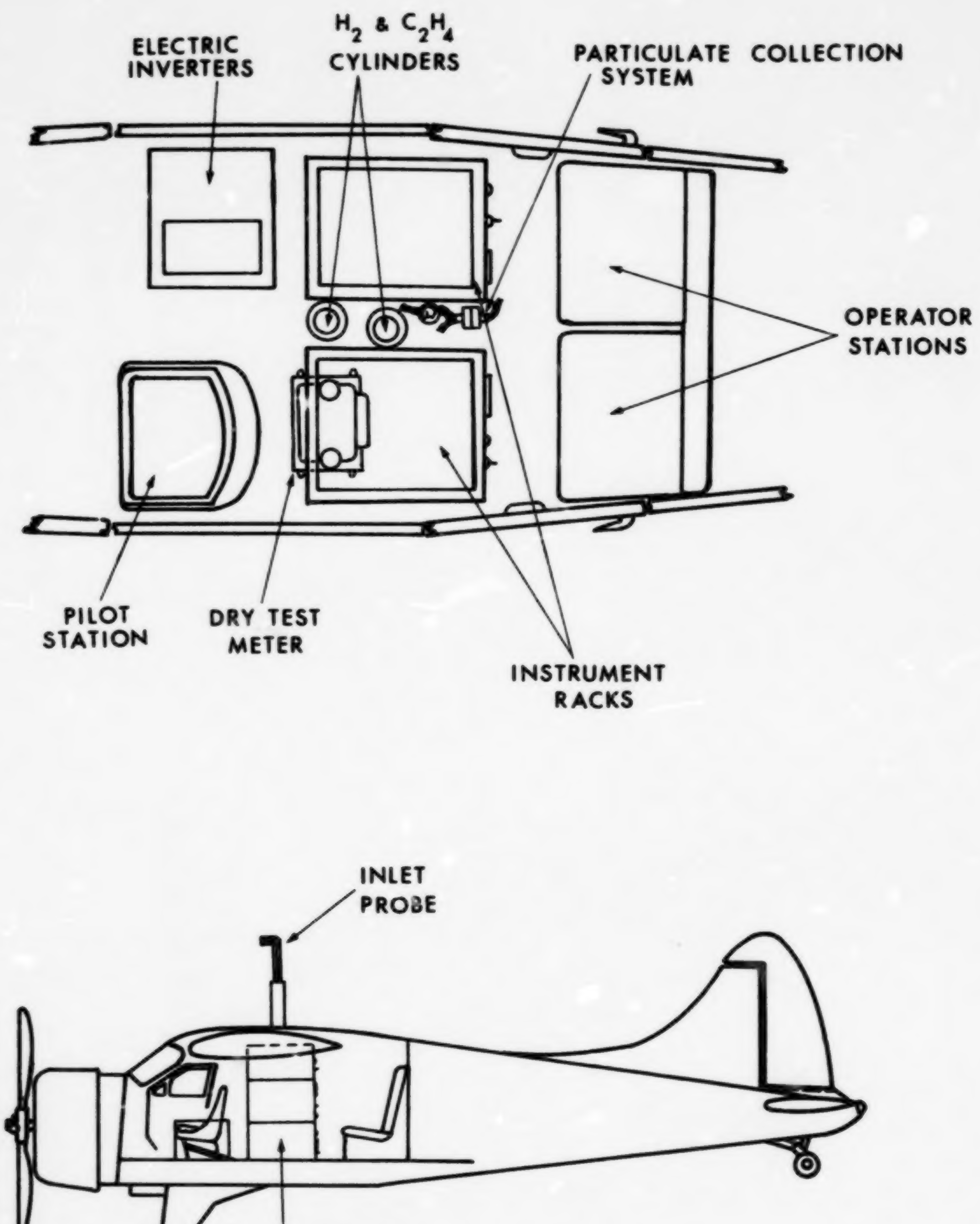
ELECTRIC INVERTERS
H_2 & C_2H_4 CYLINDERS
PARTICULATE COLLECTION SYSTEM
OPERATOR STATIONS
PILOT STATION
DRY TEST METER
INSTRUMENT RACKS
INLET PROBE
INSTRUMENT RACKS

Figure 7. Airplane instrument layout.

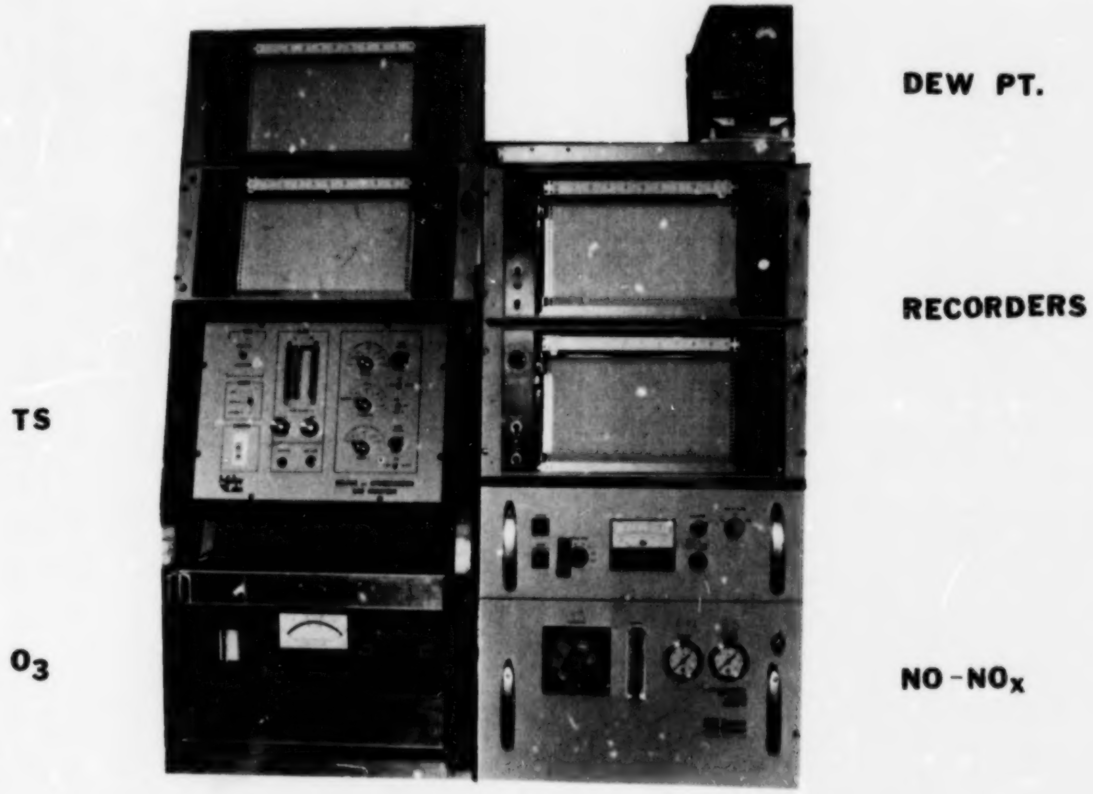
DEW PT.
RECORDERS
TS
O_3
NO-NO_x

Figure 8. U6-A instrument package.

particulate and continuous gas monitors while eliminating interferences from the propeller wash and engine exhaust. Both probes were nearly isokinetic--the gas sampling probe by allowing excess probe ram-air to bleed out the end and the particulate sampling probe by matching probe intake area and sampling flow rate to the aircraft sampling speed of 50 m s^{-1}. Vacuum for the particulate collection system was obtained from the airplane vacuum system.

The integrating nephelometer was operated without a heater. For relative humidity above about 70 percent, hygroscopic or deliquescent particles grow. This enhances their scattering coefficient and leads to increased b_{scat}. Below about 70 percent, mass concentration can be related to b_{scat} (Meteorological Research, Inc., 1972) by

$$\text{Mass } (\text{g m}^{-3}) = 0.38\ b_{scat}.$$

The second aircraft, a Bell 47A helicopter, was used in the 1977 regional transport study. The instruments installed aboard the helicopter are described in Table 2.

TABLE 2. HELICOPTER INSTRUMENT PACKAGE, BELL 47A

Parameter	Detector	Instrument
Total sulfur	Flame photometric	Meloy Labs Model SA-285
b_{scat}	Integrating nephelometer	Meteorological Research, Inc.
Temperature	Thermistor	Custom
Dewpoint	Chilled mirror	Cambridge 137-C3
	Filter collection system	
$SO_4^=$, NO_3^-, NH_4^+	37 mm Millipore filters (Fluoropore)	See text

Power for the continuous monitors was provided by the helicopter electrical system through a 1200-W Deltec inverter. The output from the instruments was applied to Hewlett-Packard 7100B, dual-channel, strip chart recorders.

The helicopter and the instrument layout are shown in Figures 9 and 10. The dual-line sampling probe was constructed from two 0.635-cm-OD stainless steel tubes, which were mounted on the right landing strut and extended forward about 1 m. This arrangement allowed for separate sampling streams for particulates and gases while eliminating rotor downwash interferences. Airflow through the probes was nearly isokinetic. Vacuum for the particulate collection system was obtained from two Gast model 1550 vacuum pumps.

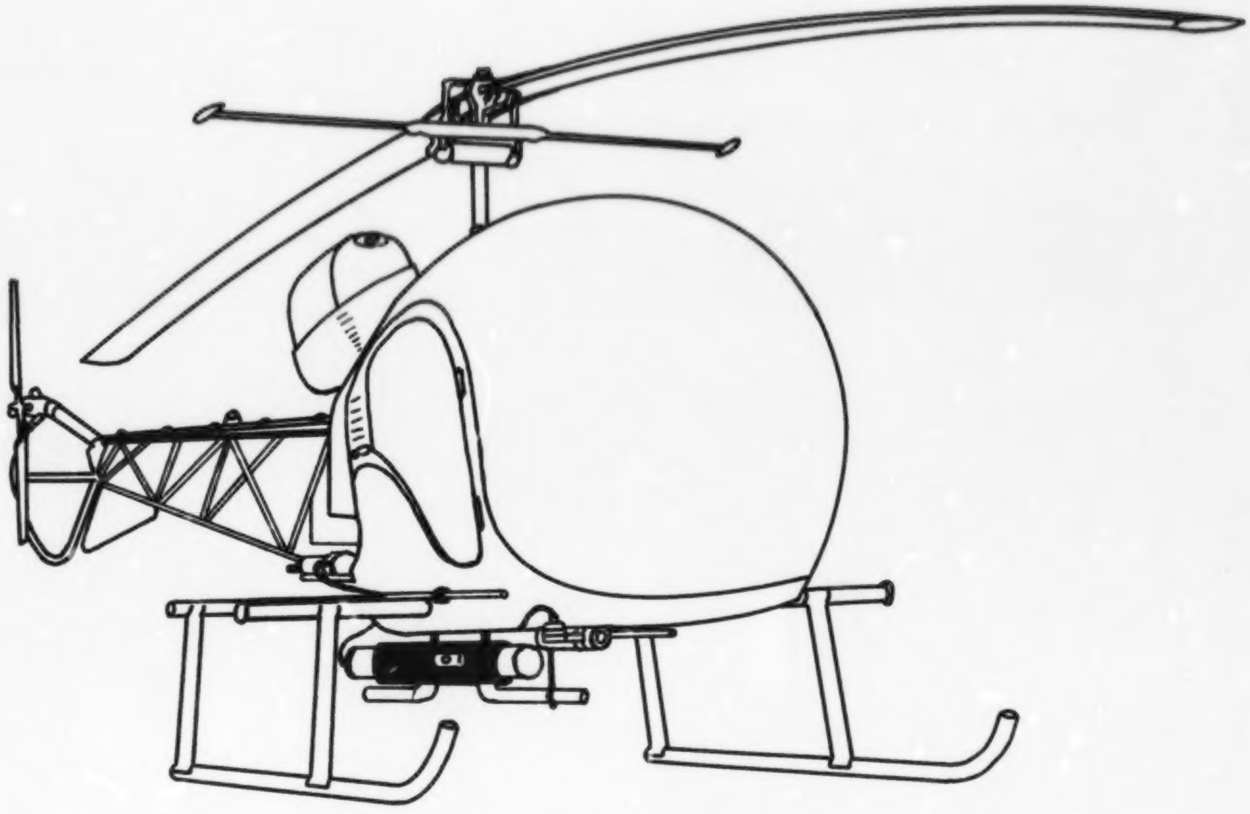

Figure 9. Bell 47A helicopter.

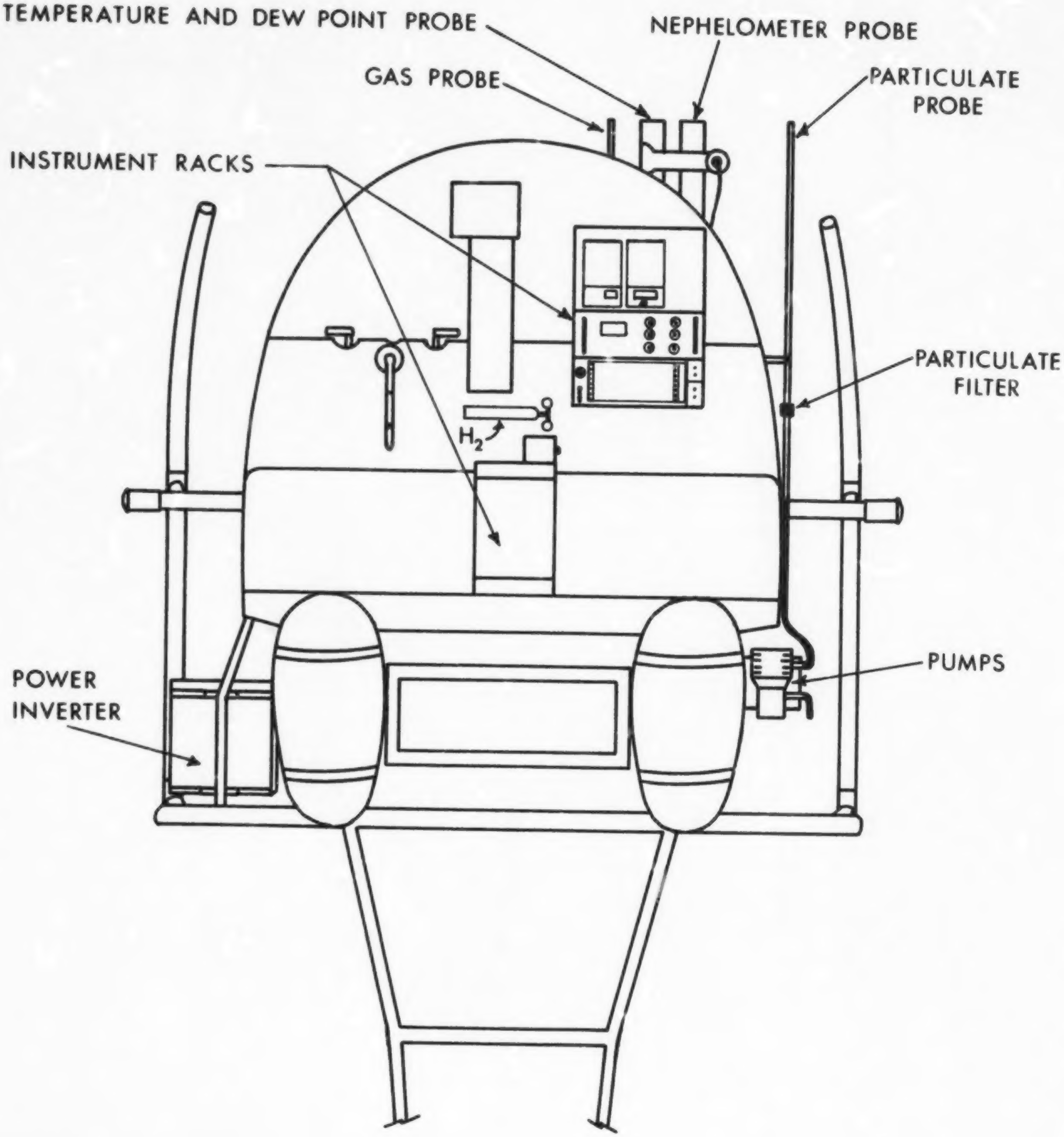
TEMPERATURE AND DEW POINT PROBE
NEPHELOMETER PROBE
GAS PROBE
PARTICULATE PROBE
INSTRUMENT RACKS
PARTICULATE FILTER
H_2
POWER INVERTER
PUMPS

Figure 10. Helicopter instrument layout.

In both studies, particulate samples were collected on 37-mm Millipore (Fluoropore) membrane filters. The 1976 study used Fluoropore filters with 0.5-μm pore size, whereas the 1977 study used filters with 1.0-μm pore size. Liu and Lee (1976) have shown that these filters have greater than 99 percent collection efficiency for aerosols in the 0.03- to 1.0-μm diameter range. The volume of air sampled was measured with Sprague dry test meters in 1976 and Matheson mass flowmeters in 1977. The average flow rate through the filters was 50 L/min, and the average volume of air sampled was 1.8 m^3.

METEOROLOGICAL MEASUREMENTS AND SUPPORT

The study area for both the 1976 and 1977 aircraft measurement programs was centered over the western Tennessee Valley region (dashed area in Figure 11). As shown by Figure 11, this area has one of the most densely instrumented meteorological networks in the Nation. TVA operates seven upper-air stations, and the NWS operates one. Of the stations, four are operated on a 24-h basis, with pibal and temperature soundings taken four times throughout the day. Most of these soundings are taken from early morning through midday. The NWS upper-air station takes temperature and wind soundings at 0600 and 1800 CST. In addition to these measurements, TVA measures wind and temperature at 13 meteorological towers, and the NWS measures near-surface and cloud parameters at five 24-h weather observation stations. This wealth of meteorological data, particularly the eight upper-air sites, has proven useful in accurately defining the spatial and temporal variations of the planetary boundary layer.

The TVA Meteorological Forecast Center (MFC) in Muscle Shoals, Alabama, provided planning and operational forecasts of mixing-layer heights and wind velocities, airmass trajectories, heights of radiation and subsidence inversions, and general weather and cloud forecasts for the study area. These forecasts were issued twice daily; an operational forecast was issued on the morning of a sampling day, and an afternoon planning forecast was issued for the following day. Updates of actual wind and temperature profiles near the aircraft sampling paths were frequently obtained on a near-real-time basis to evaluate the ongoing experiment from a meteorological standpoint. To minimize variables and still obtain a "typical" airflow pattern, the 1976 and 1977 studies were designed so that sampling would be conducted during "favorable" meteorological conditions. These favorable conditions included ceilings greater than 305 m, identifiable subsidence inversions ≤2000 m, no measurable precipitation within the study area, and persistent winds from the south through west.

SAMPLING PROCEDURE

Two full-scale long-range transport field studies were conducted, one during February and March 1976 and the other during June and July 1977. Because meteorology, chemistry, and biological activity differ significantly from spring to summer, and knowledge gained from the 1976 study influenced the design of the 1977 study, the sampling procedure description is divided by field study.

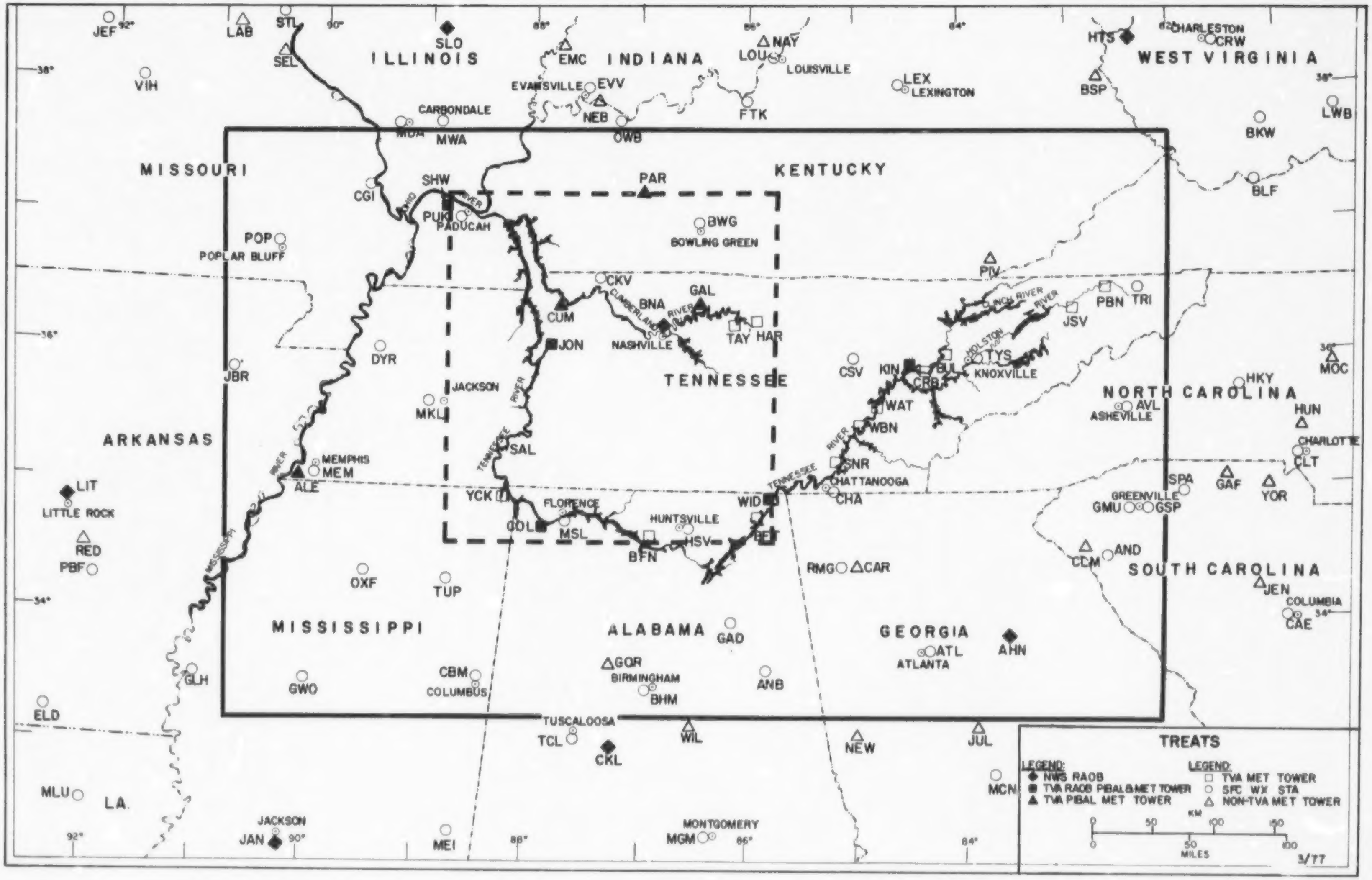
TREATS
LEGEND:
◆ NWS RAOB
■ TVA RAOB PIBAL & MET TOWER
▲ TVA PIBAL MET TOWER
□ TVA MET TOWER
○ SFC WX STA
△ NON-TVA MET TOWER
KM
0
50
100
150
MILES
0
50
100
3/77
MISSOURI
ILLINOIS
INDIANA
KENTUCKY
WEST VIRGINIA
ARKANSAS
TENNESSEE
NORTH CAROLINA
SOUTH CAROLINA
MISSISSIPPI
ALABAMA
GEORGIA
LA.
JEF
LAB
STL
SEL
VIH
SLO
EMC
EVANSVILLE
EVV
NEB
OWB
LOU
NAY
LOUISVILLE
FTK
LEX
LEXINGTON
HTS
BSP
CHARLESTON
CRW
BKW
LWB
BLF
CARBONDALE
MDA
MWA
SHW
CGI
PUK
PADUCAH
PAR
BWG
BOWLING GREEN
POP
POPLAR BLUFF
CKV
CUM
BNA
GAL
NASHVILLE
TAY
HAR
JON
DYR
JBR
JACKSON
MKL
PIV
PBN
TRI
JSV
CLINCH RIVER
HOLSTON
TYS
KNOXVILLE
CSV
KIN
BUL
CRB
WAT
WBN
SNR
CHATTANOOGA
CHA
HKY
MOC
AVL
ASHEVILLE
HUN
CHARLOTTE
CLT
SPA
GAF
YOR
GREENVILLE
GMU
GSP
CLM
AND
JEN
COLUMBIA
CAE
LIT
LITTLE ROCK
RED
PBF
MEMPHIS
MEM
ALE
SAL
YCK
FLORENCE
COL
MSL
HUNTSVILLE
HSV
BFN
WID
BEF
RMG
CAR
OXF
TUP
GAD
ATL
ATLANTA
AHN
GQR
BIRMINGHAM
BHM
ANB
CBM
COLUMBUS
GWO
GLH
ELD
TUSCALOOSA
TCL
CKL
WIL
NEW
JUL
MCN
MLU
JACKSON
JAN
MEI
MONTGOMERY
MGM
OHIO RIVER
CUMBERLAND RIVER
TENNESSEE RIVER
MISSISSIPPI RIVER
92°
90°
88°
86°
84°
82°
38°
36°
34°

Figure 11. Location and type of meteorological measurements.

1976 Study

The sampling strategy during the 1976 study was to obtain Lagrangian airmass measurements under fairly representative airflow conditions. This and other meteorological conditions, described in the Meteorological Measurements and Support subsection of Section 3, could be met only briefly during prefrontal flow. Also, due to the variability of the wind, the "window" during which the afternoon aircraft space coordinates were similar to the Lagrangian airmass coordinates was also limited.

The Meteorological Characterization subsection, Section 3, indicates that the principal flow direction is from the south through west. With this in mind, we decided that the aircraft sampling strategy should be to first make representative morning inflow measurements from south-central Tennessee through northern Alabama. This was accomplished by flying two horizontal traverses, one within the morning radiation inversion and one between the tops of the radiation inversion and the subsidence inversion. These traverses were flown at "constant altitudes" AGL; the within-inversion measurements were typically made at an altitude of about 600 m AGL. Sulfate sample requirements, more than airmass characterization requirements, dictated that the traverses last at least 1.5 h, or be about 150 km long.

After the morning sampling traverses were completed, the aircraft landed and refueled at the Muscle Shoals, Alabama, airport. At that time, the forecasted wind and weather conditions at the outflow boundary were updated. The aircraft then flew a "constant altitude" sampling flight to the outflow boundary, which was typically near south-central Kentucky and north-central Tennessee. Immediately after reaching the outflow field study boundary, sampling began. The afternoon outflow sampling procedure was similar to the morning procedure; that is, two (about 200-km) traverses were flown at different altitudes to get representative readings within the well-mixed layer. Typically, these measurements were near 600 and 1200 m AGL.

1977 Study

Three factors dictated that the single sampling strategy technique used during the 1976 study be modified. The first factor was a need, identified during the 1976 study, to determine whether significant vertical or horizontal pollutant gradients existed, especially during early daylight hours. The second factor was the availability of two aircraft; thus, simultaneous measurements at two locations were possible. The third factor, which probably proved greater than either of the other two, was the weather.

As with the 1976 study, favorable meteorological sampling conditions were identified, as described in the Meteorological Measurements and Support subsection. However, a climatological analysis of other summers and the initial weather conditions observed in May and early June 1977 indicated that obtaining all the desired conditions simultaneously would be impossible. A combination of low wind speeds, lack of directional persistence, morning ground fog, and airmass and frontal thunderstorm activity all contributed to a modified sampling strategy. This modified strategy resulted in two scenarios.

Scenario 1 was defined as airmass Lagrangian or Eulerian measurements. This scenario is similar to the 1976 sampling strategy, except that separate aircraft sampled the atmosphere at the inflow or outflow boundaries. Measurements were obtained by multiple-altitude traverses (typically four levels) through the inversion layers and usually for three time periods--early morning, late morning or midday, and afternoon. This technique allowed for both Eulerian space and time measurements in addition to the anticipated Lagrangian measurements.

In this report the terms "Eulerian" and "Lagrangian" refer only to the basis of the coordinate system. If the coordinate system is particle attached, the term "Lagrangian" is applied; the term "Eulerian" is properly applied to all other cases.

Scenario 2 was defined as airmass stagnation, or blob measurements. This scenario was similar to scenario 1 in that traverses were flown by both aircraft. However, because wind flow cannot be defined under stagnation conditions, measurements cannot be evaluated for flux, and only concentration variations in space and time can be analyzed.

The 1976 and 1977 data that were collected using these sampling strategies are summarized in Appendix B.

ANALYTICAL METHODS

Continuous Gas Analyzers

The continuous gas analyzers used in the studies were calibrated against standardized, wet chemical methods. The West-Gaeke (1956) procedure was used to calibrate the Meloy Labs flame photometric sulfur analyzers before and after experiments. During sampling, all gas monitors were continually checked for malfunctions.

The flame photometric detector is noted for its excellent sensitivity to low background levels of sulfur and its linear logarithmic response over several orders of magnitude. Unfortunately, it is also sensitive--in an instrument-specific manner--to ambient pressure, which is a function of altitude. The results from altitude tests on the Meloy 202 and 285 analyzers and the method used for adjusting the data to compensate for pressure sensitivity are given in Appendix C. Caution should be observed when using the resulting concentration numbers in an absolute sense, since these tests were made after the two study periods.

The gas analyzers provide a continuous measurement in time (or distance). To compare these continuous measurements with integrated-traverse low-volume filter particulate measurements, the continuous measurements must be integrated over the sampling traverse. The algorithm for this integration is

$$\bar{C} = 1/(t_2 - t_1) \int_{t_1}^{t_2} C(t)dt, \qquad (1)$$

where

$\bar{C}$ = integrated traverse equivalent concentration,
$C(t)$ = time continuous concentration,
t_1, t_2 = endpoint times of the traverse.

Because of large sample times (typically, $t_2 - t_1 = 15$ min) and small gradients of $C(t)$ in time, instrument response time along a traverse was not a problem.

Low-Volume Filters

The water-soluble fraction of particulate captured on the 37-mm Millipore low-volume filters was extracted with Super-Q (prefiltered, organics adsorbed, deionized, and membrane-filtered) water in an ultrasonic bath. The extracts were analyzed for $SO_4^=$, NO_3, and NH_4^+ ions. The $SO_4^=$ analyses for the 1976 study were performed by flash vaporization--flame photometry (Roberts and Friedlander 1975; Husar et al. 1975). The samples from the 1977 study were analyzed for $SO_4^=$ and NO_3^- by ion chromatography (Mulik et al. 1976). The NH_4^+ analyses were performed by the alkaline phenate method (EPA 1974b) with a Technicon autoanalyzer. The accuracy to be expected from these techniques is shown in Table 3.

High-Volume Filters

Mine Safety Appliance filters were used during the 1976 field study. Gelman Spectrograde filters were used in all TVA high-volume samplers and in State of Kentucky high-volume samplers operated for the 1977 study. The spectrograde filter was selected for the 1977 study because of its low $SO_4^=$ background and lower alkalinity compared with most other high-volume filter materials. Coutant (1977) has shown that lower alkalinity filters produce significantly less artifact $SO_4^=$ formation.

Exposed filters were weighed for particulate loading (Jutze and Foster 1976) and analyzed for water-soluble $SO_4^=$, NO_3, and NH_4^+ ion concentration. An extract for ion analysis was obtained from a 3.4-cm strip of the filter, which was hot water refluxed for 90 min. Ion concentrations were determined with the methylthymol blue analytical finish for $SO_4^=$, automated cadmium reduction method for nitrate-nitrite, and the colorimetric phenate method for ammonium (analyzed as NH_3). Because of extraction problems with the 1977 Spectrograde filters and delays in analysis, NO_3^- and NH_4^+ values are considered inaccurate and are not reported. Checks on the accuracy of the sulfate extraction showed no significant bias. Based on eight triplicate measurements (from three collocated high-volume samplers), the standard error of estimate for the precision of the measurement and laboratory analysis was found to be ±1.4 $\mu g\ m^{-3}$ or about 10 percent.

TABLE 3. ACCURACY[a] OF ANALYTICAL METHODS, 37-mm MILLIPORE FILTERS

Ion	Method	Typical blank (μg/filter)	Concentration (μg/filter)	Recovery (%)	Precision (%)
$SO_4^=$	Flash vaporization	0.4	4.0	91	4
			8.0	100	4
			16.0	98	3
$SO_4^=$	Ion chromatograph	0.2	2.0	81	25
			20.0	93	5
NO_3^-	Cadmium reduction	0.1	0.5	118	40
			1.0	104	18
			2.0	98	10
NO_3^-	Ion chromatograph	0.1	0.1	100	19
			0.5	97	20
NH_4^+	Alkaline phenate	0.3	0.5	84	36
			1.0	87	24
			2.0	92	8

[a] Based on seven replicate determinations at the given concentration level with a single operator.

TRANSFORMATION-TRANSPORT MODEL

This section presents the derivation and exploration of simple Eulerian and Lagrangian models of the SO_2-to-$SO_4^=$ transformation and transport processes to a receptor along a mean trajectory. The pollutants are considered to be confined between the ground and a capping inversion. Diffusion in the horizontal is allowed. Simple linear models of the transformation and the dry deposition processes are used. Wet removal processes are not considered, but could be easily added to either the analytical or numerical formulations. A sensitivity analysis of the Lagrangian 1-dimensional analytic formulation illustrates not only the importance and functional relationship of various model parameters, but also the integral characteristics of the long-range transport process. Model response is compared with field data in Section 4.

Model Development

The equation that describes the mean turbulent transport, diffusion, and transformation of any conservative, gas-like, airborne substance is:

$$\frac{\partial C}{\partial t}i = -\frac{\partial}{\partial x}(UC_i) - \frac{\partial}{\partial y}(VC_i) - \frac{\partial}{\partial z}(WC_i)$$

$$+ \frac{\partial}{\partial x}(K_x\frac{\partial C}{\partial x}i) + \frac{\partial}{\partial y}(K_y\frac{\partial C}{\partial y}i) + \frac{\partial}{\partial z}(K\frac{\partial C}{\partial z}i) + k_iC_i \quad . \qquad (2)$$

The term on the left side of this equation is the mean rate of increase of C_i per unit time. The first three terms on the right side define the increase of C_i resulting from 3-dimensional differential advection transport. The next three terms define the 3-dimensional turbulent flux-convergence for C_i. The last term specifies chemical transformation. Equation (2) becomes specific to a substance when appropriate conversion parameters and boundary conditions are specified (Monin and Yaglom 1971). Although it is of limited utility as it stands, Equation (2) is a useful starting point for model development, provided appropriate assumptions are made and applied with suitable boundary conditions. This approach was used to develop a simple regional transport model for SO_2 and $SO_4^=$. Variables used in this subsection are defined in the List of Abbreviations and Symbols located at the front of this report.

Analytical Model--

Consider a region of varying width (Figure 12), oriented so that its length is parallel to the mean boundary-layer wind direction. It is bounded above by an elevated inversion, below by the ground, and on either end by the vertical inflow and outflow planes. Sulfur, as SO_2 and $SO_4^=$, is carried into the region at the inflow by the mean wind and is augmented by regional sources of SO_2, both natural and man-made. The regional airborne sulfur is subjected to turbulent transport and diffusion, chemical transformation, and deposition.

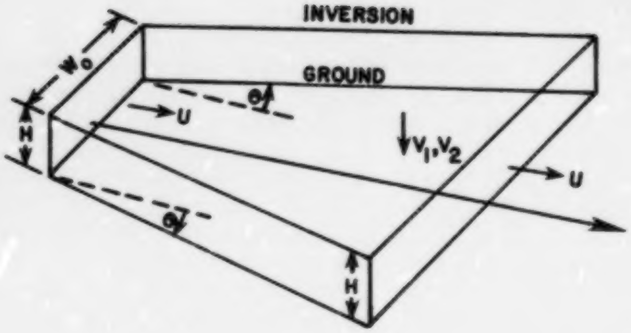

Figure 12. Region used in the development of the long-range transport model.

Equation (2) can be greatly simplified to describe this situation. To do so, eight assumptions are made.

1. $\frac{\partial C_i}{\partial t} = 0$ (steady state).
2. U = constant; $V = W = 0$.
3. $\frac{\partial}{\partial x}(UC_i) >> \frac{\partial}{\partial x}(K_x\frac{\partial C_i}{\partial x})$.
4. C_i is independent of y and z.
5. $K_y\frac{\partial C_i}{\partial y}$ is independent of x and z within the region.
6. $K_y\frac{\partial C_i}{\partial z}$ is independent of x and y within the region.
7. $K_y\frac{\partial C_i}{\partial y}\bigg|_{y = B/2} = -K_y\frac{\partial C_i}{\partial y}\bigg|_{y = -B/2}$.
8. $K_z\frac{\partial C_i}{\partial z}\bigg|_{z = 0} = -v_iC_i;\ K_z\frac{\partial C_i}{\partial z}\bigg|_{z = H} = 0$.

Letting i = 1 and integrating Equation (2) twice, once with respect to y and once with respect to z, over the region yields

$$UH\frac{d}{dx}(BC_1) = -(V_1 + Hk)BC_1. \tag{3}$$

Similarly, for i = 2, the resulting equation is

$$UH\frac{d}{dx}(BC_2) = -v_2BC_2 + 3HkBC_1/2. \tag{4}$$

Equations (3) and (4) may be considered Lagrangian by virtue of the relation $x = Ut$. These equations can be derived directly from first principles, as Scrivin and Fisher (1975) did to obtain an Equation similar to Equation (3).

The analytical solutions for Equations (3) and (4) are

$$C_1 = C_1^o \, (B_o/B) \exp \{-[(v_1/H) + k](t - t_o)\}, \qquad (5)$$

and

$$\begin{aligned} C_2 = {} & C_2^o(B_o/B) \exp [-(v_2/H)(t - t_o)] \\ & + (3/2)C_1^o(B_o/B) \{[(v_1 - v_2)/Hk] + 1\}^{-1} \\ & \cdot \{\exp [-(v_2/H)(t - t_o)] - \exp \{-[(v_1/H) + k](t - t_o)]\}. \qquad (6) \end{aligned}$$

B_o/B is the factor defining dilution due to crosswind diffusion. For single plumes Scriven and Fisher (1975) use $B = B_o + 2\theta Ut$, where θ is the (constant) angle of horizontal regional growth; Gifford (1976) suggests that, over larger distances, B is proportional to $t^{3/2}$ so that $B = bt^{3/2}$, where b is the proportionality constant. For regional transport it is appropriate to set B_o to a large value, and $B_o/B = 1$ since multiple plumes exist within the region, crosswind gradients are small, and the mass that is diffusing out is nearly balanced by that which is diffusing in.

In this form, Equations (5) and (6) do not account for sources of SO_2 within the region. This deficiency can be remedied by using the principle of superposition. If a source having emission rate Q is encountered at x', $x_o < x' < x$, assume that the effluent is spread uniformly within a plane that passes through the source and is normal to the wind. Then the SO_2 concentration in this plane, which is now taken as the initial plane, is Q/UHB', where $B = B'$ when $x = x'$, and x' is taken as the initial distance. The solution at the outflow plane is the sum of the individual solutions.

Equations (5) and (6) likewise do not apply to a region having a variable mixing depth. This deficiency can be overcome either by (1) deriving Equations (5) and (6) by assuming H is a function of x, or (2) applying Equations (5) and (6) in their present form in a stepwise manner, requiring H to be constant during any step, but allowing H to change from step to step. With this approach, the region is modeled by stacking "boxes" of possibly different dimensions end-to-end along the trajectory and modeling transport, diffusion, chemical transformation and deposition through each box in a piecewise-continuous manner. Additional details are given in the following subsection. For complex situations, the latter method is more versatile because obtaining a closed-form solution by method 1 may not be possible when H is variable. The box method can also be used to handle the presence of SO_2 sources within the region.

Simple Box Model--

With the "box" approach, the region is modeled by stacking "boxes" end-to-end along the trajectory and modeling, in a piecewise-continuous manner, transport, diffusion, chemical transformation, and deposition through each box. Figure 13 illustrates how boxes are stacked to vary mixing height and handle multiple sources.

When Equations (4) and (5) are applied across a "box," they become for SO_2

$$C_{1,j} = (1 - H_{j-1}/H_j)C_{1,b} + (H_{i-1}/H_j)C_{1,j-1} \exp[-(v_1/H_j + k)\Delta t] + Q_j/H_jU \; ; \qquad (7)$$

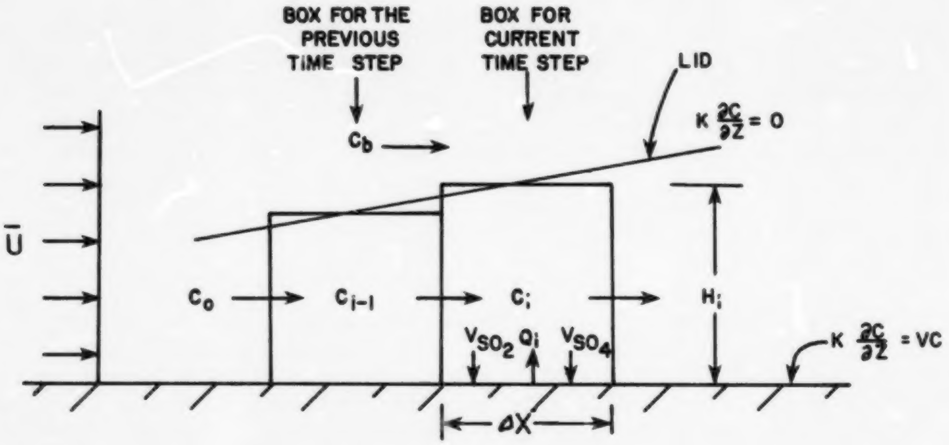

BOX FOR THE PREVIOUS TIME STEP
BOX FOR CURRENT TIME STEP
LID
$K \frac{\partial C}{\partial Z} = 0$
C_b
$\bar{U}$
C_o
C_{i-1}
C_i
H_i
V_{SO_2}
Q_i
V_{SO_4}
$K \frac{\partial C}{\partial Z} = VC$
ΔX

Figure 13. Schematic of the box model.

and for $SO_4^=$

$$C_{2,j} = (1 - H_{j-1}/H_j)C_{2,b} + (H_{j-1}/H_j)C_{2,j-1} + 3/2\, C_{1,j-1} [(v_1 - v_2/H_jk) + 1]^{-1} \exp[-(v_1/H_j + k)]\Delta t \; . \qquad (8)$$

Equations (7) and (8) are simple algebraic equations, which are Lagrangian in nature and allow for varying mixing height and sources along the trajectory. Again, the dilution term for crosswind spread has been neglected in this formulation; the solution process proceeds simply by solving Equation (7) for the J box SO_2 concentration and then using this concentration in Equation (8). This solution procedure is repeated as "boxes" are stacked end-to-end along the trajectory.

Eulerian Model--

Equation (2) could be solved (as is) with implicit finite-difference techniques since they demand nothing about the flow or diffusion situation. Unfortunately, if assumptions are not imposed, such procedures make significant demands on computer resources and knowledge of boundary conditions (Crawford 1977). If the same assumptions used to obtain Equations (7) and (8) are imposed, except that $X \neq Ut$, the following Eulerian finite-difference model is obtained:

$$C_{1,j} = \frac{(1/\Delta t)C^{o}_{1,j} + U/\Delta x(1-H_{j-1}/H_j)C_{1,b} + H_{j-1}/H_j C_{1,j-1}}{[1/\Delta t + U/\Delta x + v_1/H_j + k]} \quad ; \qquad (9)$$

$$C_{2,j} = \frac{(1/\Delta t)C^{o}_{2,j} + U/\Delta x(1-H_{j-1}/H_j)C_{2,b} + H_{j-1}/H_j C_2 + 2/3\ kC_{1,j}}{[1/\Delta t + U/\Delta x + v_2/H_j]} \ . \qquad (10)$$

Equations (9) and (10) are similar to the previous box model, and $C^{o}_{1,j}$ and $C^{o}_{2,j}$ are the box concentrations of SO_2 and $SO_4^{=}$ at the previous time step.

Lagrangian finite-difference equations similar to Equations (7) and (8) can also be obtained:

$$C_{1,j} = \frac{2/\Delta t\ [(1-H_{j-1}/H_j)C_{1,b} + H_{j-1}/H_j C_{1,j}]}{[2/\Delta t + v_1/H_j + k]} + Q_j/(UH_j) \quad ; \qquad (11)$$

$$C_{2,j} = \frac{2/\Delta t\ [(1-H_{j-1}/H_j)C_{2,b} + H_{j-1}/H_j C_{2,j}] + 2/3\ kC_{1,j}}{[2/\Delta t + v_2/H_j]} \ . \qquad (12)$$

These finite-difference equations follow the analytic ones remarkably well. For example, Equations (11) and (7) agree within a few percent for a time step of 1 h for typical values of model parameters. But for Lagrangian modeling, the truly analytic Equations (5) and (6) or (7) and (8) are preferred because they are exact within model assumptions and functionally tell more about the transport process. Figure 14 compares the boundary conditions required and solution region obtained with Lagrangian vs Eulerian models. As can be seen, the Lagrangian model requires much less input information, but also yields less predictive information.

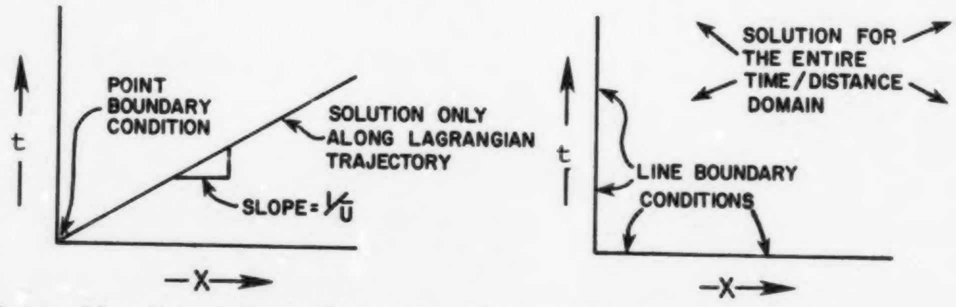
t
POINT BOUNDARY CONDITION
SOLUTION ONLY ALONG LAGRANGIAN TRAJECTORY
SLOPE = 1/U
—X→
t
SOLUTION FOR THE ENTIRE TIME/DISTANCE DOMAIN
LINE BOUNDARY CONDITIONS
—X→

Figure 14. Comparison of Lagrangian and Eulerian boundary conditions and solution domains.

Model Analysis

A sensitivity analysis of Equations (5) and (6) is useful because it reveals the functional behavior of the model relative to its various parameters and the theoretical behavior of the transport, transformation, and deposition processes insofar as they are properly described by the assumptions made to derive the model. In Equations (5) and (6), t (or $x\ U^{-1}$) is the independent variable, and H, V_1, V_2, and k, along with the initial conditions C_1^o and C_2^o, control the model response, C_1 and C_2. Following the usual approach to sensitivity analysis, we varied each of the four parameters and two initial conditions independently over a range of possible values, centered about their normal values, while the other parameters and initial conditions were held fixed at their nominal values. The effect on model response with $B_o/B = 1$ is presented in Table 4 and Figures 15 and 16. For these results, typical midday parameter values were used: H = 1500 m, $v_1 = 1\ cms^{-1}$; $v_2 = 0.1\ cms^{-1}$; and $k = 5.6 \times 10^{-6}\ s^{-1}$ (2 percent per hour). Table 4 shows the effect of a 50 percent change from the nominal value of each parameter.

TABLE 4. PERCENT VARIATION IN MODEL RESPONSE RESULTING FROM A ±50 PERCENT CHANGE IN A SINGLE PARAMETER

Model parameter	Typical value	Relative response (%) due to parameter variation: Plus 50% C_1	Plus 50% C_2	Minus 50% C_1	Minus 50% C_2
k	2% h	-21	+36	+27	-45
v_1	$1\ cm\ s^{-1}$	-25	-11	+33	+13
v_2	$0.1\ cm\ s^{-1}$	-	-2	-	+2
H	1500 m	+23	+10	-44	-23

Figure 15 illustrates the effect of transport time on model response. The C_1/C_1^o curve is exponential and is characterized by a time constant of $[(v_1/H) + k]^{-1}$. For typical midday parameter values, dry deposition of SO_2 is slightly more important than transformation of SO_2 to $SO_4^=$. These processes together imply a half-life for SO_2 of about 16 h.

On the other hand, the C_2/C_1^o curve of Figure 15 is not exponential. In fact, for $B_o/B = 1$, C_2/C_1^o reaches a maximum value at

$$t_* = t_o + \ln\ [(v_1 + kH)/v_2]/\{[(v_1 - v_2)/H] + k\}, \qquad (13)$$

or about three days for typical parameter values. For Figure 15, we assumed no initial sulfate (i.e., $C_2^o = 0$) and that $t_o = 0$. Beyond $t = t^*$, C_2/C_1^o decays more slowly--approximately exponentially at a rate

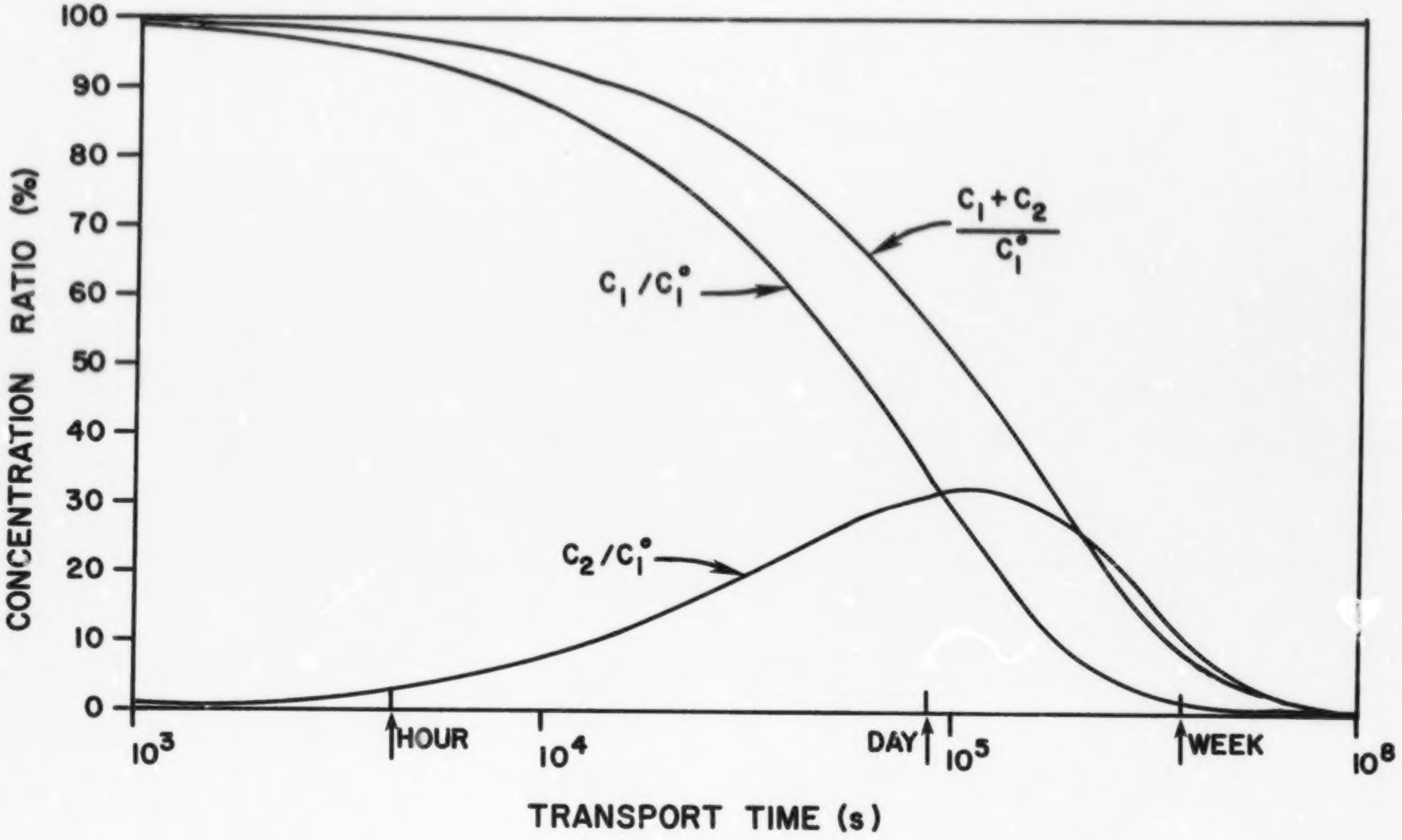

Figure 15. Predicted variation in SO_2 and $SO_4^=$ concentrations as a function of transport time.

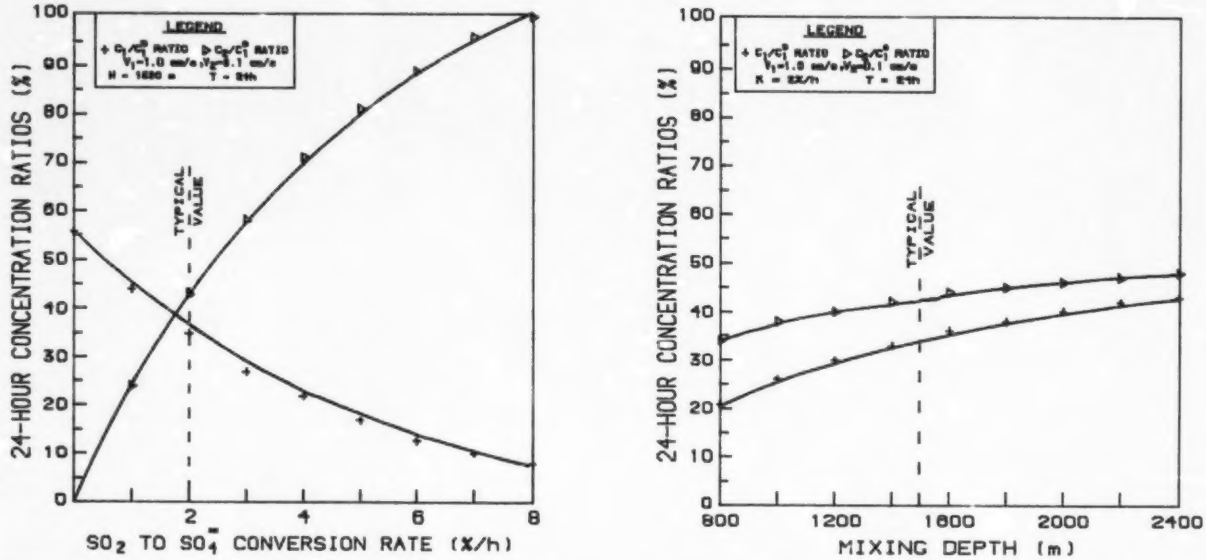

a) EFFECT OF VARIATIONS OF K, THE REACTION RATE CONSTANT, ON SO_2 AND $SO_4^=$ CONCENTRATIONS

b) EFFECT OF VARIATIONS OF H, THE MIXING DEPTH, ON SO_2 AND $SO_4^=$ CONCENTRATIONS

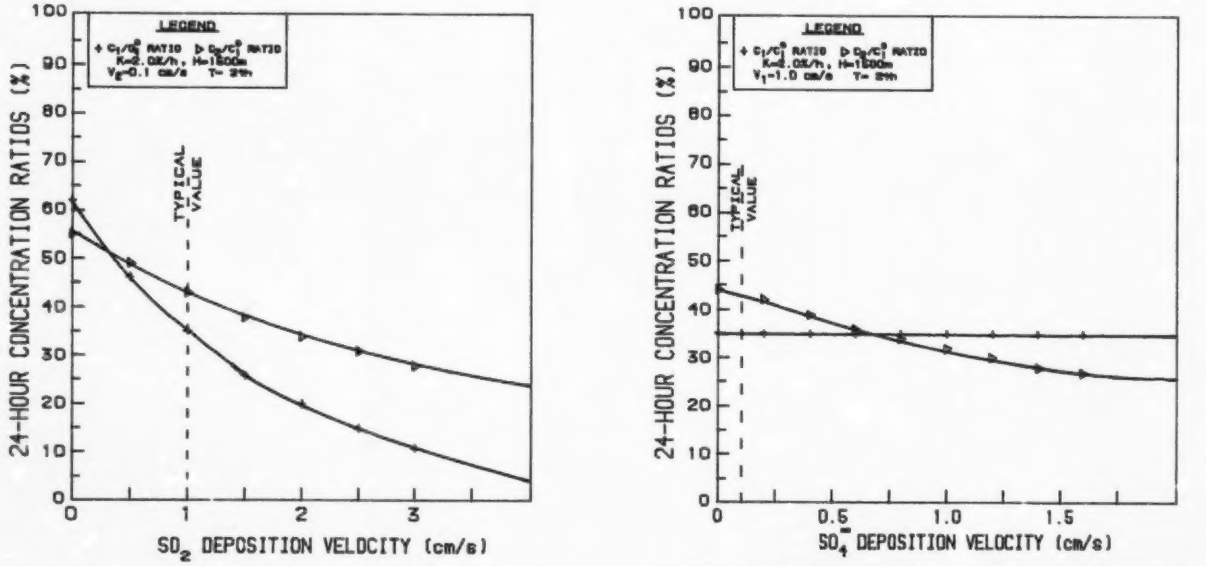

c) EFFECT OF VARIATIONS OF V_1, SO_2 DEPOSITION VELOCITY, ON SO_2 AND $SO_4^=$ CONCENTRATIONS

d) EFFECT OF VARIATIONS OF V_2, $SO_4^=$ DEPOSITION VELOCITY, ON SO_2 AND $SO_4^=$ CONCENTRATIONS

Figure 16. Effect of variations in model parameters on predicted response after 24 h of transport.

characterized by a half-life, due to dry deposition, of around 12 days. Therefore, as shown in the meteorological characterization subsection, precipitation occurs frequently enough to indicate that wet-sulfate removal processes are probably dominant.

Without wet removal, the model confirms that long-range transport over great distance is possible. Because C_2/C_1 is unique for each value of t, the average age of an airmass passing the outflow plane can be computed when this ratio is known. Assuming $C_2^o = 0$, the age is

$$t_a = \frac{\ln[1 + 2/3\{[(v_1 - v_2)/Hk] + 1\}(C_2/C_1)]}{[(v_1 - v_2)/H] + k} = t_o \ . \qquad (14)$$

Figure 16 illustrates the effect of individual parameter variation on model response after 24 h of transport. This figure shows that k and v_1 have the greatest control over response and v_2 has the least. The figure also shows that increases in either H or k will increase the C_2/C_1^o ratio.

Finally, the form of any of the models presented is such that the effect of a single phenomenon cannot be separated or therefore estimated. For example, the simplified form of Equation (5) is $C/C_o = \exp\{(-v_1/H + k)\,t\}$. It is apparent (based on the present best guess at the parameters v_1 and k) that the effect of deposition is equivalent in magnitude, direction, and form to that of chemical transformation. The sulfate equations are even more transcendental in nature. This illustrates the need for physical understanding and study of separate deposition and transformation phenomena. Comparisons with data are presented in Section 4.

In summary, the model predicts that airborne SO_2 decays exponentially with transport time. Its half-life of about 16 h results from the nearly equal effects of removal by dry deposition and transformation to $SO_4^=$. The decay rate is only a mild function of mixing height. The model also shows that $SO_4^=$, aside from the initial presence of $SO_4^=$ concentrations increases until it reaches a maximum after about three days of transport, after which it decays almost exponentially. The model indicates that $SO_4^=$ is most sensitive to changes in the transformation rate of SO_2 to $SO_4^=$. It is relatively insensitive to changes in mixing height or deposition rates.

SECTION 4

RESULTS AND DISCUSSIONS

SULFATE CONCENTRATION AND FLUX CLIMATOLOGY

Although the regional field studies supplied unique and informative field data, these data are limited to only a few specific spring and summer days. Long-term climatological data do not suffer from this deficiency, and much can be learned from variations in and interrelationships between aerometric and meteorological parameters.

Seasonal Concentration Variations

The seasonal fluctuation of a pollutant is usually the most prominent feature of a long-term data set. The analysis of four years of sixth-day suspended sulfate data taken from the five rural Tennessee Valley monitoring sites (Figure 17) reveals the strongly seasonal configuration shown in Figure 18. Suspended sulfate concentrations are lowest in the winter, highest in the summer, and intermediate in the spring and fall. The mean summer concentration of 10.4 $\mu g\ m^{-3}$ is more than double the mean winter concentration of 4.5 $\mu g\ m^{-3}$. This pattern of summer suspended sulfate maxima is consistent with the observations found in other sulfate research conducted in the eastern United States and Canada (Garvey 1975; Hitchcock 1976; ERT 1976; Lioy et al. 1977; Tony and Batchelder 1978; and Melo 1978).

Although the seasonal patterns found in these studies are similar, significant differences in magnitude do exist, with the highest sulfate levels occurring at urban sites in the northeastern United States (Altshuller 1973; Frank 1974; ERT 1976).

Many factors may be related to the seasonal pattern of suspended sulfate values. These factors fall into three major categories--emissions, transformation, and transport-related phenomena.

The anthropogenic contribution to sulfur in the atmosphere is well quantified, particularly in the industrialized regions of the world. In the past, the release of anthropogenic sulfur from these regions was strongly seasonal--high emissions in the winter when much fossil fuel (particularly coal) was used for space heating and low emissions in the summer months when space heating was not required. However, the advent of cleaner fuels, such as natural gas and low-sulfur coal, for space heating and industrial processes and the promulgation of strict air quality regulations resulted in an overall reduction in total sulfur emissions per kilowatt. During this same period, however, total sulfur emissions were not reduced, primarily because of the increased demand for fossil-fuel-generated electrical power. Across the country and particularly in the Tennessee Valley, coal-fired generating units provide the main source of electrical power. These units provide base load generating capacity, and although peak demands occur in heating and cooling seasons, the relative seasonal variation in the rate of sulfur emissions can explain only a small percentage of the

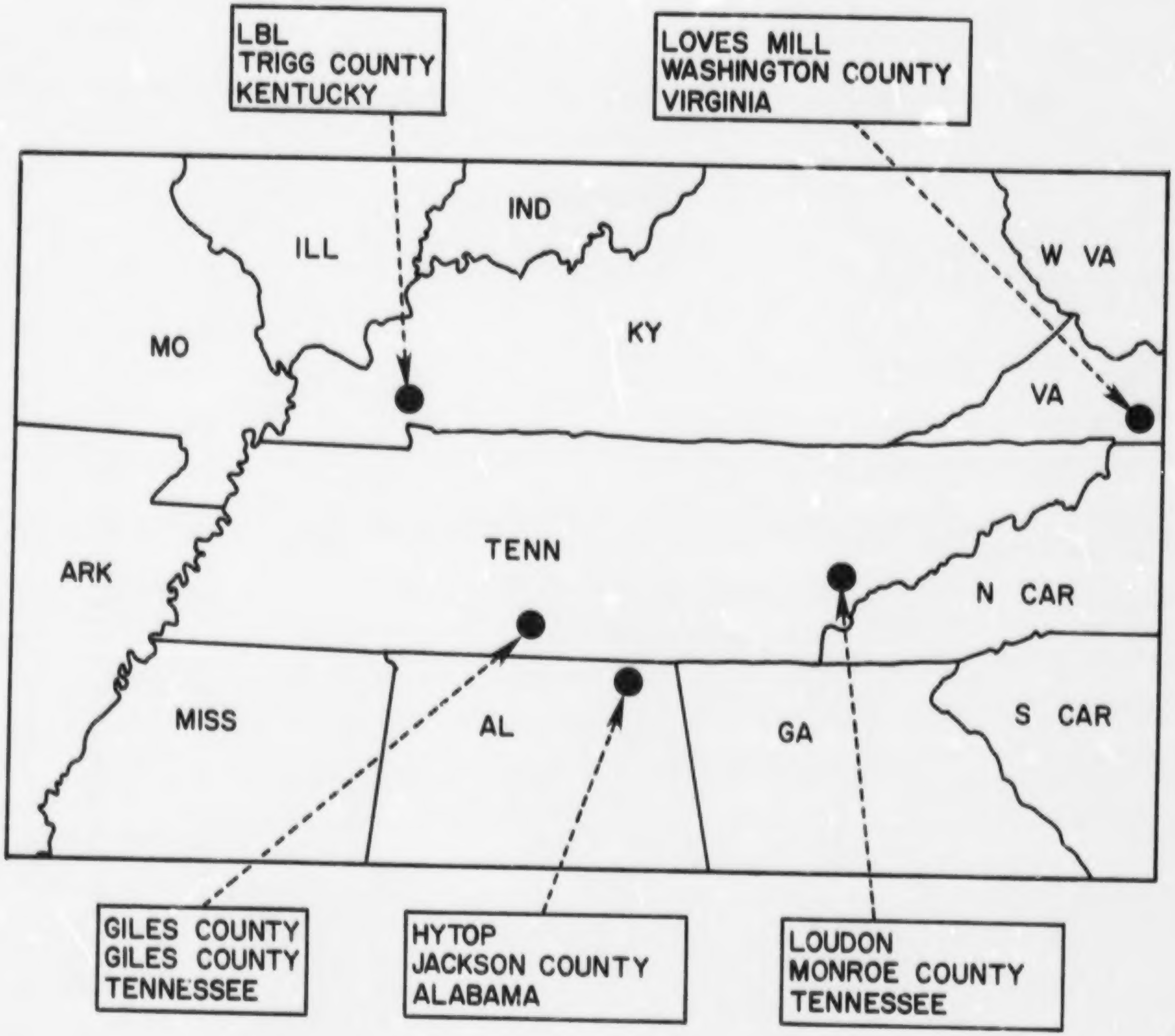
LBL
TRIGG COUNTY
KENTUCKY
LOVES MILL
WASHINGTON COUNTY
VIRGINIA
MO
ILL
IND
KY
W VA
VA
ARK
TENN
N CAR
MISS
AL
GA
S CAR
GILES COUNTY
GILES COUNTY
TENNESSEE
HYTOP
JACKSON COUNTY
ALABAMA
LOUDON
MONROE COUNTY
TENNESSEE

Figure 17. Regional air quality trend stations.

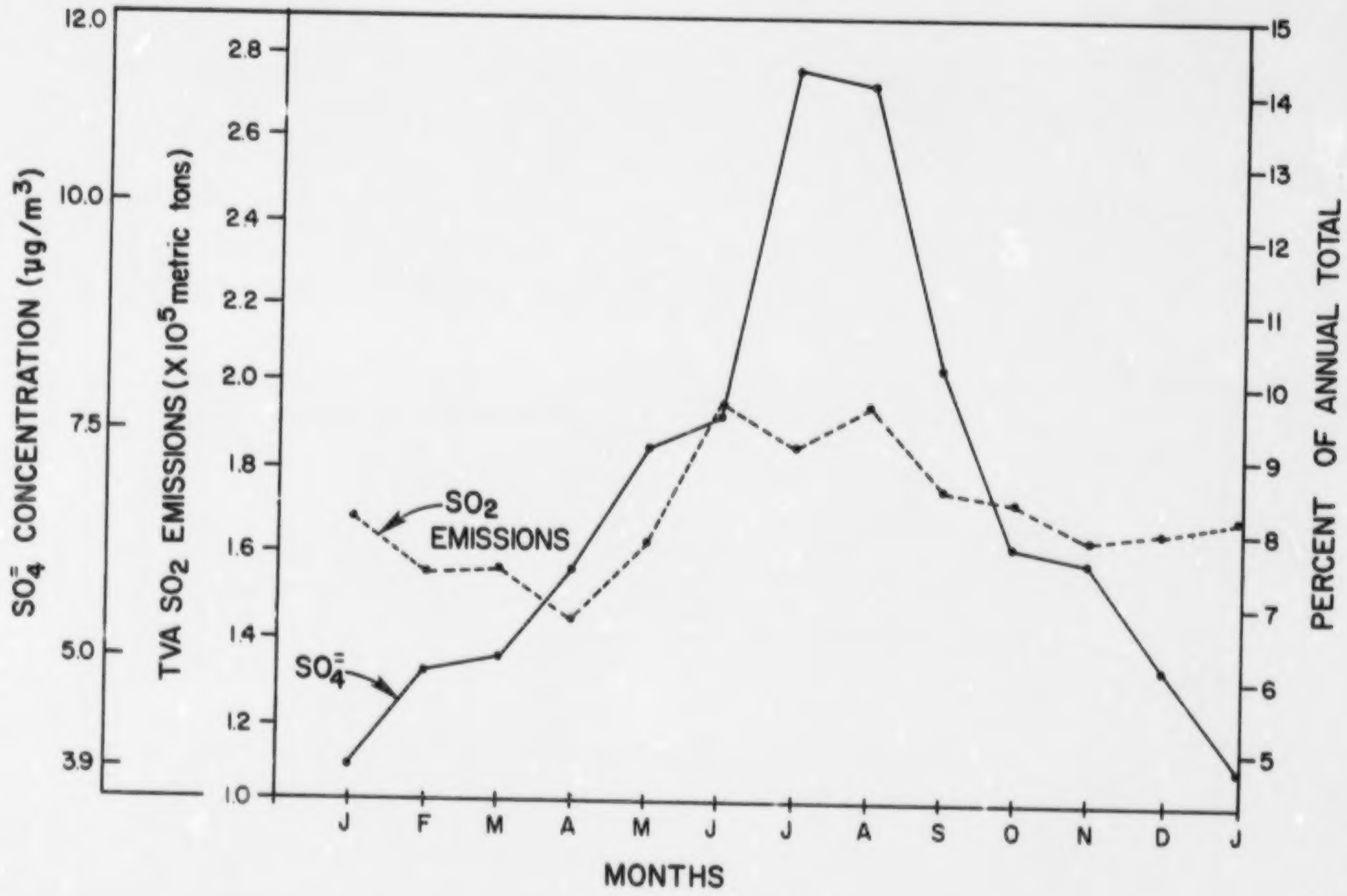

Figure 18. Monthly variations of TVA's SO_2 emissions and regional sulfate concentrations, 1974-1977.

seasonal sulfate variation (Figure 18). Therefore, anthropogenic sulfur emissions are not significantly related to the seasonal pattern of suspended sulfates in the Tennessee Valley region.

The natural contribution of sulfur to the atmosphere is not well quantified. Several researchers (e.g., Robinson and Robins 1972; Lovelock et al. 1972; Friend 1973; Hitchcock 1975) have estimated natural emissions on a global scale, but little additional information exists.

Biological emissions of atmospheric sulfur, thought to be mostly hydrogen sulfide (H_2S), are undoubtedly related to seasonal fluctuations in temperature. Biological activity and emissions of H_2S are greater with increasing temperature. This source of emissions may be partly responsible for the seasonal sulfate pattern--particularly in the TREATS region, where typical summertime southwesterly transport allows sulfur input from the potentially large natural sulfur-producing regions of low-lying marshes and swamps found in east Texas, Louisiana, and Mississippi. Natural sulfur sources and their contribution to regional airsheds are of paramount concern.

Various transformation processes and their respective rates may also be partly responsible for the high summer levels of suspended sulfate. The conversion rate for SO_2 to $SO_4^=$ is greater in the summer (about 1.4 percent per hour) than in the winter (about 0.3 percent per hour) (Meagher 1977). The increase in summer conversion rate is believed to result from increased photochemical activity. The difference in conversion rates and the relative deposition velocities of SO_2 (1 cm s^{-1}) and $SO_4^=$ (0.1 to 0.5 cm s^{-1}) indicates that high summer sulfate levels result at least partly from seasonal variations in transformation processes.

High sulfate concentrations are usually associated with stagnating anticyclonic airmasses (ERT 1976; Teknekron 1977). Within the TREATS region these stagnating conditions are more prevalent in the summer and fall months than in the other seasons (Korshover 1976). Of either continental or maritime origin, these conditions are associated with high temperature, humidity, and insolation and with low precipitation and ventilation. Meteorological factors present in these airmasses seem to provide optimal conditions for both sulfate generation and its atmospheric buildup. Some airmass characteristics are thus related to optimization of the transformation process (i.e., high temperature, insolation, and humidity), whereas others relate to concentration of the end product (i.e., low precipitation and poor ventilation). The strong frontal activity associated with the winter months exhibits contrary factors, which result in less transformation and concentration buildup.

In summary, the factors resulting in the seasonal summer sulfate concentration maxima may be relegated to three major categories: (1) increased natural and anthropogenic emissions; (2) enhanced gaseous sulfur to particulate sulfate transformation; and (3) poor transport conditions, resulting in atmospheric sulfate buildup.

Regional Sulfate Flux Rose

To better describe the flux of sulfate pollution through the TREATS region and the significant variables that influence it, a sulfate trajectory climatology analysis is presented. This analysis summarizes three years of sulfate flux data, gathered every sixth day beginning on January 4, 1976. It incorporates (1) sulfate data obtained from three TVA high-volume sampler sites centered around Nashville, Tennessee; (2) boundary-layer meteorologic parameters obtained from the NWS site at Nashville, Tennessee; and (3) synoptic weather typing (as described in the Meteorological Characterization subsection of Section 3). These parameters have been analyzed seasonally and annually. Correlations between and among variables are described, and significant findings are discussed.

The sulfate concentration numbers used are the averages from three TVA monitoring locations--Cumberland and Gallatin Steam Plants and Giles County trend station--that surround Nashville, Tennessee. A logical question is whether the proximity of the power plants to the high-volume samplers leads to spurious sulfate readings. However, as described in more detail in the Eulerian Space and Time subsection of Section 4, the sulfate measurements obtained at the plants are thought to be representative of regional levels. Also, a plot (Figure 19) of the concentration values from the Giles County trend station vs. the average of all the sites supports this conclusion. Figure 19 shows a slope of near one and a high correlation coefficient.

The meteorological parameters include average wind velocity and dewpoint temperature through the first 1500 m AGL averaged from twice daily NWS radiosondes. Also included are the weather typing parameters as described in the Meteorological Characterization subsection, Section 3. Analysis of the data (Figures 20 and 21) graphically shows that the southwest sector dominates as the favored sector for mass transport through the Tennessee Valley region. The dominance of this sector for transport is also supported by the trajectory and meteorological analyses presented earlier. An analysis of 24-h back-trajectory data shows that the favored source origination region for this southwesterly flow sector is located in southern Louisiana and Mississippi. Implications of this region as a potentially major biogenic source region are discussed in the Lagrangian flux analysis subsection.

The relative distribution of the range of aerometric and meteorological variables within sectors is also of interest. The frequency of occurrences of a given parameter by sector have been divided into three ranges.

Intercomparisons between sectors show the relative importance of each in producing elevated pollutant and wind speed levels. Due to a limited data base, the individual 22.5-degree sectors have been grouped into 90-degree sectors for analysis purposes. Even when this is done, the southeast sector still has insufficient data (8 observations) for inclusion in the analysis. The results of these annual relative frequency distributions are shown in Figure 22.

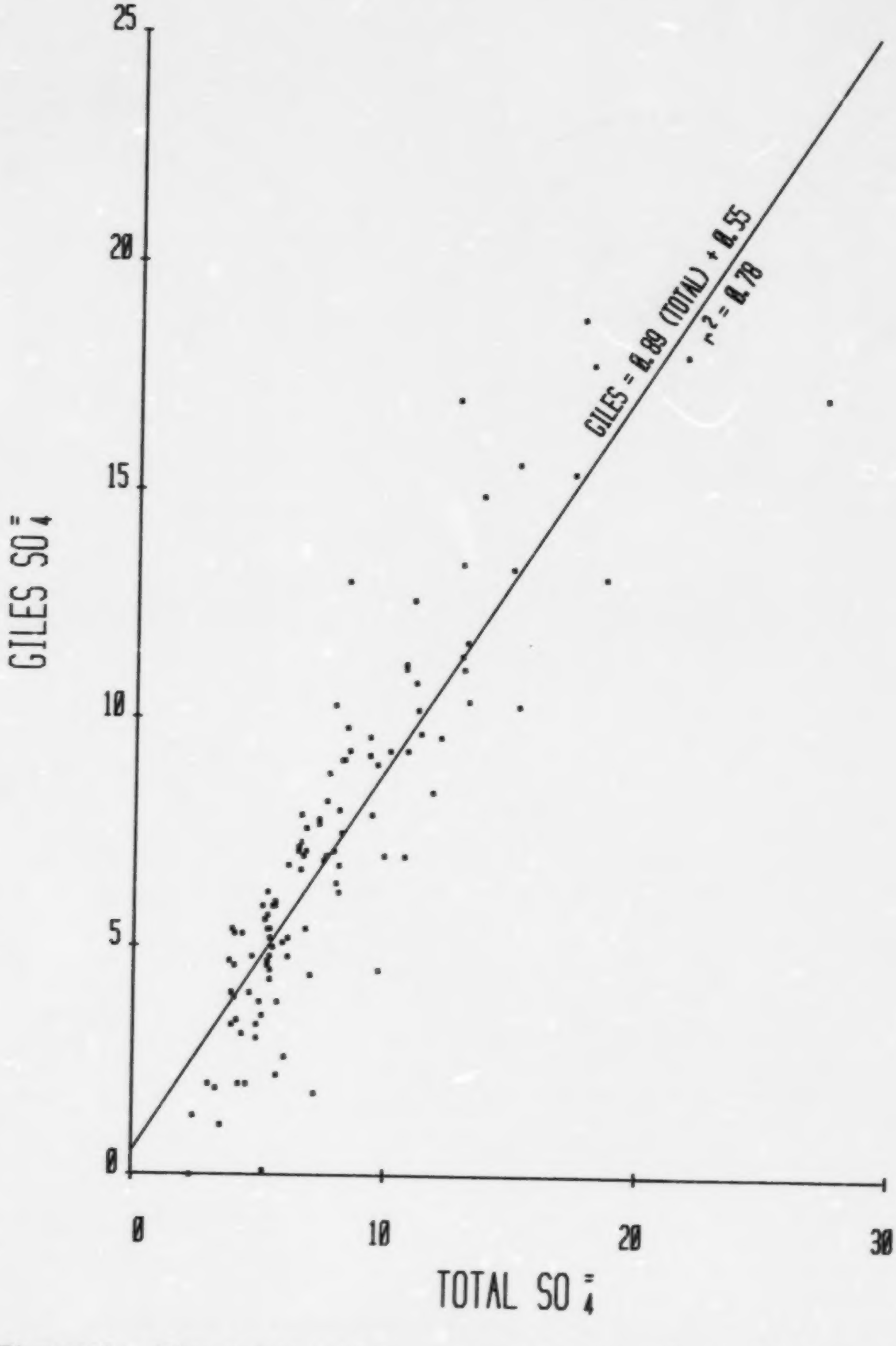

Figure 19. Giles County sulfate concentration (μg m^{-3}) vs. the average concentration of Cumberland, Gallatin, and Giles.

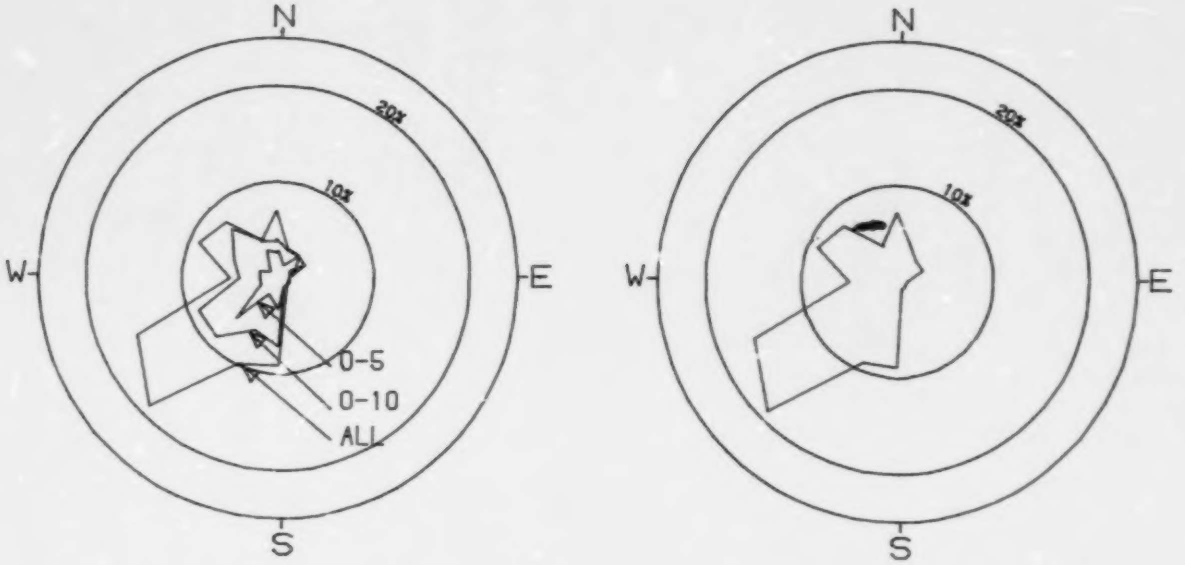

(A) WIND SPEED (m/s)

(C) WIND DIRECTION (degrees)

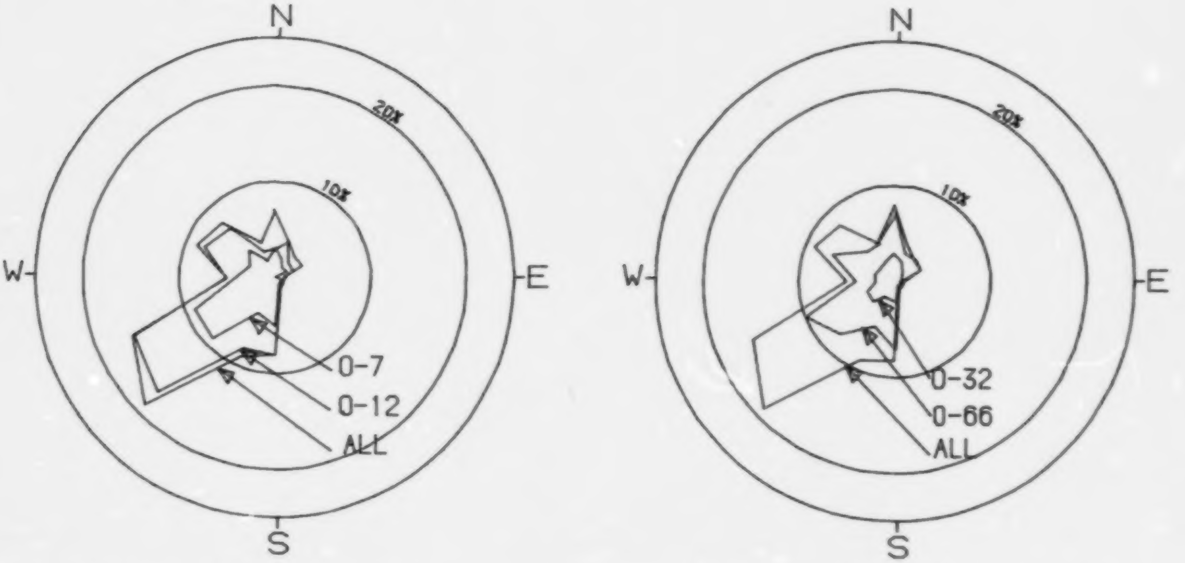

(B) SULFATE CONCENTRATION (µg/m^3)

(D) SULFATE FLUX (µg m^{-2} s^{-1})

Figure 20. Annual frequency distributions of wind speed, wind direction, sulfate concentration, and sulfate flux for Nashville, Tennessee.

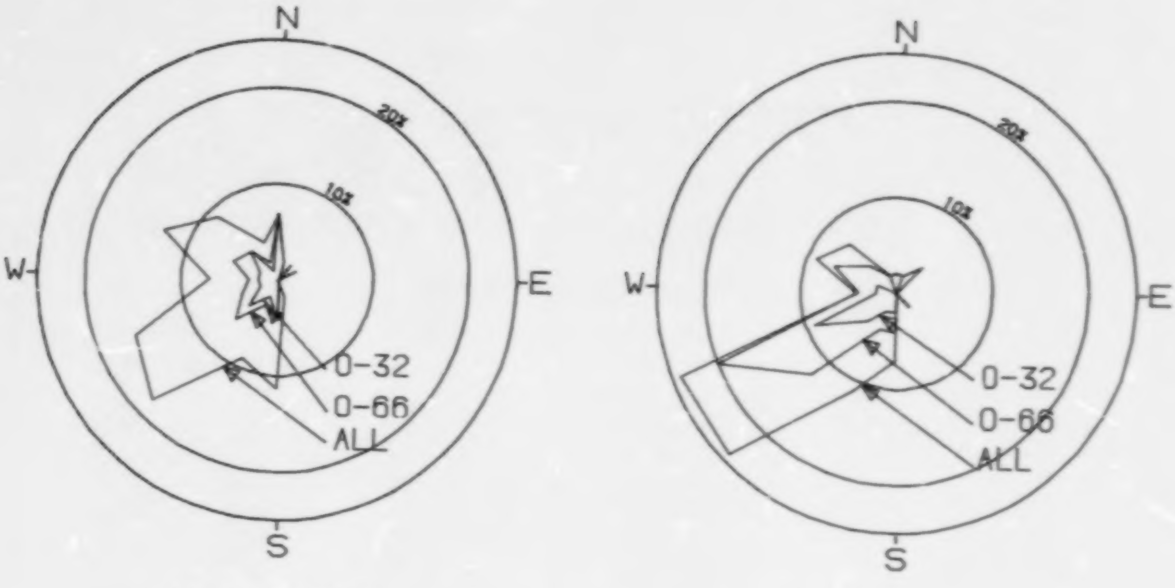

(A) WINTER

(B) SPRING

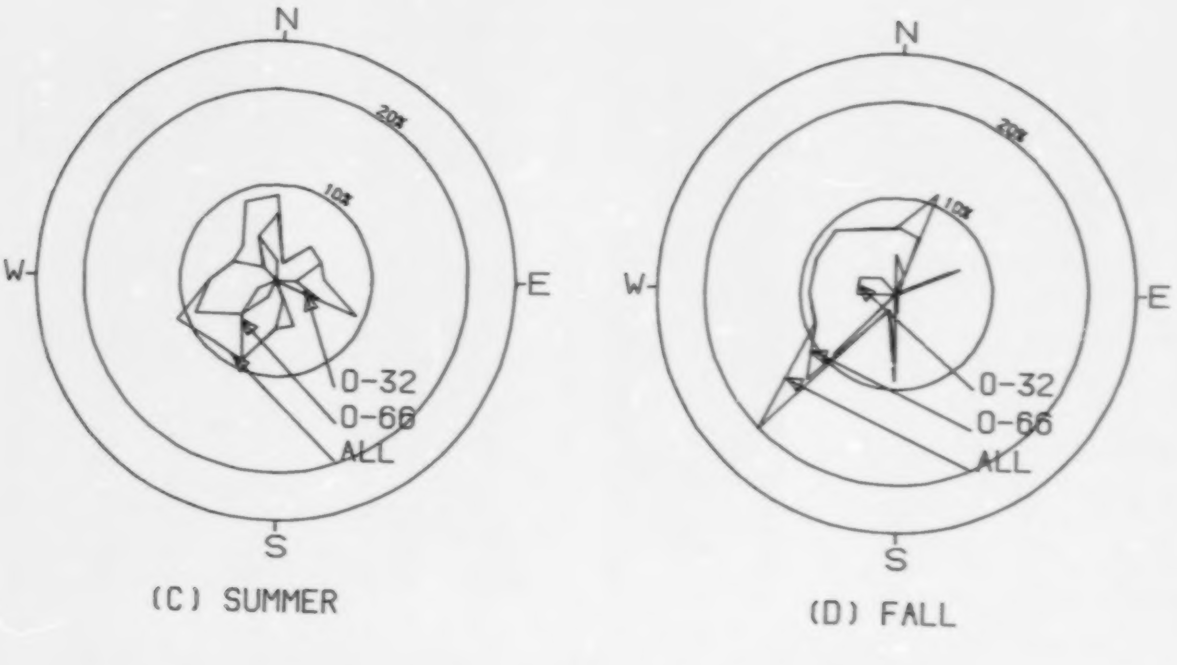

(C) SUMMER

(D) FALL

Figure 21. Seasonal frequency distributions of Nashville sulfate flux ($\mu g\ m^{-2}\ s^{-1}$).

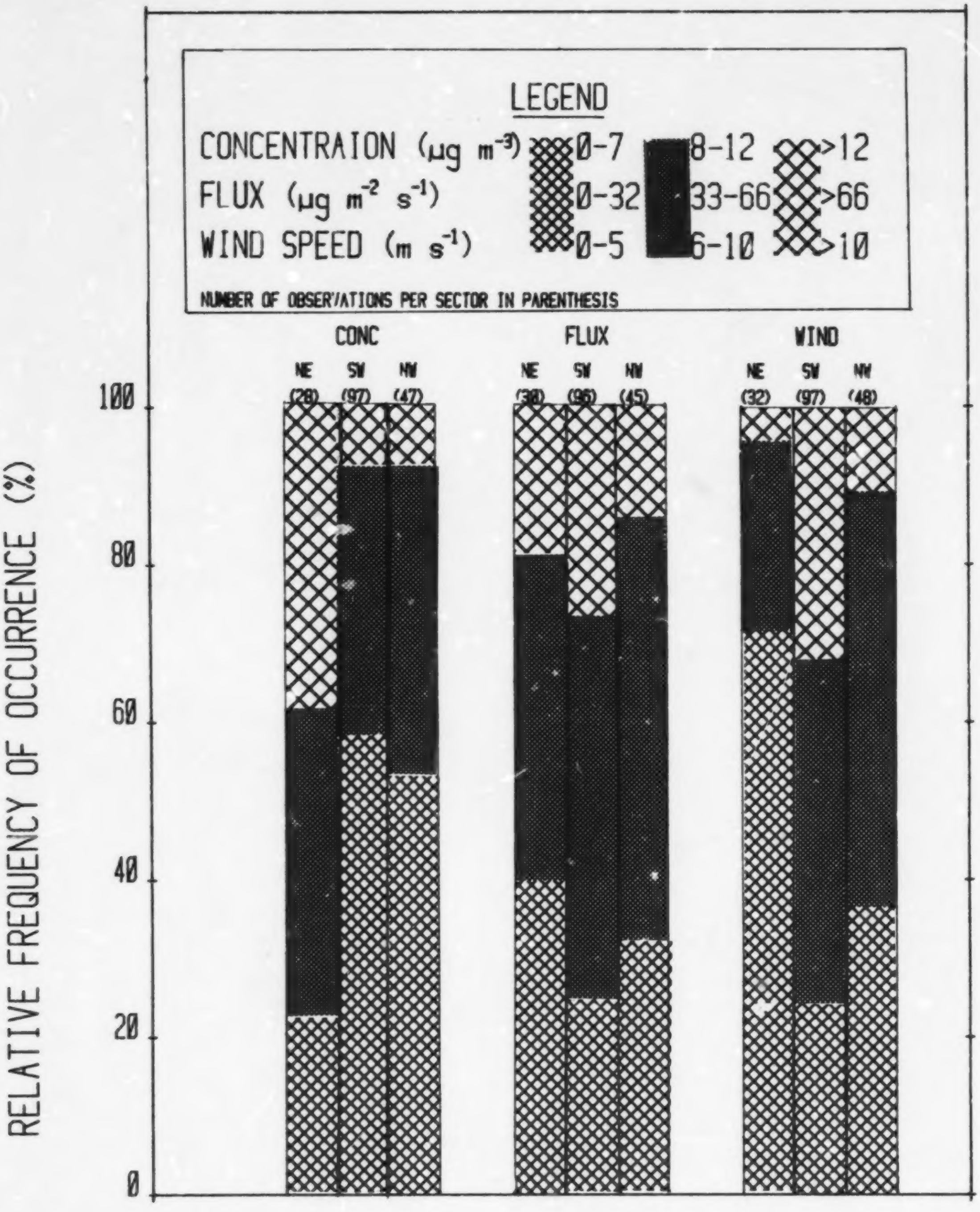

Figure 22. Relative frequency distributions.

An analysis of the data presented in Figure 22 shows that, although most sulfate is transported into the Valley from the southwest, the greatest concentration maxima occur with northeasterly flow. Reisinger and Crawford (1979) have shown that this trend can result from the transport of modified continental polar air from the high emission density region along the Ohio River valley into the study area. Also, the southwest and northwest sectors have almost identical concentration distributions, probably indicating a lesser, more diffuse source region than is associated with northeasterly flow. As will be shown subsequently, aircraft data from the two field studies also support this analysis.

The relative annual flux distribution by sector is also shown in Figure 22. Contrary to the concentration analysis, this figure indicates that the cumulative flux distribution shown in Figure 20 is a good indicator for the relative magnitude of flux by sector. An analysis of the relative flux distribution shows that, within the southwest sector, flux values are greater than 66 μg m^{-2} s^{-1} on 30 percent of the days. This is almost twice the relative occurrence of the other two sectors analyzed. Naturally, since pollutant flux is inherently tied to wind speed, the close similarity between the relative flux plot and the wind speed plot shown in Figure 22 is not surprising. Also, the wind speed plot is well correlated with the other pollutant frequency distributions, especially for the southwest sector.

An analysis of the seasonal variation in both flux and concentration, regardless of sector, is shown in Table 5.

TABLE 5. MEDIAN SULFATE FLUX AND CONCENTRATION VALUES REGARDLESS OF SECTOR

Season	Flux (μg m^{-2} s^{-1})	Concentration (μg m^{-3})
Winter	42	5
Spring	50	6
Summer	44	11
Fall	38	7

This table shows that sulfate flux peaks during the spring, whereas sulfate concentration peaks during the summer. Variations in these variables depend at least partly on variations in airmass type, wind velocity, solar radiation, and biogenic and anthropogenic emission. In an attempt to determine the relative importance of one of these parameters, airmass type, a joint frequency distribution analysis was performed. This analysis indicates that concentration and flux levels differ only slightly when the airmass type is either maritime tropical or modified continental polar. However, when modified maritime polar airmasses are present, high pollutant levels rarely occur. This, no doubt, results partly from low natural and man-made sulfur emission rates in the upwind areas of the Great Plains. Analysis of the relationship between high sulfate flux levels and meteorological characteristics indicates that the highest sulfate flux values ($\geq 100\ \mu g\ m^{-2}\ s^{-1}$) occur during southwesterly flow of maritime tropical air. This flow occurs, almost exclusively, in response to gradients related to prefrontal or Bermuda high pressure patterns.

FLUX CALCULATIONS

Measurements of regional mass transport (or flux) of a pollutant are very useful for assessing not only the impact of the studied area on itself and adjacent regions, but also the impact of adjacent regions on the studied region. Ideally, pollutant flux can be defined at any location, but measurements at inflow and outflow locations relative to the study region are the most informative. An inflow measurement defines the impact of an upwind region on the study area, whereas an outflow measurement defines the combined impact of the upwind and study regions on the downwind region. The net impact of a studied area on a downwind region is defined by differences in these measurements (i.e., outflow minus inflow). This difference, when complemented with meteorological and source information, is also useful in studying characteristics and mechanisms of the long-range transport phenomenon.

Few researchers have attempted regional flux measurements because of the measurement difficulties imposed by the large space and time scales. This section presents the methods and results of two modest field studies that attempted such measurements within the Tennessee Valley region. Our intent is not that these measurements be considered exact (no measurement is), but that they are reasonable estimates from which several significant conclusions can be made.

Estimating Concentration and Flux

The variable that describes net pollutant mass transport is pollutant flux. Pollutant flux can be defined at a point, over a line, or through a plane. The appropriate method for assessing regional impact is the pollutant flux through a plane. This is defined as

$$F_i(x,t) = \iint C_i U dy dz/(H \cdot L), \tag{15}$$

where

C_i = concentration of pollutant species i,
U = transporting wind speed (ideally normal to the measurement plane),
H = height of the plane,
L = length of the plane,
F_i = transported mass of pollutant species i per unit area per unit time.

Unfortunately, Equation (15) is impossible to evaluate rigorously because C_i and U vary, not only as a complex unknown function of position coordinates x, y, and z, but also as a function of time t. Therefore, assumptions must be made about the spatial and temporal variations of C_i and U.

By assuming that variation in time is "slow" compared with the time scale required for the measurement (about 2 h) and the horizontal inhomogeneity can be integrated out by long horizontal sampling traverses (about 150 km), then Equation (15) can be approximated as

$$F_i \cong \frac{1}{H}\left[\bar{C}_R\bar{U}_R H_R + \bar{C}_S\bar{U}_S\,(H_S - H_R) + \bar{C}_B\bar{U}_S\,(H_{max} - H_S)\right], \qquad (16)$$

where

H = average mixing height for all study days, 1600 m,

$\bar{C}_R$ = average concentration through H_R,

$\bar{U}_R$ = average wind speed through H_R,

H_R = height of radiation inversion,

$\bar{C}_S$ = average concentration from H_R to H_S,

$\bar{U}_S$ = average wind speed from H_R to H_S,

H_S = height of subsidence inversion,

$\bar{C}_B$ = background concentration for $SO_4^=$ and total sulfur, 0.8 μg m ^{3} and 20 μg m ^{3}, respectively,

H_{max} = daily maximum mixing height.

A typical illustration of how these fluxes were piecewise integrated is presented in Figure 23. For early morning measurements, F_i was approximated by the sum of three parts: (1) within the morning radiation inversion; (2) between the radiation and subsidence inversions; and (3) between the morning subsidence height and H_{max}. Thus, on days when H_S was less than the afternoon's maximum mixing height (H_{max}), a correction for $\bar{C}_B$ (the above subsidence inversion mean concentrations) from H_S to H_{max} was used in the F_i approximation. Values of $\bar{C}_B$ for SO_2 and $SO_4^=$ were obtained by averaging the limited number of actual measurements made above the subsidence inversions with the 10 percentile values determined from an analysis of all measurements made by the two aircraft. This correction allows for mass conservation when comparing mass flux during the diurnal cycle and is especially important when comparing early morning to midday measurements. When the morning subsidence inversion height is greater than the afternoon mixing height, mass concentration is assumed to result from meteorological subsidence of superior air. Thus, no corrections are made under these conditions. Also, so that intercomparison between days can be made, the sulfur flux values for all days have been normalized to the grand mean subsidence inversion height measured on all field study

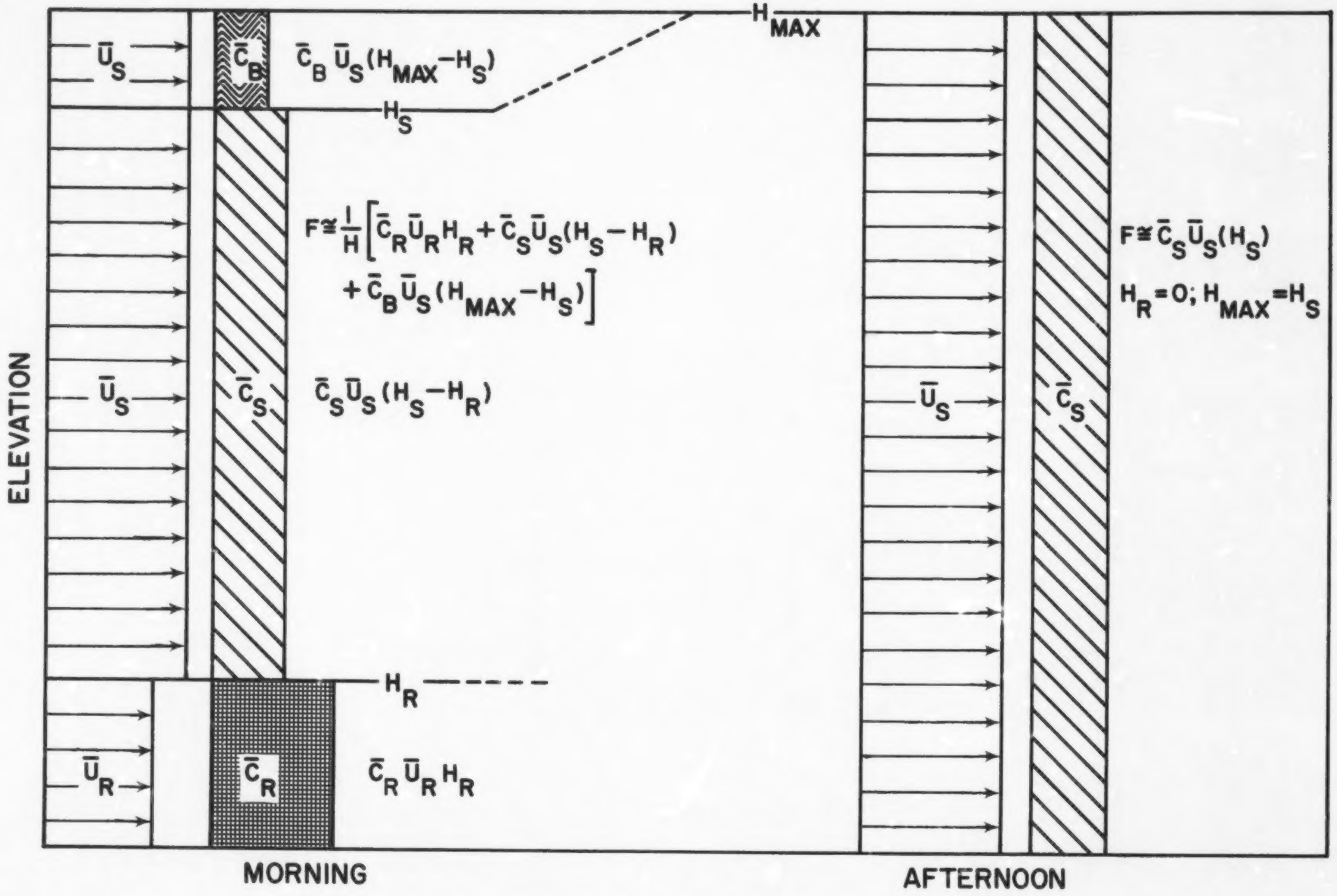
H_{MAX}
$\bar{U}_S$
$\bar{C}_B$
$\bar{C}_B \bar{U}_S (H_{MAX} - H_S)$
H_S
$F \cong \frac{1}{H}\left[\bar{C}_R \bar{U}_R H_R + \bar{C}_S \bar{U}_S (H_S - H_R) + \bar{C}_B \bar{U}_S (H_{MAX} - H_S)\right]$
ELEVATION
$\bar{U}_S$
$\bar{C}_S$
$\bar{C}_S \bar{U}_S (H_S - H_R)$
H_R
$\bar{U}_R$
$\bar{C}_R$
$\bar{C}_R \bar{U}_R H_R$
MORNING
$\bar{U}_S$
$\bar{C}_S$
$F \cong \bar{C}_S \bar{U}_S (H_S)$
$H_R = 0; H_{MAX} = H_S$
AFTERNOON

Figure 23. Schematic of typical flux calculation procedure.

sampling days, H (1600 m). In the following subsections, the methods of approximating the variables listed in Equation (16) are discussed.

Estimating $\bar{U}$, H_R, and H_S--

Any accurate calculation of mass flux inherently depends on a good estimate of wind speed. In like manner, an accurate estimate of the mass balance depends on a good estimate of mixing height. For both the 1976 and 1977 studies, the TVA and NWS upper-air stations closest to and most representative of the airmass sampled were used to estimate actual mixing height and resultant wind speeds. These stations and their representative wind speed and mixing height values for the Eulerian and Lagrangian days are listed in Appendix C. H_R was simply defined as any surface-based inversion with $\partial T/\partial z \geq 0$. To determine the best estimate of the actual average mixing height for a group of measurements, the representative sounding was plotted, and the near-surface temperature measured at midsampling time was used to find the dry adiabatic intersection of the sounding. Variation can possibly occur when estimating the actual mixing height, especially during midmorning, which is the time when the radiation inversions usually dissipate. However, on the average, this method is a good approximation to the true mixing height (Holzworth 1972).

After the mixing height was determined, the layer resultant wind velocity was determined. This velocity multiplied by the mean layer concentrations and normalized for H produces the flux values presented in the following analyses.

Estimating SO_x and NH_4^+ Concentrations--

Sampling limitations necessitated estimation of $\bar{C}_R$, $\bar{C}_S$, and $\bar{C}$, the mean transport layer concentration, from a few (two to four) discrete horizontal integrated average values and "typical" pollutant profile shapes. Figures 24 and 25 show the typical profiles of sulfate and total sulfur, as determined from actual measurements during the TREATS 1976 and 1977 field studies. The observed sulfur values were interpreted by considering the appropriate profile and were averaged both within and between inversion layers to obtain the most representative estimates for $\bar{C}_R$, $\bar{C}_S$, and $\bar{C}$. Because most of the NH_4^+ is assumed to be in the form of $(NH_4)_2SO_4$, the typical sulfate profiles were also used to estimate the average for NH_4^+. $\bar{C}_B$ for NH_4^+ was assumed to be the stoichiometric amount needed to react with the background $SO_4^=$ (i.e., 0.3 $\mu g\ m^{-3}$ of NH_4^+).

Estimating NO_3^- and O_3 Concentrations--

In a manner similar to the estimation for sulfur and ammonium salts, discrete horizontal integrated values were obtained for nitrate and ozone. The most significant differences between these pollutant profiles and the typical sulfur profiles were their high scatter and

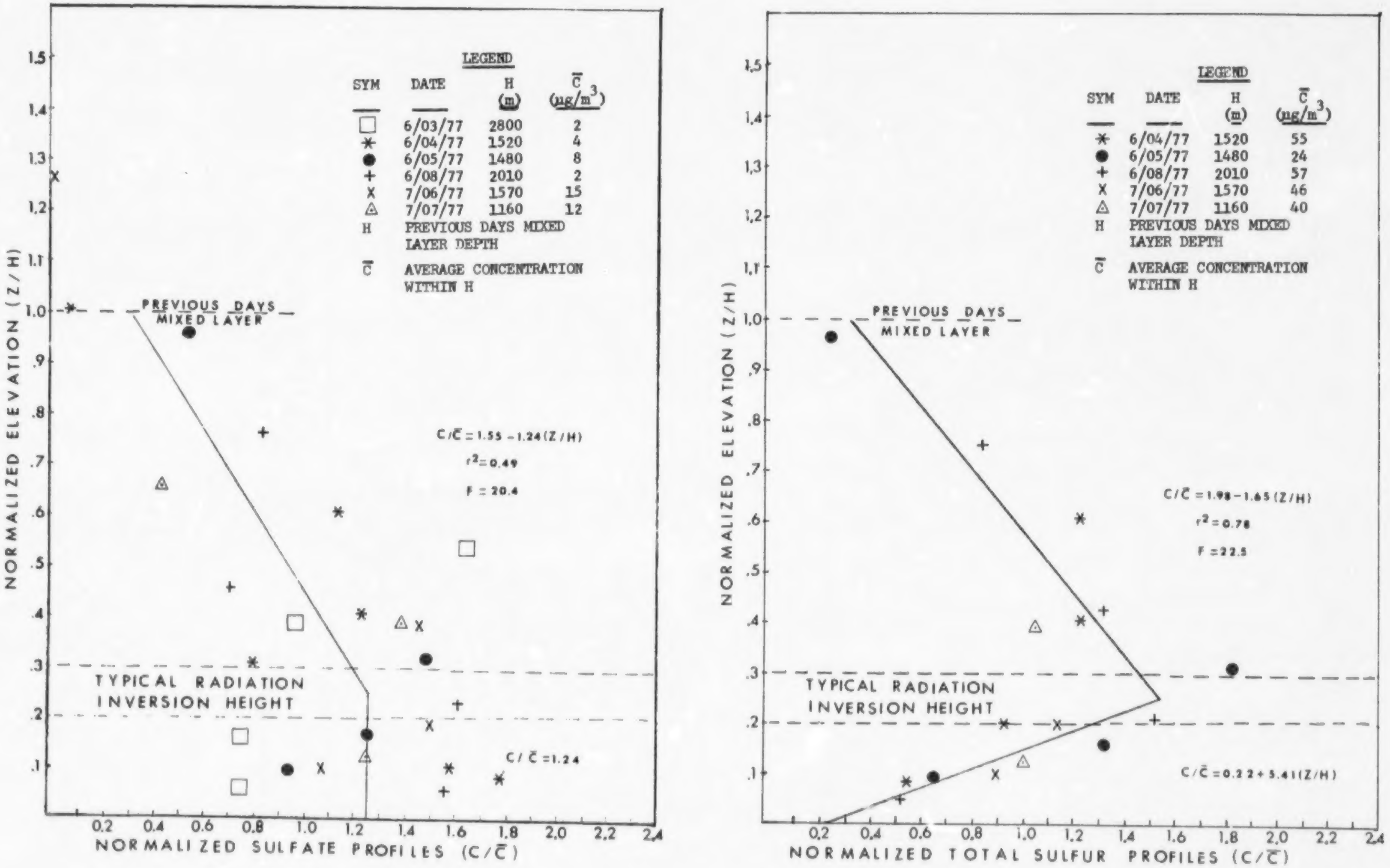

Figure 24. Typical early morning sulfur profiles.

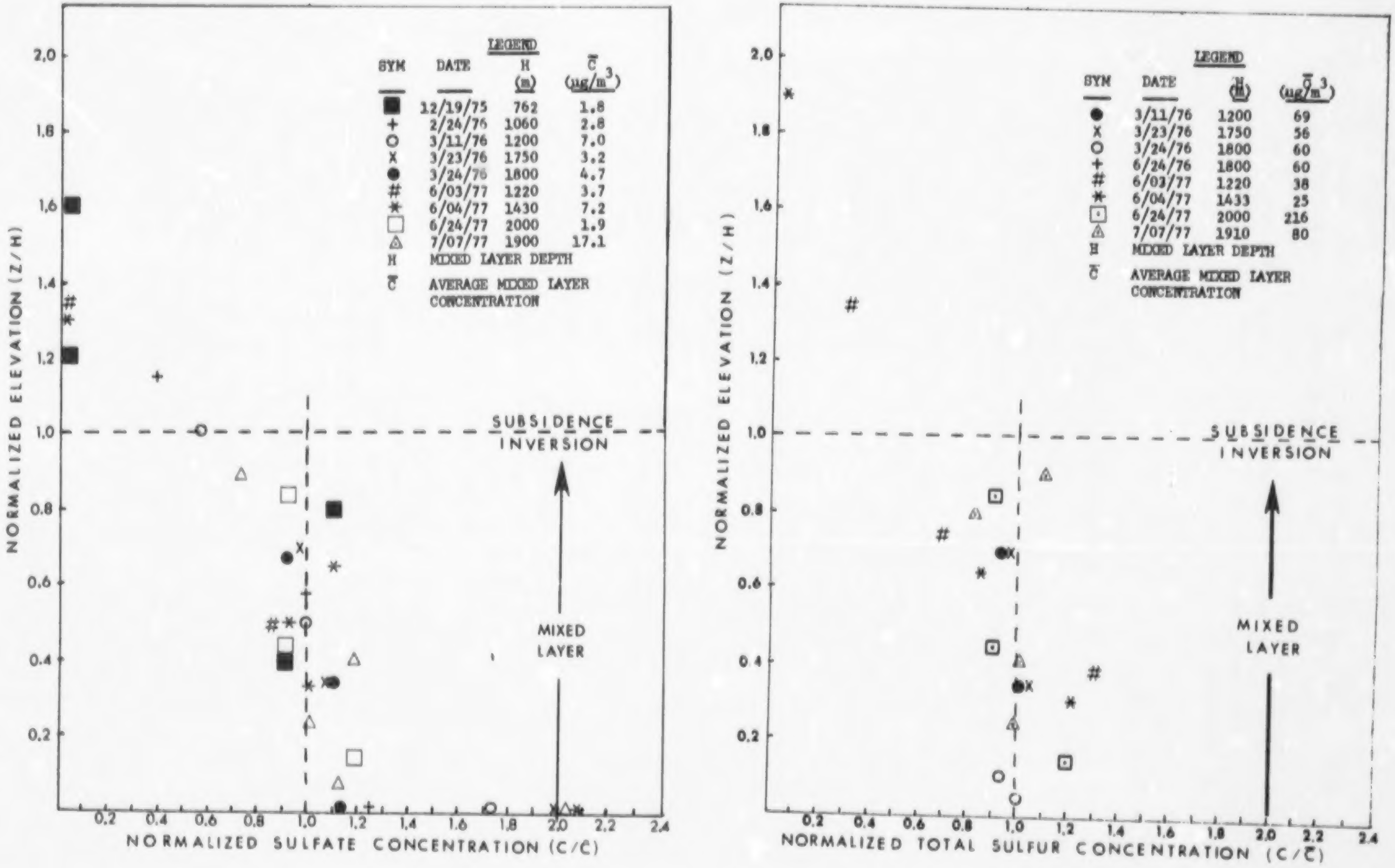

Figure 25. Typical midday sulfur profiles.

lack of shape, as illustrated by Figures 26 and 27. Because of this scatter, a vertical weighing factor, based on actual measurement location within the mixed layer, was considered to be more representative of the mean layer concentrations than any other estimation technique. No attempt was made to correct for background concentrations above the subsidence inversion when calculating $\bar{C}$.

Flux Measurement Criteria--

For the flux analysis to be reasonably accurate and useful, certain criteria are required:

1. The direction of airflow has to be relatively steady; that is, the directional variation of the mean transport wind in both space and time must be less than or equal to ±45°.
2. Both inflow and outflow measurements must be made to obtain daily Eulerian or Lagrangian concentration values. These measurements must be made over a sufficiently wide spatial extent, in both the horizontal and vertical, to be representative of the airmass sampled.
3. The meteorological conditions specified in the Meteorological Measurements and Support subsection of Section 3 must be met.

These criteria were met on five Lagrangian days and six Eulerian days during the two studies. Only one Lagrangian day was sampled during the 1977 summer study, whereas four Eulerian days were sampled. Three of the inflow-outflow Eulerian measurement days in 1977 were made during northerly wind flow.

A Lagrangian event (day) is defined as outflow aircraft measurement of the same airmass that was previously sampled at the inflow end, plus or minus 1 h. All other airmass measurements were defined as Eulerian. The average time of a set of aircraft traverses at both inflow and outflow is the time used for Lagrangian-Eulerian calculations.

For the Lagrangian days, the second criterion usually imposed an airmass age of 7 h to the outflow sampled airmass. This occurred for two reasons: (1) The aircraft had limited performance capabilities, which restricted them to daytime hours and limited cruise speeds (<100 knots); and (2) the large distance (~250 km) between inflow and outflow measurement points required a fairly rapid airmass inflow-to-outflow traverse time so that darkness would not curtail sampling operations. Because inflow measurement times usually averaged 0800 h these requirements limited Lagrangian operations to a fairly narrow "window" of favorable wind flow speeds of from 8 to 12 m s^{-1} (i.e., airmass age of 6 to 8 h). Figure 28 graphically shows both the Lagrangian and Eulerian measurement regimes. Here the earliest measurement defines the relative origin for other measurements for the same day. Only days with both inflow and outflow measurements are plotted.

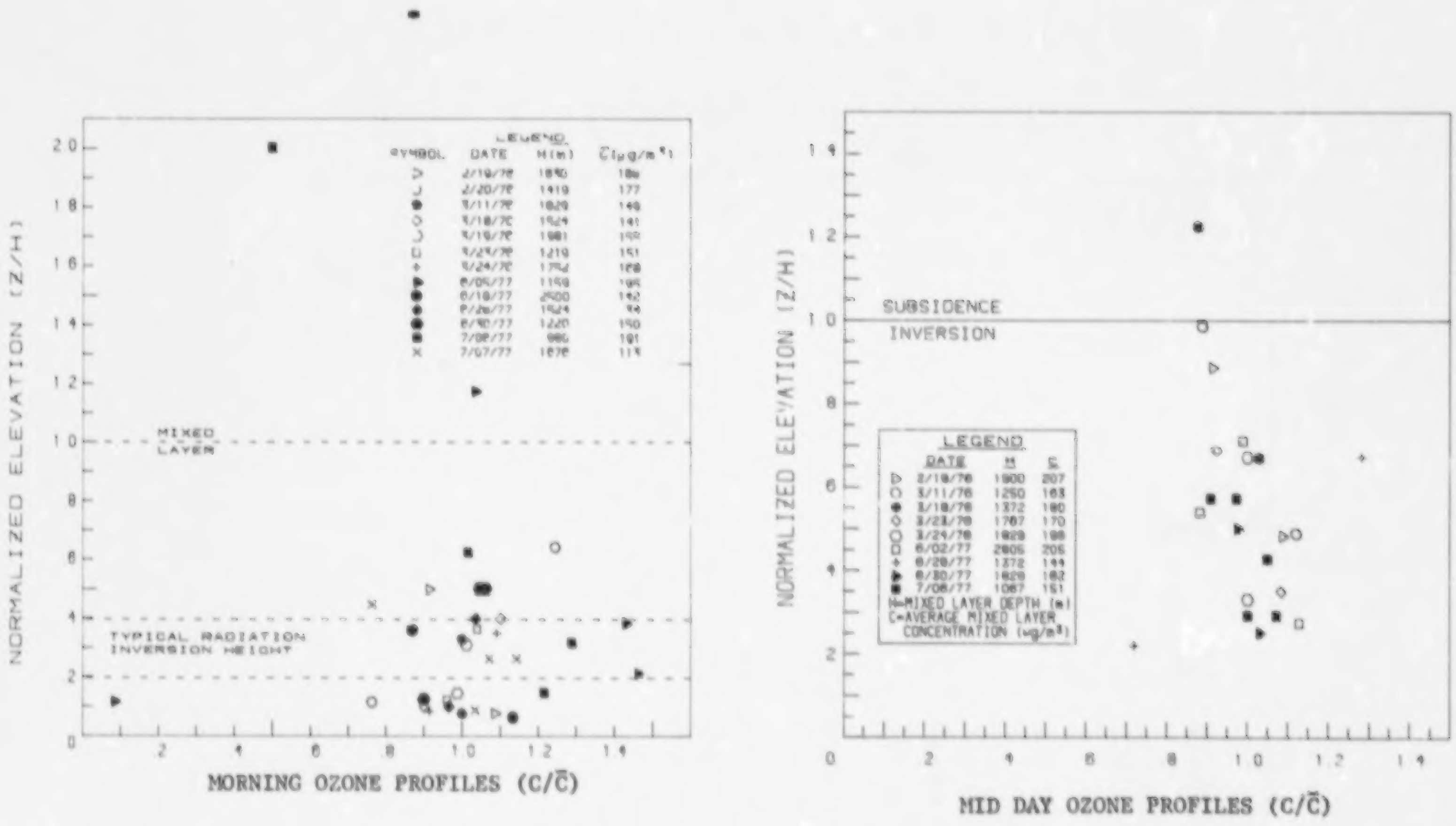

Figure 26. Typical early morning and midday normalized ozone profiles.

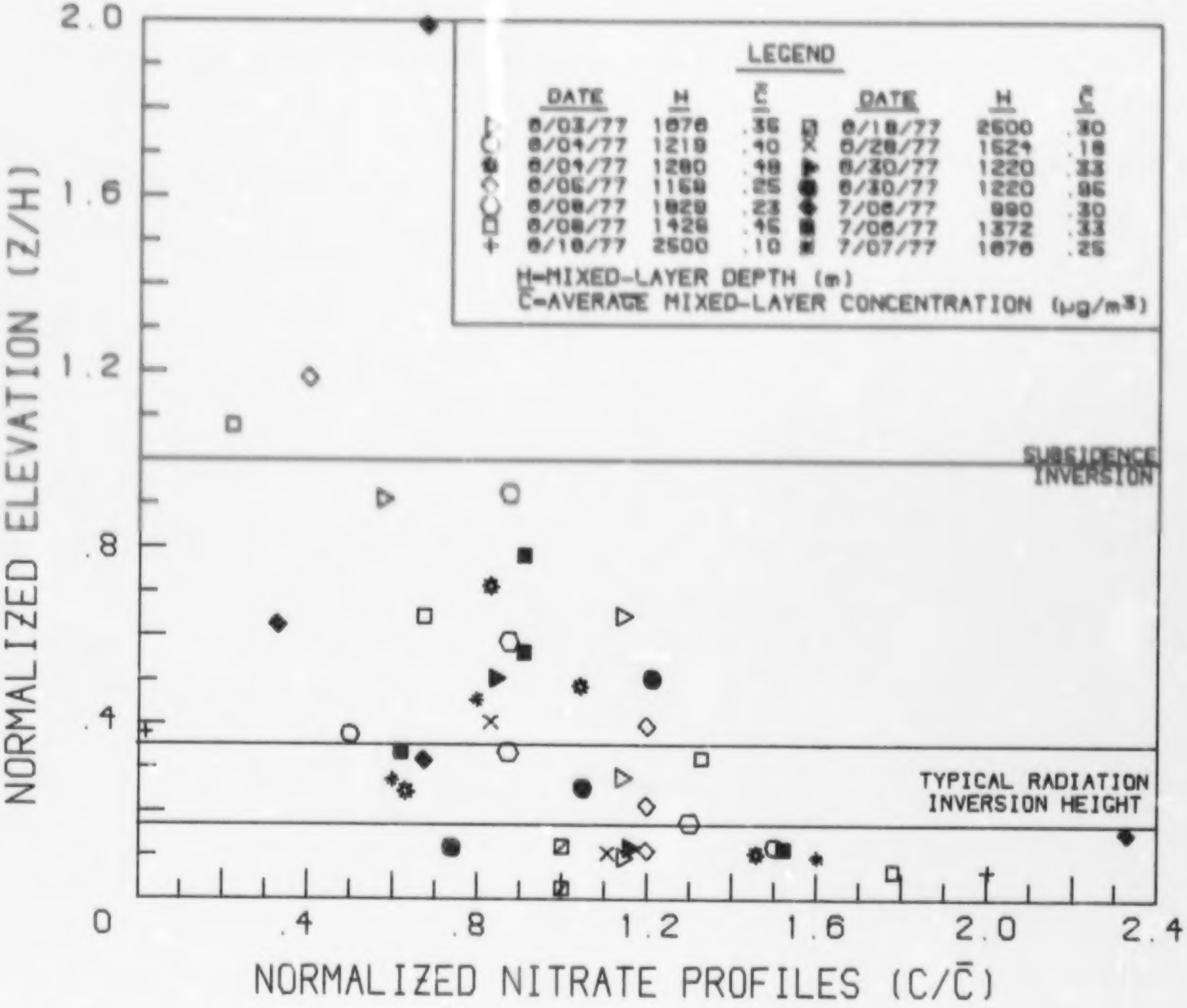

Figure 27. Typical early morning nitrate profiles.

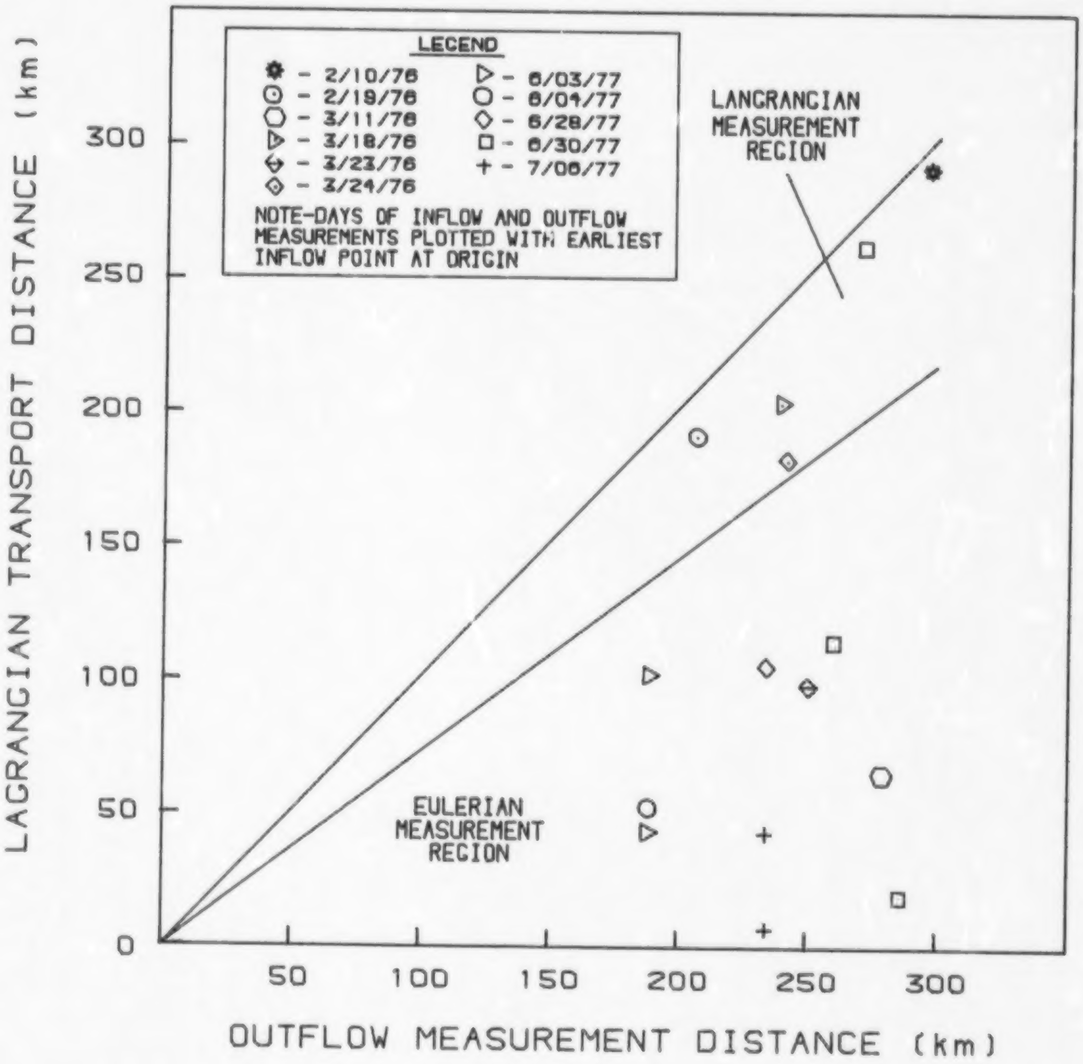

Figure 28. Airmass transport distance vs. inflow-to-outflow sampling distance.

The bias toward sampling during southwesterly flow conditions results from three factors:

1. As stated previously, "typical" meteorological conditions were desired. As evidenced from Section 3, flow from the southwest is typical.

2. High sulfate pollution episodes have been documented with southwest-to-northeast flow of maritime tropical air from the Gulf of Mexico (Perhac 1977; Smith and Niemann 1977).

3. Wind velocity sufficiently steady and strong enough to allow for Lagrangian measurements occurred almost exclusively with flow from the southwest.

Tabular Summary of Flux Calculations--

The Lagrangian and Eulerian aircraft sampling data for both 1976 and 1977 are summarized in Table 6. All days when Valley-wide measurements were made are listed in this table. The complete data set for all aircraft measurements is given in Appendix D. Due to instrument problems, only relative changes can be analyzed for the 1977 measurements made by the Meloy 202 total sulfur instrument. This instrument was almost exclusively used for measurements at the northern end of the Valley (i.e., Scottsville, Kentucky, area), and its readings are identified by a superscript "i" after the total sulfur reading. In the following sections, the data from Table 6 are analyzed by measurement type. A detailed synoptic meteorological summary for the Lagrangian and Eulerian days is given in Appendix E.

EULERIAN SPACE AND TIME VARIATIONS

The Eulerian space and time variations of four pollutants--total sulfur, $SO_4^=$, NO_3^-, and NH_4^+--are explored. Eulerian space variations are explored by grouping measurements that were made at similar times, but in different horizontal or vertical space locations. Similarly, Eulerian time variations are explored by grouping measurements that were made at the same locations, but at different times. Aircraft measurements fitting into these two groups occurred exclusively during the 1977 summer study. The aircraft data used in these analyses are taken from Table 6.

High-volume measurements of total suspended particulates and $SO_4^=$ are taken from both study periods. The high-volume sulfate is analyzed separately from the aircraft sulfate because of an interesting discontinuity between the two measurements. This discontinuity is discussed further in the Vertical Variations subsection.

Eulerian Space Variations

Eulerian measurements were separated in both horizontal and vertical space. Typically, measurements were made at two locations separated by an average horizontal distance of over 200 km. These sampling locations

TABLE 6. SUMMARY OF LAGRANGIAN AND EULERIAN MEASUREMENTS

Sampling Days With Both Inflow and Outflow Measurements

						Pollutant concentration ($\mu g\ m^{-3}$)[e]														Pollutant flux[h] ($\mu g\ m^{-2}\ s^{-1}$)				
						Inflow						Outflow								Inflow		Outflow		
Date	Time[a]	Sampling[b] methodology	WD[c] (°)	WS (m/s)	DST[d] (km)	$SO_4^=$	NH_4^+	$NH_4^+/SO_4^=$	TS[i]	NO_3^-	O_3	$SO_4^=$	NH_4^+	$NH_4^+/SO_4^=$	TS[i]	NO_3^-	O_3	Q[f]	H_s(m)[g]	$SO_4^=$	TS[i]	$SO_4^=$	TS[i]	Center point of traverse
2/10/76	0916	L	217	13.6	293	1.8	0.5	1.5	42	<LDL	-								915	24.5	571			Florence, AL
	1526											4.5	1.4	1.6	39	<LDL	-	781	915			60.6	530	Scottsville, KY
2/19/76	0927	L	274	9.8	200	1.2	0.4	1.9	67	<LDL	-								1900	14.2	818			Parsons, TN
	1455											2.3	1.4	1.2	66	<LDL	-	1462	1900			19.9	568	Smithville, TN
3/11/76	0908	E	200	3.6	278	4.5	1.3	1.6	49	<LDL	-								1829	15.5	157			Florence, AL
	1425											5.6	2.0	1.9	67	<LDL	-		1250			30.6	320	Scottsville, KY
3/18/76	0838	L	226	10.5	234	3.2	0.8	1.4	71	<LDL	-								1524	29.0	642			Decatur, AL
	1418											3.2	1.6	2.7	52	<LDL	-	1121	1372			33.5	544	Scottsville, KY
3/23/76	0834	E	210	2.5	250	2.9	1.8	3.2	85	<LDL	-								1767	3.3	81			Florence, AL
	1345											3.3	1.0	1.6	57	<LDL	-		1767			24.0	413	Scottsville, KY
3/24/76	0800	L	198	9.5	242	2.8	0.9	1.7	52	<LDL	-								1829	27.2	495			Decatur, AL
	1332											4.7	1.3	1.4	60	<LDL	-	750	1829			56.3	727	Scottsville, KY
6/3/77	0743	E	021	3.5	190	1.5	0.4	1.3	LR	0.4	-							NA	1646	8.9	LR			Florence, AL
	1030					3.6	0.9	1.4	37	0.3	-								1646	14.8	150			Threet, AL
	1110											8.6	1.6	1.0	LR	0.9	-		1676			26.6	LR	Savannah, TN
	1440					1.6	LR	LR	LR	0.7	-								1524	3.4	LR			Threet, AL
	1505											4.7	1.7	1.9	71	0.4	-		1524			12.6	183	Gordo, TN
6/4/77	0726	E	004	1.3	190	3.8	1.1	1.6	LR	0.2	-							NA	1524	6.1	LR			Threet, AL
	0717											9.5	1.4	0.8	126	0.5	-		1524			10.8	144	Scottsville, KY
	1030					4.1	1.5	2.0	31	0.2	-								1524	5.4	41			Cypress Inn, TN
	1453					6.6	1.8	1.4	22	0.3	-								1524	14.5	49			Courtland, AL
	1518											6.7	2.1	0.6	59	0.6	-		1524			18.4	164	Scottsville, KY
6/28/77	0723	E	240	8.7	234							1.6	0.1	0.7	32	0.2	118	NA	1524			16.0	334	Scottsville, KY
	1025					3.4	0.7	1.0	237	2.9	-								1372	26.2	1829			Waynesboro, TN
	1025											2.1	0.3	0.8	16	0.6	118		1372			16.2	123	Scottsville, KY
	1345					3.9	0.5	0.7	134	3.1	-								1372	27.1	938			Houston, TN
	1335											4.5	1.1	1.3	16	0.6	149		1372			31.7	114	Carthage, TN
	1651					3.4	0.5	0.8	93	2.4	-								1372	23.6	644			Lutts, TN
6/30/77	0637	L	233	9.7	234	1.9	0.4	1.1	63	1.1	-								1829	20.0	660			Savannah, TN
	0713											2.3	0.7	1.5	21	0.3	153		1829			23.4	216	Scottsville, KY
	1033					2.6	0.5	0.9	76	1.0	-								1829	24.6	707			Savannah, TN
	1000											2.7	0.4	0.8	LR	LR	221		1829			25.9	LR	Scottsville, KY
	1345					3.2	0.9	1.4	62	1.2	-							1234	1829	36.8	591			Savannah, TN
	1406											2.3	1.2	2.7	14	0.6	161	NA	1829			31.6	196	Scottsville, KY
7/6/77	0646	E	357	2.0	234							16.6	2.7	0.9	99	0.3	-		1372			54.1	322	Threet, AL
	0815					19.3	2.1	0.6	40	0.2	208								1372	11.6	24			Scottsville, KY
	1030											16.1	4.4	1.5	83	0.7	-		1372			30.4	157	Waterloo, AL
	1240					11.7	2.0	0.91	51	0.4	143								1067	14.8	65			Central City, KY
	1425											16.2	4.3	1.4	72	0.7	-		1036			33.6	149	Waterloo, AL
	1533					16.3	2.6	0.84	45	0.2	153								1067	20.7	57			Scottsville, KY

TABLE 6 (continued)

Other Eulerian Days

Date	Time[a]	Sampling[b] class	WD[c] (°)	WS (m/s)	Pollutant concentration ($\mu g\ m^{-3}$)[e] $SO_4^=$	NH_4^+	$NH_4^+/SO_4^=$	TS[i]	NO_3^-	O_3	H_s(m)[g]	Pollutant flux[h] ($\mu g\ m^{-2}\ s^{-1}$) $SO_4^=$	TS[i]	Center point of traverse
6/5/77	0702	O	327	5.0	22.7	3.0	0.7	186	0.3	-	1677	114.2	934	Threet, AL
	1137	O			7.8	2.9	2.0	57	0.6	-	1677	41.7	307	Center Star, AL
	1500	O			10.8	1.6	0.8	52	0.5	-	1677	61.9	300	Anderson, AL
	0658	N	285	2.9	5.9	1.3	1.2	21	0.2	215	1677	16.6	60	Scottsville, KY
	1045	N			7.4	2.2	1.6	42	0.7	246	1677	31.8	180	Scottsville, KY
	1430	N			13.1	3.7	1.5	30	0.4	267	1677	28.8	66	Portland, TN
6/8/77	0716	N	287	4.4	1.3	0.4	1.7	45	0.2	LR	1829	9.0	323	Franklin, KY
	1105	N			2.0	0.9	2.4	34	0.3	141	1829	9.6	161	Franklin, KY
	0645	B	VRB		3.6	1.3	2.0	89	0.4	-	1829	NA	NA	Red Bank, AL
	1015	B			1.8	0.7	2.2	61	0.3	-	1829	NA	NA	Wolf Springs, AL
7/7/77	0721	N	274	4.9	8.5	1.3	0.8	25	0.2	98	1900	40.9	160	Lewisburg, KY
	1115	N			9.2	2.1	1.2	31	0.1	111	1900	48.9	167	Central City, KY
	1100	O	317	3.2	12.1	3.2	1.4	103	0.5	-	1900	41.7	355	Waterloo, AL
	1428	O			22.8	2.9	0.7	80	0.5	-	1900	105.7	369	Red Bank, AL

[a] Midtime of sampling traverses.

[b] L = Lagrangian; E = Eulerian; B = blob; O = outflow; N = neither.

[c] Mean wind direction and speed for the sampling day.

[d] Distance in kilometers between average midpoint of inflow and outflow sampling traverses.

[e] Abbreviations: - = pollutant not measured; LR = lost record; NA = not applicable; <LDL = less than lower detectable limit; $NH_4^+/SO_4^=$ = molar ratio; TS as SO_2.

[f] TVA emissions in metric tons affecting outflow Lagrangian airmass.

[g] Height of subsidence inversion through which C was calculated.

[h] Calculated through H_s; normalized to H = 1600 m.

[i] Questionable data, good only in a relative sense by sampling class (instrument).

were typically in south-central Kentucky and northwestern Alabama. These locations characterized either inflow, outflow, neither, or blob (stagnation) conditions, depending on meteorology. Such measurements were also made at various elevations.

Horizontal Variations--

When winds were steady enough, inflow and outflow measurements were made. Five such days were sampled during the 1977 summer study. Again, the limitation of this data base to just five summer days allows only tentative findings. Plots of $SO_4^=$, NH_4^+, total sulfur, and NO_3^- aircraft values, listed by measurement type and flow direction, are presented in Figures 29 through 32. Intercomparison by pollutant shows that, with northerly flow, average values of $SO_4^=$ concentrations (Figure 29) vary significantly from inflow to outflow and from day to day. However, with southwesterly flow the situation is reversed. Little spatial or temporal variation is evident. Although this difference may be due only to the limited number of days sampled, it could also be due to the variation in SO_2 emission density. Large sulfur sources are immediately upwind from the inflow (northern) boundary during northerly wind flow, whereas just the opposite is the case for the inflow (southern) boundary with southwesterly flow. Similarly, for ammonium (Figure 30) the northerly inflow boundary shows greater variability and higher concentrations vs. those at the southern inflow boundary. Nitrate concentrations (Figure 32) show an opposite correlation, indicating that its major source regions differ significantly (possibly natural vs man-made). The average inflow and outflow concentrations and standard deviations by pollutant for three days with northerly flow and for the two days with southwesterly flow are shown in Table 7.

TABLE 7. INFLOW-OUTFLOW CONCENTRATIONS[a] (μg m^{-3}) BY FLOW DIRECTION

Pollutant	Flow direction: North-northeast Inflow	North-northeast Outflow	South-southwest Inflow	South-southwest Outflow
$SO_4^=$	7.6 (6.6)	11.2 (5.0)	3.1 (0.7)	2.6 (1.0)
NH_4^+	1.5 (0.7)	2.6 (1.3)	0.6 (0.2)	0.6 (0.5)
NO_3^-	0.3 (0.2)	0.6 (0.2)	2.0 (1.0)	0.5 (0.2)

[a] Standard deviations in parentheses.

Significant increases occur in the average concentrations of all three pollutants from inflow to outflow with northerly winds, whereas no significant change occurs from inflow to outflow with southwesterly flow, except for the nitrates. The nitrates show a large inflow concentration with southerly flow and a small outflow concentration.

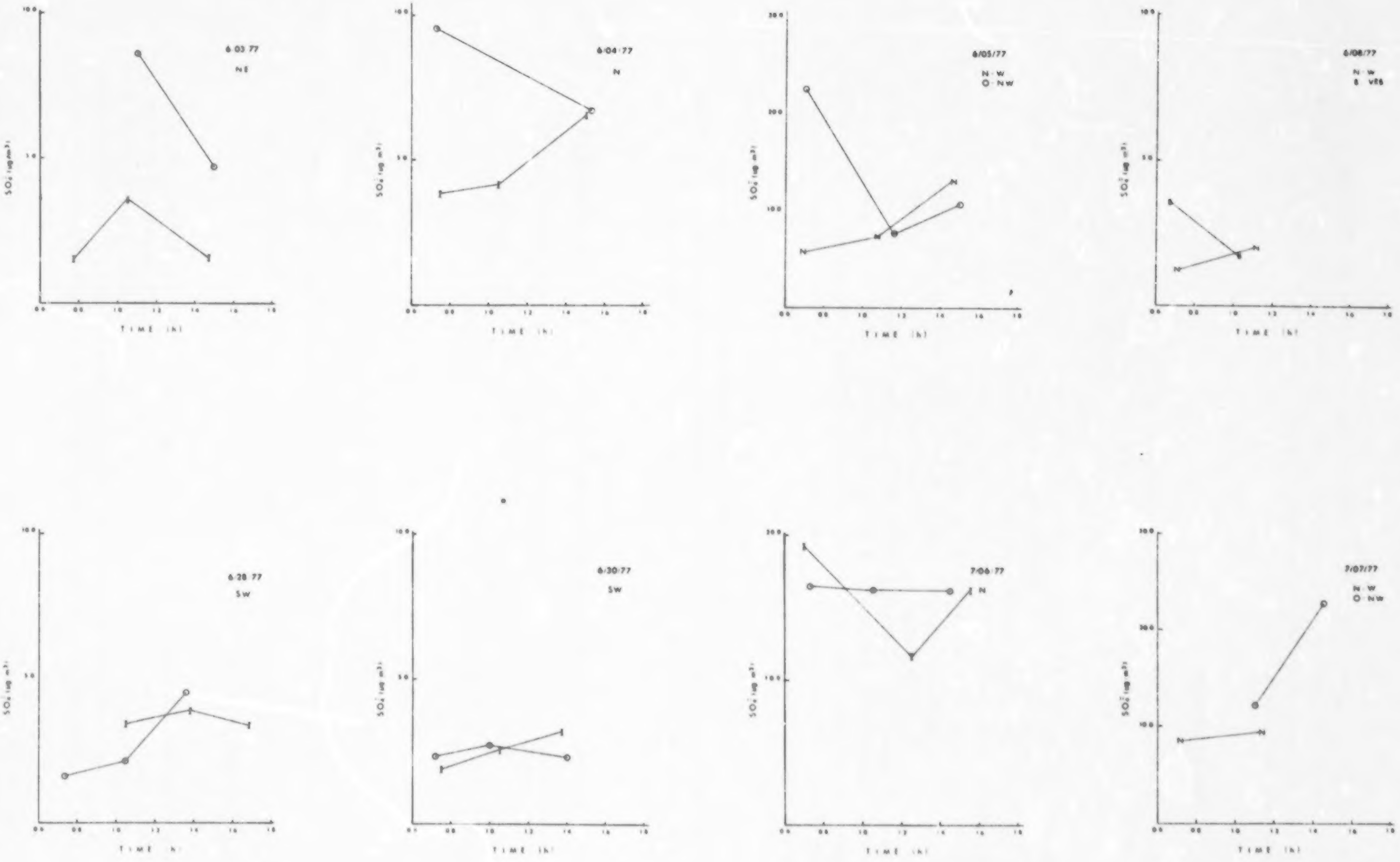

Figure 29. Temporal variation of sulfate (I = inflow, O = outflow, N = neither, B = blob; wind direction in upper right corner of each axis).

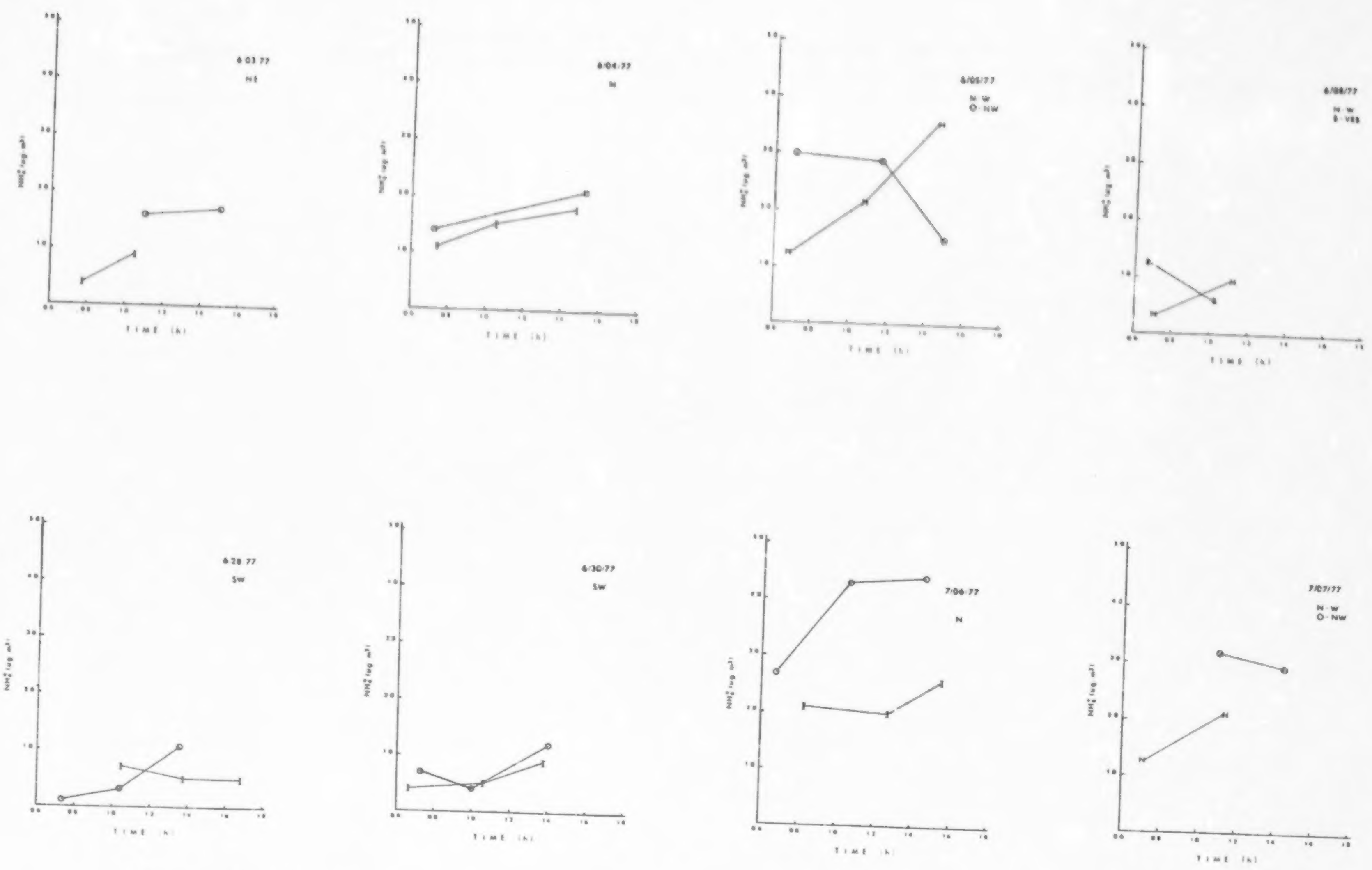

Figure 30. Temporal variation of ammonium (I = inflow, O = outflow, N = neither, B = blob; wind direction in upper right corner of each axis).

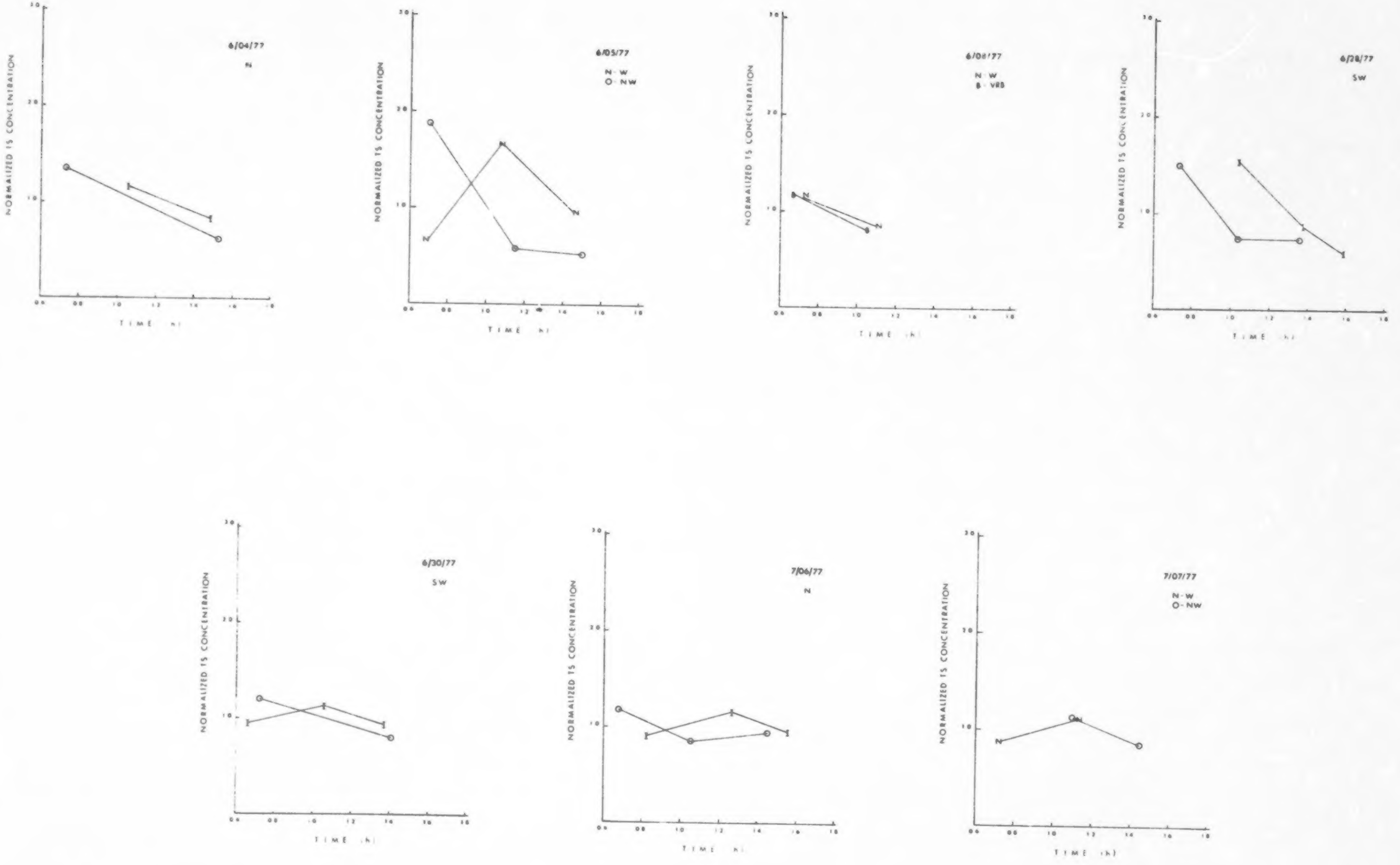

Figure 31. Temporal variation of normalized total sulfur (I = inflow, O = outflow, N = neither, B = blob; wind direction in upper right corner of each axis).

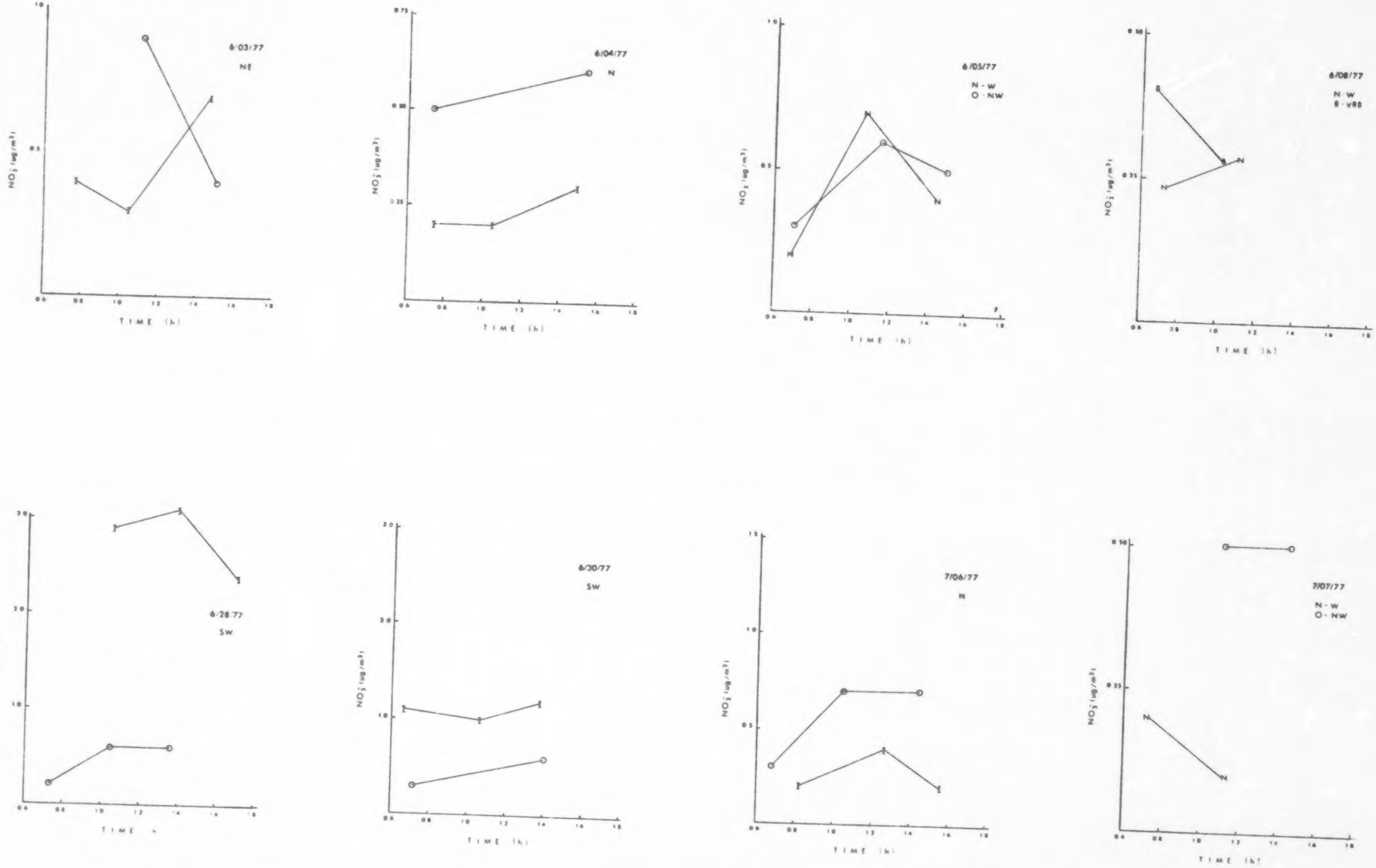

Figure 32. Temporal variation of nitrate (I = inflow, O = outflow, N = neither, B = blob; wind direction in upper right corner of each axis).

Traditionally, total filterable sulfates have been measured as water-soluble sulfates from glass-fiber, high-volume filters. Although serious questions as to the adequacy of this sampling method have often been raised, governmental agencies and private industry continue to use the high-volume method. Therefore, establishment of a relationship between high-volume concentrations, upper air concentrations, and interregional transport would be useful.

High-volume filter data, mostly for daytime periods, from the two studies are presented in Appendix D. These data are obtained from fixed monitors, most of which are located near TVA power plants (Figure 3). Depending on wind flow conditions, these sites are designated as being representative of inflow, outflow, or neither (in between). A presentation of inflow-outflow-neither high-volume measurements by wind direction is shown in Table 8.

TABLE 8. HIGH-VOLUME CONCENTRATIONS ($\mu g\ m^{-3}$) BY FLOW DIRECTION

Number of days	Wind direction	Inflow		Outflow		Neither		Average	
		TSP	$SO_4^=$	TSP	$SO_4^=$	TSP	$SO_4^=$	TSP	$SO_4^=$
7	WNW (270-329°)	79	12.1	93	17.5	79	15.4	84	15.0
3	N (330-029°)	92	15.1	86	17.3	85	17.5	88	16.6
Average		85	13.6	89	17.4	82	16.5	85	15.8
4	S (150-209°)	62	6.6	86	8.0	55	7.2	68	7.3
12	WSW (210-269°)	76	8.0	60	6.6	50	6.4	62	7.0
Average		69	7.3	73	7.3	53	6.8	65	7.2
Weighted grand average		75	9.7	79	11.2	65	10.5	71	10.5

Analysis of these data shows that, similar to the aircraft data, sulfate concentrations differ significantly with various wind flows. West-northwesterly through northerly flow is accompanied by high sulfate concentrations at both inflow and outflow, whereas the opposite is true for southerly or west-southwesterly flow. Total suspended particulates follow the same pattern; only the relative magnitude of the changes are less. For all days, the average increase in sulfate from inflow to outflow is 15 percent, whereas total suspended particulates show no significant change.

Vertical Variations--

Typical early morning and midday sulfur profiles are illustrated in Figures 24 and 25 respectively. To generate these plots, data were normalized and pooled, regardless of location. Both plots illustrate a somewhat unexpected behavior. The early morning profiles scale well in the vertical when the previous day's mixed-layer depth is used. At the lower boundary (Z/H = 0), the data suggest that through the night SO_2 (the main component of the total sulfur plot) is selectively removed, whereas $SO_4^=$ shows no apparent trend. This could indicate a significant difference in nighttime SO_2 vs. $SO_4^=$ deposition velocities. The midday sulfur profiles of Figure 25 illustrate just what is expected--a uniformly mixed layer--except for ground-level $SO_4^=$, which was determined by high-volume sampling.

The difference between similar spatial and temporal measurements of aircraft and ground-level sulfate is graphically shown in Table 9 and Figure 33. A paired-t test shows that this difference--aircraft concentrations nearly half the high-volume concentrations--is statistically significant ($p = 0.99$). Because most monitoring sites are located at the power plants, a bias was at first believed to have been introduced by local source effects. This bias might result from primary sulfate emissions, artifact sulfate formation, or a more frequent exposure to secondarily formed $SO_4^=$. However, Bailey and Ruddock (1978) have shown that primary sulfate emissions from TVA power plants are typically low (~1 percent by molar ratio), and artifact sulfate formation on Gelman Spectrograde filters, as discussed in the Analytical Methods subsection, is also low. Also, the average conversion rate of SO_2 to $SO_4^=$ [<2 percent per hour (Meagher et al. 1977)] and the relatively low deposition velocity of $SO_4^=$ indicate that this pollutant is long-lived and therefore widely dispersed. This is supported by an analysis of high-volume data from the two field studies.

A high-volume sampler located at the Giles County trend station was compared with the average of four samplers located at the nearest TVA coal-fired power plant, the Colbert Steam Plant. These two measurement sites are separated by over 100 km. A plot of the Giles sulfate data vs. the Colbert data for 18 simultaneous measurements obtained during the two studies is shown in Figure 34. A slope statistically not different from one and a high correlation coefficient ($r^2 = 0.77$) indicate the regional nature of the sulfate pollution and the representativeness of the power plant sulfate values in indicating regional sulfate levels.

Additional correlations among five trend stations and between Giles County and the average of Cumberland and Gallatin Steam Plants, as tabulated in Table 10, show that, although all correlations are good, the correlation between Giles and the average of the two power plants is better than the correlations between trend stations. This result is probably due to the variabilities inherent in the measurement technique itself. Thus, because two or more high-volume samplers exist at each power plant, the resultant smoothed or averaged measurement concentration may be more representative of regional sulfate levels.

Terra and Hilst (1978) of the Electric Power Research Institute's SURE program reported midday ozone bulges near the ground (surface to 200 m AGL) during their summer measurement program. These ozone bulges are an indication of photochemical reactions and may be tied to hydroxyl radical production, a favored reactant with SO_2 that probably leads to sulfate formation. Unfortunately, our study had no ground-level or near-ground-level ozone measurements; thus, this hypothesis for explaining the high $SO_4^=$ readings measured near ground level for the TREATS data could not be checked.

TABLE 9. COMPARISON OF GROUND-LEVEL AND UPPER-AIR SULFATE CONCENTRATIONS

Date	Sample class[a]	Aircraft measured concentration[b] ($\mu g\ m^{-3}$)	Closest high-volume station(s)	High-volume concentration[c] ($\mu g\ m^{-3}$)
6/03/77	O	5.5	Colbert	17.0
6/05/77	N	9.3	Colbert	17.0
6/08/77	B	4.0	Colbert	9.0
6/24/77	I	2.8	Colbert	4.5
6/28/77	I	2.8	Johnsonville	13.0
6/30/77	I	3.0	Colbert	5.3
7/06/77	N	19.8	Paradise and Gallatin	27.1
7/06/77	O	17.9	OACD and Colbert	28.7
7/07/77	N	14.4	Cumberland and Paradise	27.2

[a] I = inflow, O = outflow, B = blob, and N = neither.

[b] Each air concentration is an average of at least two measurements spanning at least 4 h and within 50 to 305 m AGL.

[c] Results from at least two high-volume monitors were averaged. Both 9- and 24-h results are presented; values for 6/24/77, 6/30/77, and 7/6/77 are 24-h samples.

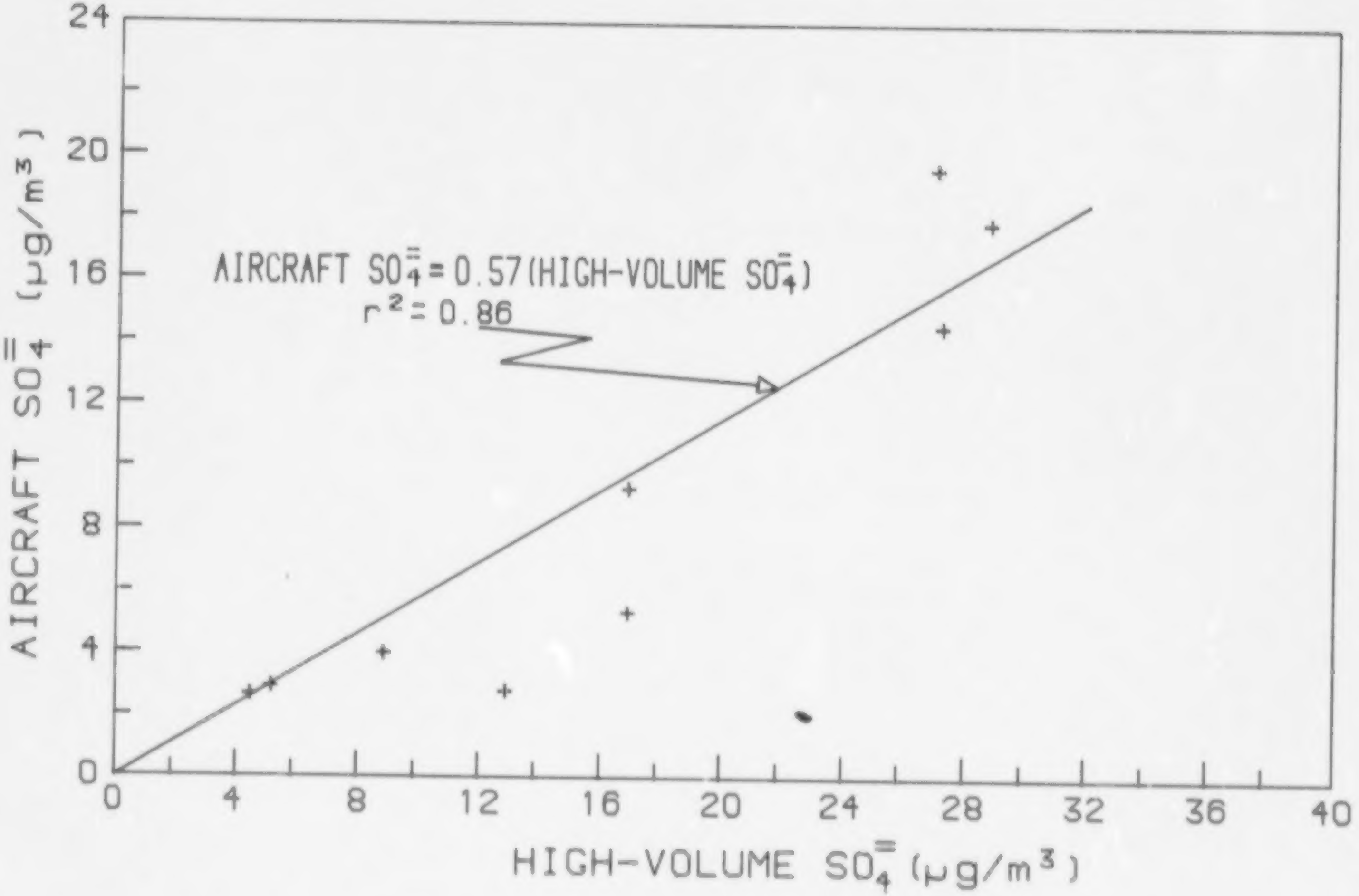

Figure 33. Comparison of ground-level to upper-air sulfate concentrations.

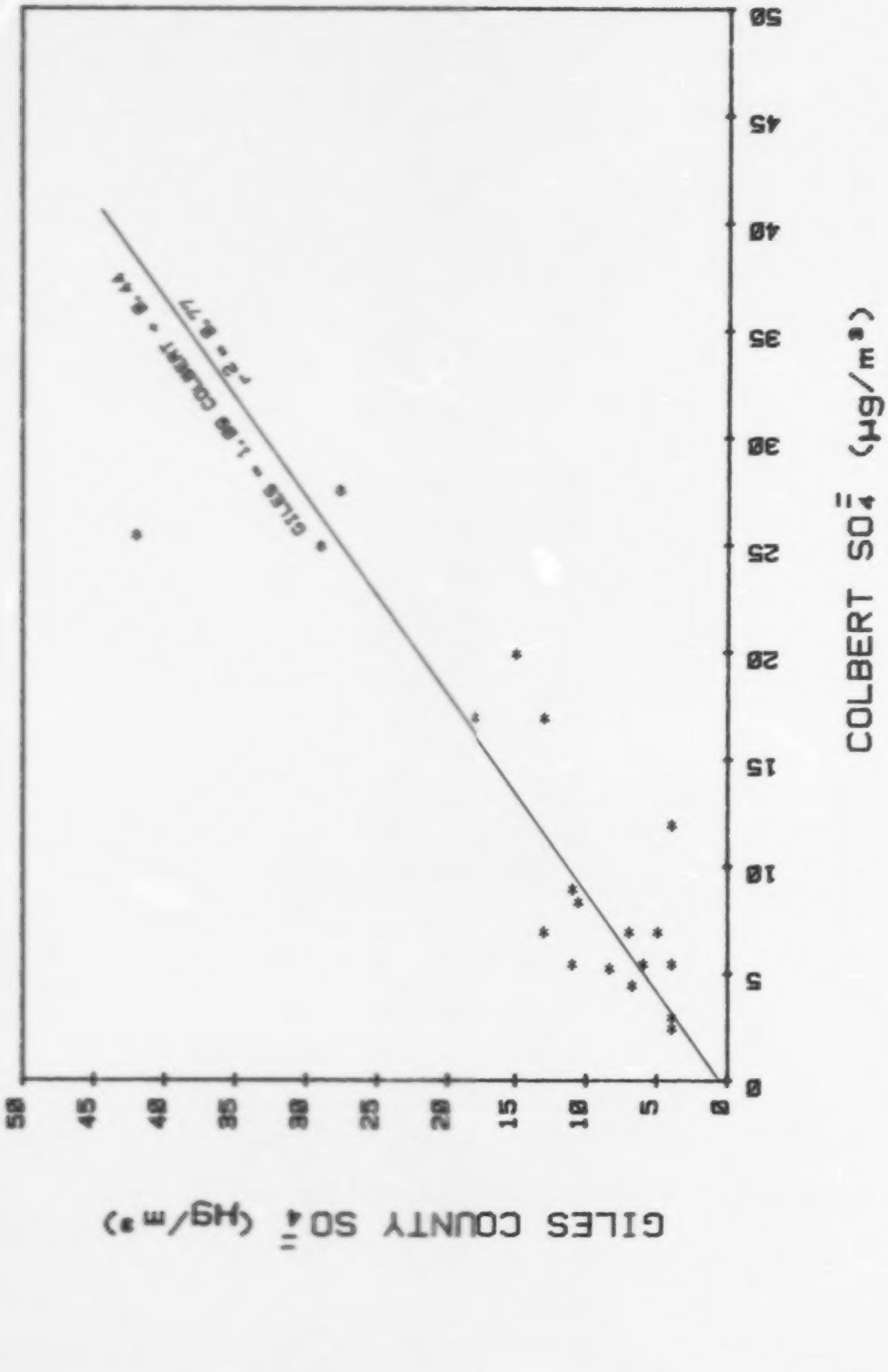

Figure 34. Giles County sulfate concentration vs Colbert.

TABLE 10. SUSPENDED SULFATE CORRELATION MATRIX

	Air quality trend stations					
	Loves Mill	Loudon	Hytop	Giles County	Land Between the Lakes	Valley-wide
Loves Mill		0.58[a] (250)	0.55 (320)	0.54 (450)	0.47 (520)	0.73
Loudon	86[b]		0.69 (185)	0.58 (225)	0.45 (350)	0.83
Hytop	92	89		0.66 (80)	0.51 (260)	0.83
Giles County	82	80	217		0.46 (175)	0.83
Land Between the Lakes	93	89	227	222		0.67
Valley-wide	97	93	98	88	100	

	Selected trend and power plant stations[c]			
	Giles County	Cumberland	Gallatin	Average
Giles County		0.71[a] (125)	0.78 (115)	0.89
Cumberland	112[b]		0.85 (110)	0.93
Gallatin	112	113		0.95
Average	112	112	112	

[a] Based on high-volume data collected simultaneously every sixth day; parenthesized numbers are the distance between sites in kilometers.

[b] Number of data points in correlation.

[c] Data from around a power plant were averaged.

These analyses do not indicate the reason for the large discontinuity evident in the aircraft vs. ground-level sulfate measurements. However, dispersion and deposition theory would indicate that this phenomenon is an aberration; therefore, we speculate that this phenomenon results from artifact $SO_4^=$ formation on the Gelman Spectrograde filters. Until such time as an explanation is forthcoming, the two data sets will be analyzed separately.

Eulerian Time Variations

Analyses of the time dependence of the various pollutant concentrations are presented in this section. The data shown in Figures 29 through 32 also show temporal variations for the various pollutants measured at different locations throughout the Valley. A temporal analysis of the data indicates diurnal variations between and within pollutants. For instance, the sulfate concentration plots show a fairly flat profile with southwesterly wind flow, whereas large variations usually occur with westerly through northerly flow. However, the flux of sulfate generally increases throughout the day, with significant departures evident on June 3 and 5, 1977. Ammonium, an ion thought to be strongly tied to the sulfates, also shows a fairly flat profile on the southwesterly flow days, but has significant departures from the sulfate profile shapes on other days. The molar ratio ($NH_4^+/SO_4^=$) presents no identifiable temporal trend. However, a relatively high ratio occurred on the stagnate or blob day, June 8, 1977, indicating that a much more aged airmass was sampled. The normalized measurements of total sulfur concentration definitely show a trend toward lower values from morning to afternoon, whereas nitrate values show no discernible pattern. However, as previously mentioned, the inflow nitrate values measured during southwesterly flow are significantly higher than any other inflow or outflow nitrate values measured.

Some of these phenomena are explainable. For instance, the decrease in total sulfur concentration with time may be related to an increase in turbulent mixing, thus leading to increased removal. Conversely, the sulfate concentration data do not follow any pattern; due to its longevity, it should be a more regional and uniformly distributed pollutant. The high inflow concentrations of nitrate during southwesterly flow indicate a significantly different source region than that within or north of the field study area. Because no large anthropogenic NO_x sources exist within 500 km upwind from the southwestern field study boundary, it seems probable that a natural area type source region is responsible for this anomaly.

LAGRANGIAN FLUX ANALYSIS

This section presents (1) the results of Lagrangian field study data, (2) comparisons of model predictions vs. actual data, and (3) additional predictions based on measured inflow boundary conditions and model simulation of transport to the outflow. Both the field study data and model predictions support several unexpected conclusions concerning TVA's regional and interregional impact and the significance of upwind sources.

Field Results

Five Lagrangian days (Figure 28) were sampled during the two field studies--four during the 1976 spring study and one during the 1977 summer study. A breakdown of the Lagrangian days and the flux calculations is shown in Table 6. This analysis shows that all Lagrangian measurements were made under relatively brisk southwesterly through westerly flow. Four of the five Lagrangian measurement days occurred during prefrontal flow of maritime tropical air. The only exception was on February 19, 1976, when a weak front moved through the area early in the morning and westerly flow occurred thereafter. No significant rainfall occurred on any of these days; however, cloud ceilings at ≤ 2000 m were present on February 10, 1976, and June 30, 1977. Also, solar radiation was considerably limited on February 10, 1976, March 24, 1976, and June 30, 1977, due to high cloud cover.

Analysis of these limited field data shows that, for the four Lagrangian days with both inflow and outflow total sulfur and sulfate measurements, the average daily sulfate flux from inflow to outflow increased by 47 percent, with a standard deviation of 35 percent, whereas the total sulfur (gaseous and particulate) flux decreased. Plots of both the Lagrangian and Eulerian inflow-outflow sulfate and total sulfur flux measurements are shown in Figures 35 and 36. Although both the inflow and outflow sulfate concentrations are relatively low, there appears to be a significant percentage increase in outflow sulfate flux. Also, total sulfur flux decreases slightly from inflow to outflow. However, neither of these conclusions is statistically significant (due to a high standard deviation and a limited number of data points).

The average measured mole ratios of $NH_4^+/SO_4^=$ are 1.5±0.3 at the inflow vs 1.9±0.7 at the outflow. This is a 27 percent increase from inflow to outflow. Although this difference may be real, statistically it is not significant. The scatter (Figure 37) for the composite of Lagrangian and Eulerian sulfate and ammonium measurement comparisons is large.

If the measured sulfate is assumed to be derived only from ammonium sulfate [$(NH_4)_2SO_4$], ammonium acid sulfate (NH_4HSO_4), and sulfuric acid (H_2SO_4) and if all ammonium is associated with sulfate, then limits can be placed on the relative abundance of these compounds. The minimum and maximum percentages of each compound that could yield the observed ratios are given in Table 11. The sulfur acid data includes all sulfate compounds other than the ammonium salts.

TABLE 11. SULFATE SPECIATION

Compound	Inflow (%)	Outflow (%)
$(NH_4)_2SO_4$	50-75	91-96
NH_4HSO_4	0-50	0-9
H_2SO_4	0-25	0-5

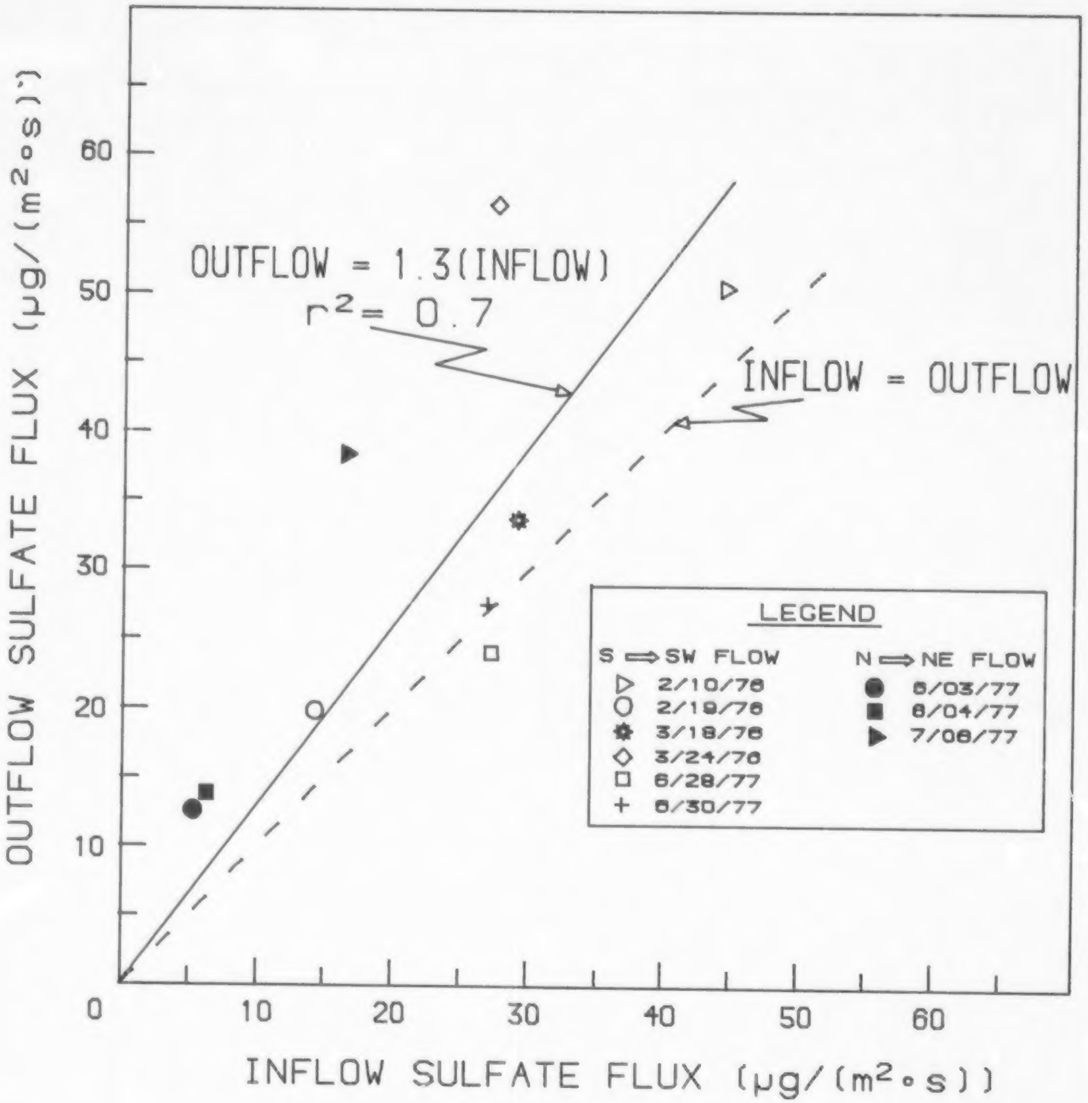

Figure 35. Comparison of inflow to outflow sulfate flux.

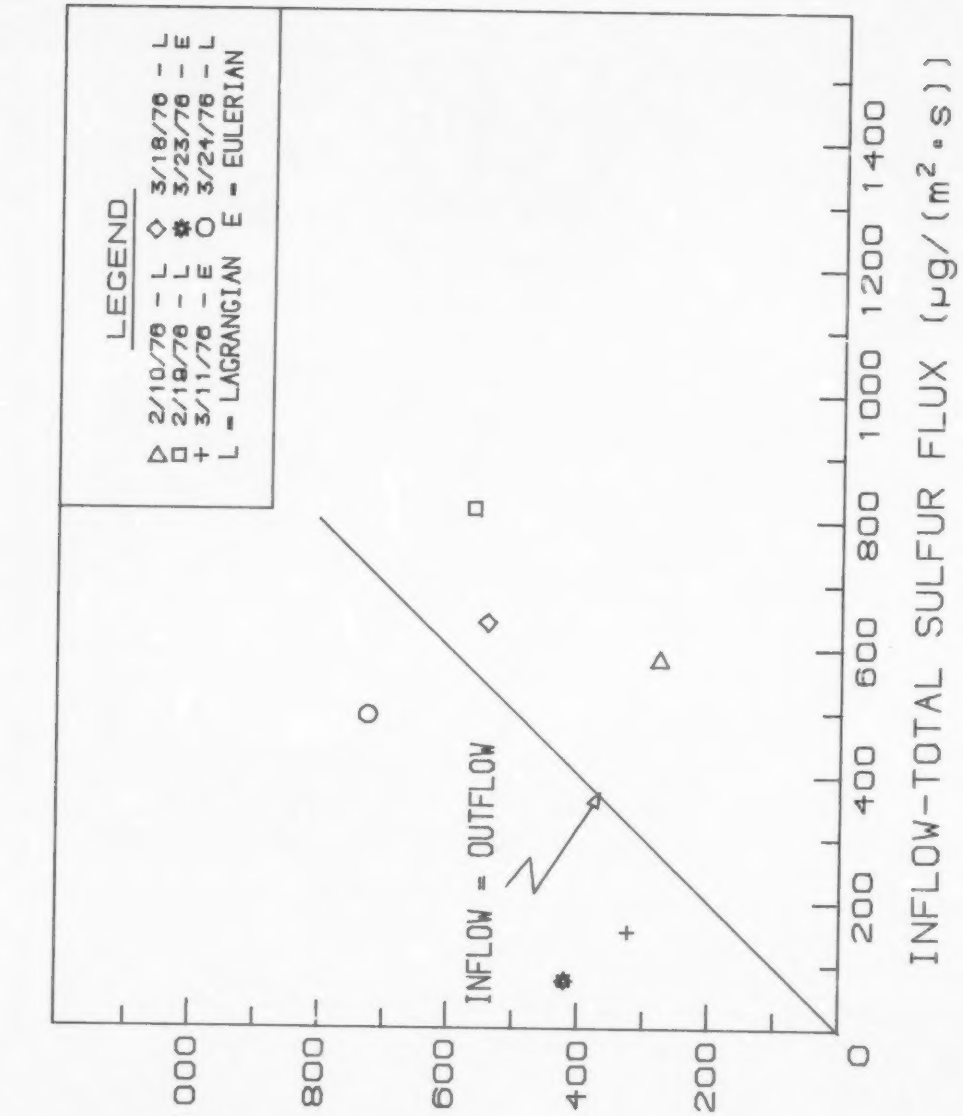

Figure 36. Comparison of inflow to outflow total sulfur flux.

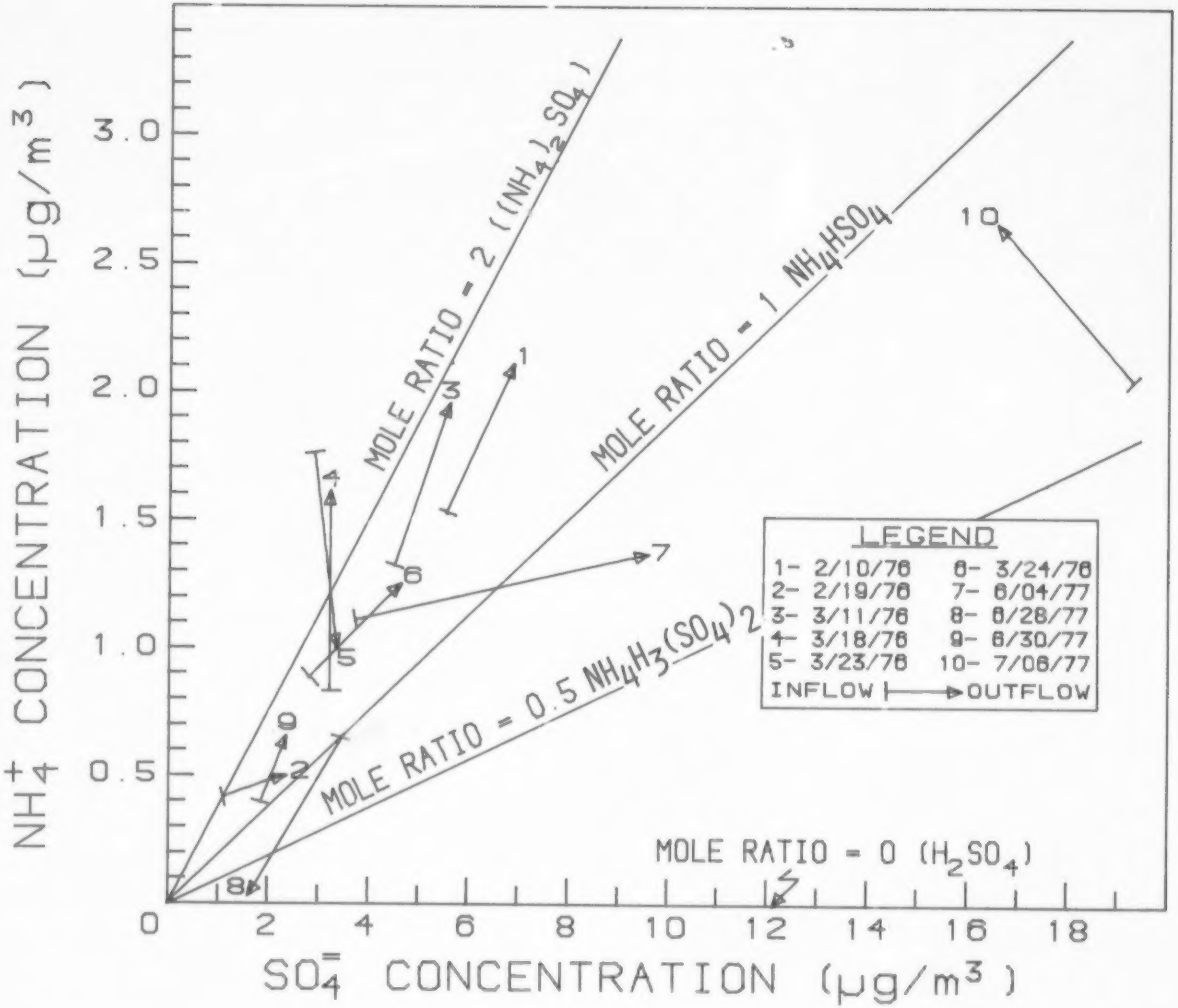

Figure 37. Inflow to outflow concentrations and mole ratio changes.

Nitrate (NO_3^-) concentrations are all below the minimum detectable limit for the 1976 samples, whereas for the one Lagrangian day in 1977, the nitrate averaged 1.1 μg m^{-3} at inflow and 0.6 μg m^{-3} at outflow.

Model Results

Equations (5) and (6) of the Transformation-Transport Model subsection of Section 3 are the analytical models used for the comparisons and predictions of this subsection. Given a set of inflow boundary conditions, superposition was used to account for multiple sources along a trajectory path. The parameters used were specified as $B_o/B = 0.0$, $V_1 = 1.0$ cm/s, $V_2 = 0.5$ cm s^{-1}, K = 0.3 percent per hour; and H was specified as observed for the given day being simulated. The deposition velocities are as suggested by Hicks and Wesley (1978). Although their sulfate deposition velocity is high in comparison with other reported values, it has minor influence on model simulations (see Model Analysis subsection). The SO_2 to $SO_4^=$ transformation rate of 0.3 percent per hour is intentionally low with respect to the recommended value of 2 percent per hour (Husar et al. 1977). This lower rate was selected because it is more representative of actual measurements made within TVA power plant plumes at lower atmospheric temperatures (5 to 10°C) and higher plume dilution ratios (Meagher et al. 1977). Also, chemical transformations within the Tennessee Valley region should proceed at a somewhat slower rate because of the relatively low levels of urban pollutants.

Figure 38 illustrates observed vs. predicted outflow total sulfur (symbols) and sulfate concentrations (small letters). The five days presented were characterized by wind speeds around 8.5 m s^{-1}, mixing heights of 1530 m, and trajectory lengths of 300 km. The predictions are surprisingly good considering the simplicity of the model and model input.

The relative change in total sulfur flux across the TREATS field study region is illustrated in Figure 39. Here the observed data points are represented by circled letters, and the predicted data points (using inflow measured values as boundary conditions) are shown by noncircled letters. Although some of these predicted points are noted as Eulerian, this is only because of the data tagging system used. That is, the model can only yield Lagrangian results. When the modeled results are added, the range of inflow-to-outflow flux values is significantly increased. If the outflow total sulfur flux decreases, as indicated by the limited observed data, then the removal by deposition exceeds TVA's rate of emission, a conclusion supported by the model.

Both observed and predicted inflow-to-outflow sulfate flux are illustrated in Figure 40. This plot indicates that, although the outflow sulfate flux is about twice the inflow flux, the average outflow sulfate concentration is only 5.4 μg m^{-3}.

Model results indicate that sulfur emissions from upwind sources are primarily responsible for the gaseous and particulate flux values measured. The following subsection integrates the results from this and previous subsections in an attempt to identify emission rates and locations of significant upwind sulfur sources.

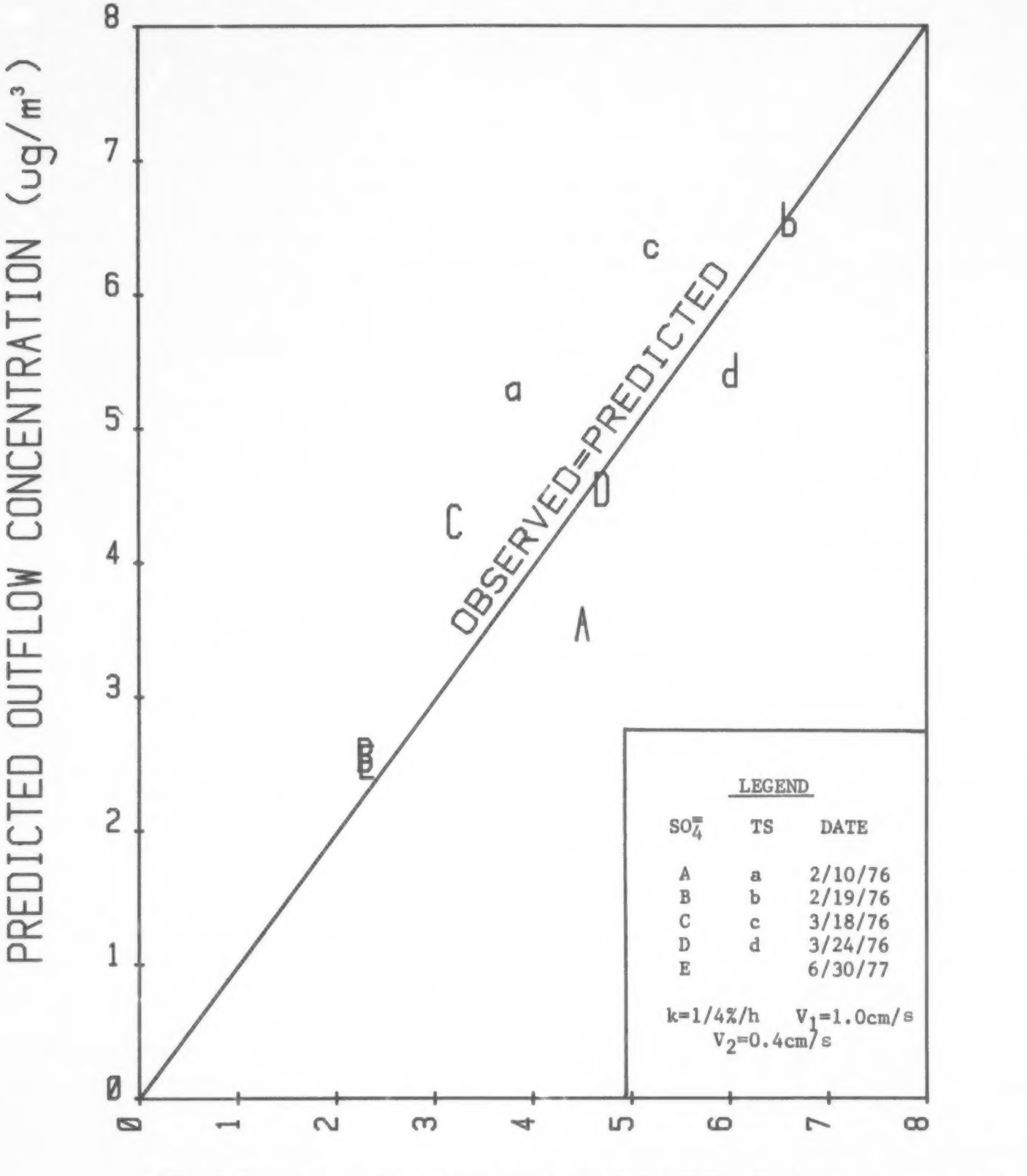

Figure 38. Observed vs. predicted outflow total sulfur (X 10^2) and sulfate concentrations

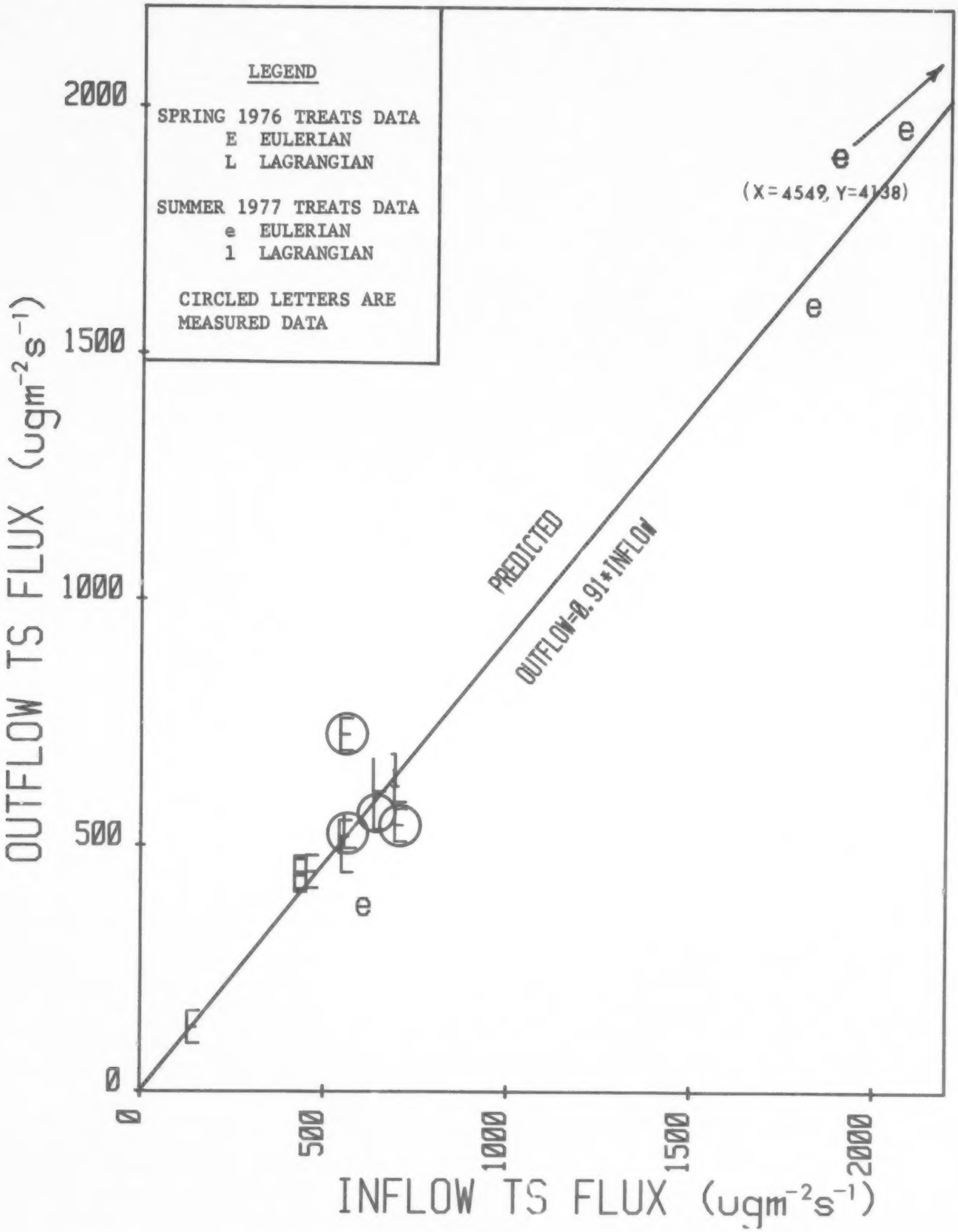

Figure 39. Relative change in total sulfur flux across the TREATS field study region.

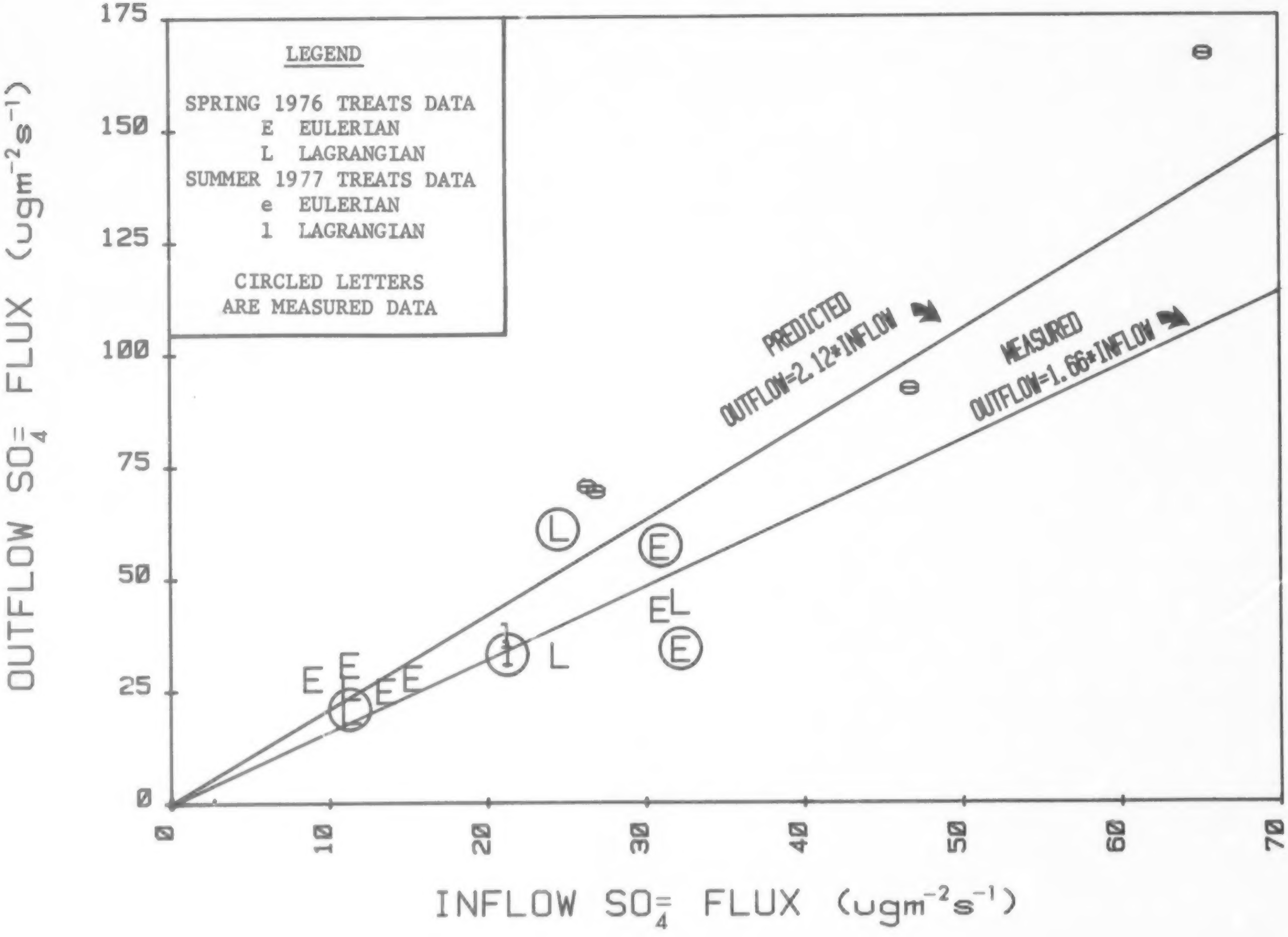

Figure 40. Sulfate flux changes across the TREATS field study region.

Upwind Sources

A large influx of total sulfur pollutants occurs when the flow is southwesterly. This influx is evident from both aircraft (spring and summer studies) and seasonal and annual ground-level sampling (high-volume sulfate data). These inflow (and outflow) fluxes are typically of the same order of magnitude as the regional emission flux contribution. The obvious question is, "What is the location(s) and magnitude of the upwind source region(s)?" In trying to answer this question, we look first at the upwind anthropogenic source regions and second at possible biogenic sources.

An analysis of man-made SO_2 emissions from the southwest quadrant (Figures 2 and 3) shows that no large sulfur sources exist within 500 km of the inflow field study boundary. Further analysis (private communications with B. Gilbert, EPA, Region IV, 1979) reveals that the area from central Texas eastward to the Alabama-Mississippi border, including the States of Arkansas, Louisiana, and Mississippi, has about the same daily SO_2 emission rate as all 12 TVA coal-fired power plants (i.e., ~5000 metric tons/day). To evaluate the significance of these emissions on the inflow measurements made for the four Lagrangian days, the transformation-transport model was used. Average meteorologic and aerometric parameters were used, and all emissions were assumed to originate at the approximate center (i.e., central Louisiana) of the land area included in the upwind source region. Using typical deposition velocities ($V_1 = 1.0$ cm s^{-1}, $V_2 = 0.5$ cm s^{-1}), Equations (5) and (6) show that, on the average, the upwind anthropogenic sources contribute about 50 percent to the measured sulfate flux. Other man-made sources farther upwind also probably contributed to the measured inflow values; however, due to the relatively short half-life of SO_2 (~16 h) and the low measured inflow sulfate flux, emissions from any other sources farther upwind would not be likely to have a very significant effect.

The above results seem to point to a large biogenic source region as the only possible explanation for the high influx readings observed. Various large wetland areas (e.g., inland and tidal marshes, bogs, etc.) exist along the Gulf Coast region of east Texas, Mississippi, Alabama, and Louisiana and in Arkansas (Shaw and Fredine, undated). However, quantification of the relative importance of each type of wetland in producing natural sulfur emissions is limited (Adams et al. 1979). Thus, in a crude attempt to determine whether these extensive wetlands (about 8.6×10^4 km^2) could supply the needed gaseous sulfur, the transformation-transport model was run (using the boundary conditions used in making the anthropogenic calculations) backward in time to estimate the emission rates, airmass age, and average source location needed to explain the concentrations measured. These calculations result in an estimated rate of emission of 2.02 Tg y^{-1} (as SO_2), a mean age of 10 h, and a source distance of about 300 km. The age and distance results compare well with the central location and mean transport times from the principal swampland areas of Louisiana (~500 km). Also, when the estimated emission rate is applied evenly across the wetland areas, the average sulfur emission flux rate from wetlands alone is ~10 g m^{-2} y^{-1}. This estimate is one to two orders of magnitude higher than current approximations of wetland emissions (Adams et al. 1979). However, our estimate does not include emissions from nonwetland soils or emissions from the Gulf of Mexico. Also, as stated by Adams et al., their approximations likely underestimate actual natural emissions due to sampling system losses.

REFERENCES

Adams, D. F.; Farwell, S. O.; Robinson, E.; and Pack, M. R. 1979. *Assessment of biogenic sulfur emissions in the SURE area*. Final report prepared for Electric Power Research Institute, Palo Alto, California; Research Project, 856-1.

Altshuller, A. P. 1973. Atmospheric sulfur dioxide and sulfate--distribution of concentration at urban and nonurban sites in the United States. *Environ. Sci. Technol*. 7:709-712.

Altshuller, A. P. 1976. Regional transport and transformation of sulfur dioxide to sulfates in the U.S. *JAPCA* 26:318.

Bailey, E. M., and Ruddock, H. A. 1979. *Measurements of sulfuric acid at Tennessee Valley Authority coal-fired power plants using the condenser method*. TVA/EP-79/05, Division of Environmental Planning, Tennessee Valley Authority, Muscle Shoals, Alabama.

Bolin, B.; Granat, L.; Ingelstam, L.; Johannesson, M.; Matesson, E.; Oden, S.; Rodhe, H.; and Tamm, C. O. 1971. *Air pollution across national boundaries*. *The impact of sulfur in air and precipitation*. Sweden's Case Study for the United Nations Conference on the Human Environment, P. A. Norstedt and Sons, Stockholm, Sweden.

Bolin, B., and Pearson, C. 1975. Regional dispersion and deposition of atmospheric pollutants with particular application to sulfur pollution over western Europe. *Tellus* 24:281-310.

Braekke, H., Ed. 1976. *Impact of acid precipitation on forest and freshwater ecosystems in Norway*. SNSF Fagrapport FRG, Aas-NCH, Norway.

Coutant, R. W. 1977. Effect of environmental variables on collection of atmospheric sulfate. *Environ. Sci. Technol*. 11:873.

Crawford, T. L. 1977. *Numerical modeling of complex two and three dimensional flow and diffusion problems in the natural air environment*. Ph.D. Thesis, University of Waterloo, Waterloo, Ontario.

Eliassen, A., and Saltbones, J. 1974. Decay and transformation rates of SO_2, as estimated from emission data, trajectories, and measured air concentrations. *Atmos. Environ*. 9:425-429.

Environmental Protection Agency. 1974*a*. *Health consequences of sulfur oxides--a report from CHESS, 1970-1971*. EPA-650/1-74-004.

Environmental Protection Agency. 1974*b*. *Manual of methods for chemical analysis of water and wastes*, pp. 168-174.

Environmental Research and Technology, Inc. 1976. *Design of the Sulfate Regional Experiment (SURE)*. EC-125, vol. IX, prepared for Electric Power Research Institute, Palo Alto, California.

Federal Register. 1978. 43(43):8962-9059.

Frank, N. H. 1974. Temporal and spatial relationships of sulfate, total suspended particulates, and sulfur dioxide. Presented at 67th APCA Annual Meeting, Denver, Colorado.

Friend, J. P. 1973. The global sulfur cycle. Chemistry of the Lower Atmosphere. New York, pp. 177-201.

Gartrell, F. E.; Thomas, F. W.; and Carpenter, S. B. 1963. Atmospheric oxidation of SO_2 in coal-burning power plant plumes. Amer. Ind. Hyg. Assoc. J. 24:113.

Garvey, J. H. 1975. Sulfate monitoring in the town of Huntington, New York--statistical analysis. Engineering Report EN-1405, Long Island Lighting Company.

Gifford, F. A. 1976. Tropospheric relative diffusion observations. J. Appl. Meteorol. 16:311-313.

Hansen, M. H.; Ingvorsen, K.; and Jorgensen, B. B. 1978. Mechanisms of hydrogen sulfide release from coastal marine sediments to the atmosphere. Limnol. Oceanogr. 23:68-76.

Hausknecht, D. F., and Ziskind, R. A. 1975. Effects of sulfur oxides on the lung: An analytical base. Research Project 205, prepared for Electric Power Research Institute, Palo Alto, California.

Hicks, B. B., and Wesley, M. L. 1978. Recent results for particle deposition obtained by the Eddy correlation method. ERC No. 78-12, Argonne National Laboratory.

Hitchcock, D. R. 1975. Dimethyl sulfide emissions to the global atmosphere. Chemosphere 3:137.

Hitchcock, D. R. 1976. Atmospheric sulfates from biological sources. JAPCA 26:210-215.

Holzworth, G. C. 1972. Mixing heights, wind speeds, and potential for urban air pollution throughout the contiguous United States. EPA Pub. No. AP-101, Environmental Protection Agency, Office of Air Programs.

Husar, J. D.; Husar, R. B.; and Stubuts, P. K. 1975. Determination of submicron amounts of atmospheric particulate sulfur. Anal. Chem. 47:2062-2064.

Husar, R. B.; Lodge, J. P.; and Moore, D. J., Eds. 1977. Sulfur in the atmosphere. Dubrovnik Conference, Pergamon Press, Oxford, England.

Jutze, G. A., and Foster, K. E. 1967. Recommended standard method for atmospheric sampling of fine particulate matter by filter media--high-volume sampler. JAPCA 17:17.

Korshover, J. 1976. Climatology of stagnating anticyclones east of the Rocky Mountains, 1936-1975. NOAA Technical Memorandum ERL ARL-55, Air Resources Laboratory, Silver Springs, Maryland.

Liggett, W. S., and Parkhurst, W. J. 1977. Suspended particulates and sulfates at rural locations in the Tennessee Valley. TVA Internal Report I-AQ-77-14, Division of Environmenal Planning, Tennessee Valley Authority, Chattanooga, Tennessee.

Lioy, P. J.; Wolff, G. T.; Czachor, J. S.; Coffey, P. E.; Stasiuk, W. N.; and Romano, D. 1977. Evidence of high atmospheric concentrations of sulfates detected at rural sites in the northeast. J. Environ. Sci. Health A12: 1-14.

Liu, B.H.Y., and Lee, K. W. 1976. Efficiency of membrane and nucleopore filters for submicrometer aerosols. Environ. Sci. Technol. 10:345-350.

Lovelock, J. E.; Maggs, R. J.; and Rasmussen, R. A. 1972. Atmospheric dimethyl sulfide and the natural sulfur cycle. Nature 237:452.

Meagher, J. F.; Stockburger, L., III; Bailey, E. M.; and Huff, O. 1977. Chemical interaction in coal-fired power plant plumes. II. Sulfur dioxide oxidation - a progress report. TVA Internal Report I-AQ-77-20. Division of Environmental Planning, Tennessee Valley Authority, Muscle Shoals, Alabama.

Melo, O. T. 1978. Aerosol and precipitation sampling in southern Ontario - 1976 results. Internal Report No. 78-125-K, Ontario Hydro.

Meteorology Research, Inc. 1972. Integrating nephelometer and recorder - instrument manual. Altadena, California.

Monin, R. S., and Yaglom, A. M. 1971. Statistical fluid mechanics: Mechanics of turbulence, vol. 1. MIT Press, Cambridge, Massachusetts.

Mulik, J.; Puckett, R.; and Sawicki, E. 1976. Ion chromatographic analysis of sulfate and nitrate in ambient aerosols. Anal. Lett. 9:653-663.

Perhac, R. M. 1978. Sulfate regional experiment in Northeastern United States: The "SURE" program. Atmos. Environ. 12:641-647.

Reisinger, L. M., and Crawford, T. L. 1979. August 1976 sulfate episodes in the Tennessee Valley region. TVA/EP-79/04, Division of Environmental Planning, Tennessee Valley Authority, Muscle Shoals, Alabama.

Reisinger, L. M., and Sharma, V. 1977. Regional sulfur dioxide emission inventory. TVA Internal Report I-AQ-77-18, Division of Environmental Planning, Tennessee Valley Authority, Muscle Shoals, Alabama.

Roberts, P. T., and Friedlander, S. K. 1975. Conversion of SO_2 to sulfur particulate in the Los Angeles atmosphere. Environ. Health Perspect. 10:103-108.

Rowe, M. D.; Morris, S. C.; and Hamilton, L. D. 1978. Potential ambient standards for atmospheric sulfates: An account of a workshop. JAPCA 28:772.

Robinson, E., and Robbins, R. C. 1972. Emissions, concentrations and fate of gaseous atmospheric pollutants. *Air pollution control, vol. II*, Strauss, W., Ed., pp. 1-93. Wiley (Interscience), New York.

Scriven, R. A., and Fisher, B.E.A. 1975. The long-range transport of airborne material and its removal by deposition and washout. I. General considerations. *Atmos. Environ.* 9:49-56.

Shaw, S. P., and Fredine, C. G. Undated. *Wetlands of the United States. Circular 39, Fish and Wildlife Service, U.S. Dept of the Interior.*

Smith, F. B., and Jeffrey, G. H. 1975. Airborne transport of sulphur dioxide from the United Kingdom. *Atmos. Environ*. 9:643-659.

Smith, L. F., and Niemann, B. L. 1977. The Ohio River Basin Energy Study: The Future of Air Resources and Other Factors Affecting Energy Development. Paper presented at the Third International Conference on Environmental Problems of the Extractive Industries, Dayton, Ohio.

Teknekron. 1978. An integrated technology assessment of electric utility energy systems. Vol. III: Air quality impact model and results. Teknekron, Inc., Berkeley, California.

Terra, S., and Hilst, G. 1978. SURE takes to the air. *EPRI J.* 12:14-17.

Tony, E. Y., and Batchelder, R. B. 1978. *Compilation and analysis of data sets for the evaluation of regional sulfate models*. Teknekron, Inc., Berkeley, California.

Trijonis, J., and Yvan, K. 1978. *Visibility in the Northeast--long-term visibility trends and visibility/pollutant relationships*. EPA 600/3-78-075, Environmental Protection Agency, Research Triangle Park, North Carolina.

West, P. W., and Gaeke, G. C. 1956. Fixation of sulfur dioxide as sulfitomercurate III and subsequent colorimetric determination. *Anal. Chem*. 28:1816.

Yocom, J. E., and Grappone, N. 1976. *Effects of power plant emissions on materials*. EC-139, Summary report prepared for Electric Power Research Institute, Palo Alto, California.

APPENDIX A

SYNOPTIC WEATHER TYPING

APPENDIX A

SYNOPTIC WEATHER TYPING

A quasi-objective weather typing scheme has been devised. The area of interest is defined by a 500-nautical-mile (nmi) radius from Nashville, Tennessee. Data for five parameters were obtained from NWS daily weather maps for every sixth day for a 5-year period beginning on November 5, 1973. Thus, over 235 data points were generated for each parameter. These five parameters describe (1) predominant frontal systems and associated pressure centers; (2) distance (range) of the most significant pressure center from Nashville, Tennessee; (3) direction from Nashville, Tennessee (degrees from true north) of this pressure center; (4) airmass type (e.g., maritime tropical, continental polar); and (5) relative frequency of measurable precipitation ($\geq$0.01 in.).

These parameters are further divided into categories. These categories and their annual and seasonal distributions are presented in Tables A.1 through A.5.

Annually, 27 percent of the frontal system-pressure center parameter can be described by the high-pressure center (HPC) without front category, while the next most frequent occurrence is divided almost equally between HPC associated with cold fronts west of Nashville or with stationary fronts (~16 percent each). Seasonally, the only significant variation occurs during the summer months, when stationary fronts account for 36 percent of the weather occurrences.

Joint frequency distributions (JFD) between some of the parameters were analyzed. First, comparisons between the distance and pressure-frontal parameters indicate that, although HPC without cold fronts occur most frequently, their relative distance from Nashville is often within a 100- to 399-nmi range (53 percent). Directional considerations indicate that most of the pressure centers within this range (28 percent) occur in the 045- to 089-degree sector. Also, for pressure centers greater than 500 nmi, 46 percent occur within sectors 2 and 3 (045 to 134 degrees), whereas an additional 31 percent occur within sectors 7 and 8 (270 to 359 degrees). Seasonally, the annual JFD varies only slightly for the pressure system defining parameters 1, 2, and 3.

An analysis of the direction and airmass parameters shows that, when pressure centers are southeast of Nashville, there is an 81 percent chance that the airmass type affecting the Tennessee Valley region will be of maritime tropical origin. This, no doubt, is in response to the summertime Bermuda high (48 percent occurrence). For the approximately 50 percent of the time when pressure centers are within a 500-nmi radius of Nashville, Tennessee, the most favored range is from 300 to 399 nmi (16 percent). Except for the range from 0 to 99 nmi (3 percent), the other three categories all occur at about the same frequency (11 percent). Seasonally, summer has the largest frequency (23 percent) for the 300- to 399-nmi range.

TABLE A.1. PERCENT FREQUENCY DISTRIBUTION FOR PRESSURE-FRONTAL PARAMETER

Weather type[a]	Season Winter	 Spring	 Summer	 Fall	Annual
Cold front west with HPC	16	20	11	17	16
Cold front east with HPC	15	8	2	16	10
Cyclone with or without front	5	8	7	0	5
HPC without front	38	26	20	26	27
Stationary front with HPC	11	16	23	17	17
Stationary front with LPC	8	7	13	6	8
Stationary front without pressure center	0	0	7	0	2
East-west cold front south of BNA with HPC	3	7	8	6	6
East-west cold front north of BNA with HPC	3	8	10	12	8

[a] Abbreviations: HPC = high-pressure center; LPC = low-pressure center; BNA = Nashville station.

TABLE A.2. PERCENT FREQUENCY DISTRIBUTION FOR RANGE PARAMETER

Distance (nmi)	Season				Annual
	Winter	Spring	Summer	Fall	
0-99	2	3	2	3	2
100-199	11	18	9	7	11
200-299	8	7	11	12	9
300-399	13	13	23	17	17
400-499	16	13	14	9	13
≥500	49	46	41	52	47

TABLE A.3. PERCENT DISTRIBUTION FOR DIRECTION PARAMETER

Direction (degrees from true north)	Season				
	Winter	Spring	Summer	Fall	Annual
0-44	5	7	4	3	4
45-89	23	25	29	28	26
90-134	13	16	23	16	17
135-179	7	8	13	3	7
180-224	10	10	4	3	6
225-269	13	5	5	10	9
270-314	15	20	9	14	15
315-359	15	10	14	23	16

TABLE A.4. PERCENT DISTRIBUTION FOR AIRMASS TYPE PARAMETER

Airmass type	Season				Annual
	Winter	Spring	Summer	Fall	
Continental polar	21	8	0	10	10
Modified maritime polar	25	15	3	20	16
Maritime tropical	25	44	75	28	42
Modified continental polar	25	30	18	36	27
Modified maritime tropical	5	3	3	6	4

TABLE A.5. PERCENT FREQUENCY DISTRIBUTION FOR RAINFALL PARAMETER

Number of stations recording precipitation	Season				Annual
	Winter	Spring	Summer	Fall	
0	48	41	39	57	46
1	15	10	23	12	15
2	10	20	18	16	16
3	11	11	16	6	11
4	16	18	3	10	12

Pressure center locations occur most frequently (26 percent) in the 045- to 089-degree sector from Nashville; three other sectors (090 to 134 degrees, 270 to 314 degrees, and 315 to 359 degrees) all have occurrences at about the same frequency (16 percent). Again, the most significant departure occurs during the summer, when 52 percent of all pressure centers are located in the 045- to 089-degree and 090- to 134-degree sectors. Also, during the autumn, 51 percent of the directional location is defined by two sectors, the 045- to 089-degree and the 315- to 359-degree sectors. These results indicate the strong influence of the Bermuda high on weather patterns in the southeastern United States.

Annually, the airmass typing parameter is dominated by maritime tropical airmasses (42 percent), with the next most frequent type being modified continental polar (27 percent). Wide variations occur seasonally. Winter is almost equally divided among all the airmass types; spring shows a bias toward maritime tropical (44 percent) and modified continental polar (30 percent); summer is strongly dominated by maritime tropical (75 percent); and autumn has a slight bias toward modified continental polar (36 percent).

Annually, an analysis of the rainfall parameter indicates that 46 percent of the time no rainfall occurs at any of the four stations, and that an almost equal probability exists of having either one or two stations recording measurable precipitation (16 percent).

JFD analysis of the frequency of precipitation vs. airmass type indicates that, when maritime tropical airmasses are affecting the area, a 70 percent chance exists that at least one station will receive measurable precipitation. Conversely, when other airmass types are influencing the area, only a 40-percent chance exists of at least one station receiving measurable precipitation.

APPENDIX B

TABULATION OF TREATS 1976 and 1977 AIRCRAFT FIELD STUDY DATA

ABBREVIATIONS AND UNITS FOR APPENDIX B

DATE	Date of sample, month, day, year
TIME	Midpoint time of sample, h and min
SHIP	Aircraft used for sample, B-deHavilland Beaver U6-A, H-Bell 47A helicopter
XFROM	X-coordinate* at start of sample, km
YFROM	Y-coordinate at start of sample, km
XTO	X-coordinate at end of sample, km
YTO	Y-coordinate at end of sample, km
ELEV	Typical elevation of sample, m AGL
STYPE	Sample type, T (traverse), S (spiral)
SCLASS	Sample classification, I (inflow), O (outflow), N (neither I or O), B [blob (no significant airmass transport)], T (travel from inflow location to outflow and vice versa)
$SO_4^=$	Sulfate ion concentrations, μg m^{-3}
NO_3^-	Nitrate ion concentrations, μg m^{-3}
NH_4^+	Ammonium ion concentrations, μg m^{-3}
TS	Total sulfur concentrations, μg m^{-3} as SO_2
O_3	Ozone concentrations, μg m^{-3}
BSCAT	Atmospheric extinction coefficient due to light scattering by both gases and particulate, E-4 m^{-1}
TEMP	Ambient temperature, °C
DP	Dewpoint temperature, °C

---

*The origin of the coordinate system is Nashville, Tennessee. The Y-axis is rotated 1.8 degrees east of true north.

THREATS AIRCRAFT FIELD STUDY DATA

DATE	TIME	SHIP	XFROM	YFROM	XTO	YTO	ELEV	STYPE	SCLASS	SO4	NO3	NH4	TS	O3	BSCAT	TEMP	DP	COMMENT
10676	1216	B	-204	-186	-88	-186	686	T	I	2.5	0.0	0.6	.	.	.	1.6	.	
10676	1511	B	-88	-186	-204	-186	975	T	I	1.1	0.0	0.3	.	.	.	7.0	.	
21076	915	B	-8	-219	-182	-60	152	T	I	7.6	0.0	2.0	77	.	.	11.0	7.9	SPLIT SAMPLE
21076	917	B	-182	-60	-8	-219	914	T	I	1.7	0.0	0.5	64	.	.	10.4	3.4	
21076	1312	B	-78	-156	30	92	1524	T	T	4.3	0.0	1.2	47	.	.	10.5	-3.3	
21076	1442	B	30	92	128	146	914	T	O	6.0	0.0	1.7	8	.	.	11.1	6.1	
21076	1611	B	128	146	30	92	305	T	O	7.8	0.0	2.4	69	.	.	15.0	8.0	GALLATIN PLUME
21176	1205	B	30	92	-78	-156	610	T	T	1.1	0.0	0.8	71	.	.	6.0	.	TEMP PROFILE DURING SAMPLE
21976	840	B	-101	-156	-147	69	152	T	I	2.3	0.1	0.3	86	209	.	12.0	-0.8	
21976	1019	B	-147	69	-101	-156	914	T	I	0.8	0.0	0.0	80	172	.	8.5	-7.1	
21976	1407	H	76	-151	75	93	914	T	O	2.5	0.1	0.4	88	226	.	8.8	-3.8	
21976	1506	B	-78	-156	79	-151	1676	T	T	1.3	0.0	0.2	87	235	.	9.1	-11.3	SPLIT SAMPLE-SOME MELOY THOUBL
21976	1544	B	75	93	79	-151	1676	T	O	2.1	0.0	0.6	63	188	.	4.8	-5.4	
22076	756	B	-78	-156	92	-160	152	T	I	2.5	0.1	0.6	85	135	.	10.7	-0.9	
22076	927	B	92	-160	-78	-156	914	T	I	0.8	0.0	0.5	69	218	.	12.3	-3.7	
22476	1307	B	-8	-219	-182	-60	610	T	I	2.8	0.0	0.4	.	299	.	12.0	-5.5	SPLIT SAMPLE
22476	1307	A	-182	-60	-8	-219	1219	T	I	1.1	0.0	0.4	.	.	.	15.5	-14.0	
31176	901	A	-8	-219	-182	-60	152	T	I	5.9	0.0	2.0	71	149	.	11.1	4.6	SPLIT SAMPLE
31176	915	A	-182	-60	-8	-219	610	T	I	5.2	0.0	1.4	63	149	.	9.7	2.8	
31176	1222	A	-78	-156	-13	68	1219	T	T	4.3	0.0	1.4	56	157	.	8.0	-1.0	
31176	1340	B	-13	68	128	146	1219	T	O	4.0	0.0	1.6	65	153	.	7.5	-1.2	
31176	1510	A	128	146	-13	68	610	T	O	7.1	0.0	2.1	69	173	.	12.4	3.4	GALLATIN PLUME
31176	1638	B	-13	68	-78	-156	610	T	T	8.3	0.0	2.5	64	177	.	13.2	3.2	
31876	819	A	-119	-156	93	-180	152	T	I	3.7	0.0	0.8	78	126	.	9.1	-3.1	
31876	857	B	-78	-156	93	-180	610	T	I	3.4	0.0	1.0	92	155	.	8.1	-2.9	SPLIT SAMPLE
31876	1213	B	-78	-156	113	2	1676	T	T	2.1	0.0	0.5	87	161	.	4.9	-12.7	TEMP PROFILE DURING SAMPLE
31876	1334	B	113	-12	-14	140	1676	T	O	3.9	0.1	2.0	47	173	.	3.5	.	
31876	1502	A	-14	140	113	-12	914	T	O	2.5	0.0	1.2	57	186	.	10.9	-2.1	GALLATIN PLUME
31876	1636	B	113	2	-78	-156	1067	T	T	3.6	0.9	.0	59	186	.	11.3	-2.9	
31976	709	A	-119	-156	83	-180	305	T	I	3.1	0.6	0.1	58	153	.	11.9	2.4	
31976	739	A	-78	-156	93	-180	610	T	I	2.3	0.0	0.8	57	157	.	11.3	2.4	SPLIT SAMPLE
31976	1125	A	-78	-156	33	-35	762	T	T	5.0	0.2	1.2	59	149	.	12.0	4.8	
32376	823	B	-8	-219	-182	-60	152	T	I	3.9	0.1	1.0	69	145	.	10.8	-3.0	SPLIT SAMPLE
32376	845	B	-182	-60	-8	-219	457	T	I	1.8	0.1	3.2	52	157	.	8.8	-4.6	
32376	1119	A	-78	-156	-14	75	1372	T	T	2.9	0.0	1.5	55	157	.	5.0	-8.0	
32376	1239	A	-14	75	128	146	1219	T	O	3.1	0.0	1.2	54	157	.	4.9	-8.5	
32376	1452	H	128	146	-14	75	610	T	O	3.5	0.0	0.8	59	183	.	12.0	-7.9	GALLATIN PLUME
32376	1630	A	-14	75	-78	-156	610	T	T	4.4	0.1	0.9	62	186	.	14.5	-6.8	
32476	751	H	93	-180	-119	-156	152	T	I	4.0	0.1	1.2	72	153	.	12.3	-2.0	
32476	808	A	-119	-156	93	-180	610	T	I	2.9	0.0	1.0	64	183	.	11.3	-2.6	SPLIT SAMPLE
32476	1113	A	-78	-156	-14	75	610	T	T	4.0	0.0	1.3	62	196	.	11.3	-2.0	
32476	1228	A	-8	75	128	146	610	T	O	5.0	0.1	1.2	62	196	.	12.1	-2.3	GALLATIN PLUME
32476	1436	B	128	146	-8	75	1219	T	O	4.3	0.0	1.3	58	196	.	10.0	-5.1	
32476	1610	A	-14	75	-78	-156	610	T	T	2.3	0.1	0.6	63	196	.	12.9	-2.5	
52077	1341	A	-78	-156	-31	-163	274	T	B	19.3	0.9	3.5	294	.	.	20.0	.	
52077	1422	A	-31	-163	-48	-163	372	T	M	14.2	0.2	2.9	157	.	.	17.9	.	
52077	1451	A	-78	-156	.	.	418	S	B	15.9	0.4	2.4	122	.	.	18.0	.	
52077	1515	H	-61	-158	-27	-171	610	T	M	21.3	0.5	3.6	.	.	.	25.0	11.0	
52077	1541	H	-27	-171	-61	-160	305	T	M	19.2	0.6	3.5	.	.	.	25.0	12.0	
60177	1650	B	-78	-156	40	70	914	T	N	4.5	0.6	0.9	39	246	100	20.0	8.0	
60177	1750	B	40	70	30	92	2896	T	N	0.1	0.2	0.0	.	108	50	5.5	-11.0	
60277	1435	A	30	92	101	167	762	T	I	5.2	0.5	2.0	42	233	100	20.0	9.0	
60277	1505	A	101	167	38	124	1524	T	I	4.3	0.3	2.7	23	180	129	13.0	6.5	
60277	1535	A	76	124	101	167	1981	T	I	5.6	0.2	2.0	.	203	179	8.5	3.5	

TREATS AIRCRAFT FIELD STUDY DATA

DATE	TIME	SHIP	XFROM	YFROM	XTO	YTO	ELEV	STYPE	SCLASS	SO4	NO3	NH4	TS	O3	BSCAT	TEMP	DP	COMMENT
60277	1615	B	101	167	30	92	3048	S	I	6.4	0.4	1.7	.	451	150	8.0	1.0	SPIRAL-10,000' TO 3700'
60377	705	B	30	92	83	46	152	T	I	1.4	0.4	0.3	.	.	100	16.5	8.0	
60377	730	B	83	46	30	92	457	T	I	1.4	0.4	0.5	.	.	76	19.0	7.5	
60377	755	B	30	92	83	46	1067	T	I	1.8	0.4	0.3	.	.	89	15.0	4.5	
60377	825	B	83	46	30	92	1524	T	I	3.1	0.2	0.6	.	.	121	9.0	4.0	
60377	1015	B	30	92	76	7	610	T	I	3.2	0.4	0.8	49	.	111	18.0	8.5	
60377	1045	B	76	7	30	92	1219	T	I	4.2	0.3	1.1	26	.	111	14.5	7.0	
60377	1115	B	30	92	76	7	1646	T	I	0.2	0.2	0.0	12	.	71	12.0	-2.0	
60377	1425	B	30	92	64	23	610	T	I	0.7	0.6	0.3	.	.	.	21.5	8.5	FIRE EXTINGUISHED DISCHARGED
60377	1455	B	64	23	30	92	1128	T	I	2.5	0.9	3.0	.	.	84	17.0	7.5	FIRE EXTINGUISHED DISCHARGED
60377	1525	B	30	92	53	27	1646	T	I	1.8	0.8	0.4	.	.	84	13.0	1.0	FIRE EXTINGUISHER PROBLEMS
60377	1040	H	-78	-156	-131	-117	305	T	O	.	0.1	0.0	.	.	100	22.5	3.0	POWER SUPPLY PROBLEMS
60377	1115	H	-131	-105	-144	-87	305	T	O	12.0	1.2	1.1	.	.	121	22.5	3.0	POWER SUPPLY PROBLEMS
60377	1135	H	-139	-87	-114	-134	1067	T	O	5.2	0.6	1.4	.	.	79	16.0	7.0	POWER SUPPLY PROBLEMS
60377	1425	H	-78	-156	-99	-117	305	T	O	5.6	0.8	2.1	46	.	71	24.5	9.5	
60377	1455	H	-99	-117	-132	-72	305	T	O	4.3	0.6	1.5	68	.	66	24.5	9.0	
60377	1530	H	-132	-72	-105	-114	762	T	O	.	0.1	1.6	82	.	71	20.0	8.5	SO4 QUESTIONABLE
60377	1555	H	-105	-114	-84	-152	762	T	O	4.3	0.5	1.5	88	.	76	20.5	8.5	
60477	640	B	30	92	27	25	152	T	N	5.8	0.6	1.8	.	.	150	20.5	10.5	
60477	715	B	27	25	51	101	457	T	N	2.9	0.2	0.9	.	.	129	21.0	9.5	
60477	740	B	51	101	27	25	1067	T	N	3.0	0.1	1.0	.	.	121	15.5	7.0	
60477	810	B	27	25	51	101	1524	T	N	0.3	0.1	0.0	.	.	61	16.5	-20.0	
60477	1015	B	56	101	28	20	457	T	I	6.6	0.4	2.1	49	.	139	21.0	10.5	
60477	1045	B	28	20	56	101	914	T	I	4.3	0.1	1.3	26	.	150	17.0	9.0	
60477	1115	B	56	101	28	20	1372	T	I	1.9	0.1	0.5	15	.	89	16.0	-2.5	
60477	1145	B	28	20	56	101	1829	T	I	0.1	0.1	0.0	.	.	55	15.5	-20.0	
60477	1425	B	51	101	27	25	457	T	I	7.1	0.3	1.9	32	.	150	24.0	10.0	
60477	1450	B	27	25	51	101	914	T	I	7.9	0.2	2.2	14	.	171	20.0	9.0	
60477	1525	B	51	101	27	25	1372	T	I	6.1	0.3	1.6	.	.	161	16.0	7.5	
60477	1550	B	27	25	51	101	1829	T	I	0.0	0.2	0.0	.	.	55	16.5	-20.0	
60477	610	H	-78	-156	-112	-104	122	T	I	6.5	0.7	1.8	31	.	100	22.0	10.0	
60477	645	H	-112	-104	-78	-156	305	T	I	2.5	0.3	0.6	51	.	71	23.0	8.5	
60477	725	H	-78	-156	-112	-104	610	T	O	4.5	0.5	1.2	67	.	76	20.5	8.5	
60477	755	H	-112	-104	-78	-156	914	T	O	4.2	0.4	1.1	70	.	79	17.5	7.0	
60477	1455	H	-77	-165	-29	-162	762	T	O	7.0	0.6	2.2	55	.	82	22.0	6.5	
60477	1540	H	-29	-162	-78	-156	305	T	O	6.3	0.5	2.0	64	.	84	27.0	7.0	
60577	630	B	30	92	99	23	122	T	N	6.9	0.3	1.8	16	17	300	19.0	14.0	
60577	655	B	99	23	30	92	244	T	N	7.7	0.3	1.8	32	284	200	24.5	11.0	
60577	730	B	30	92	99	23	457	T	N	11.9	0.3	2.3	44	279	200	24.0	9.5	0732 GALLATIN PLUME
60577	800	B	99	23	30	92	1372	T	N	0.5	0.1	0.0	6	200	50	19.0	-14.0	
60577	1015	B	30	92	99	23	457	T	N	3.9	0.8	0.9	56	297	261	24.0	10.5	
60577	1045	B	99	23	30	92	914	T	N	11.9	1.1	3.6	35	273	250	20.0	10.0	
60577	1115	B	30	92	99	23	1372	T	N	9.6	0.2	3.0	.	158	79	19.0	7.0	
60577	1145	B	99	23	30	92	2134	T	N	0.9	0.1	0.0	.	106	61	15.0	2.0	SLIDES 5-8
60577	1415	B	30	92	28	20	610	T	N	14.3	0.5	4.1	36	292	261	25.5	13.0	
60577	1445	B	28	20	30	92	1219	T	N	11.9	0.3	3.3	24	237	326	20.0	12.0	SLIDES 9 & 10
60577	1515	B	30	92	16	40	1829	T	N	1.4	0.0	0.4	.	267	221	15.0	10.5	
60577	615	H	-87	-152	-124	-115	152	T	O	7.6	0.6	1.8	37	.	116	25.0	10.0	
60577	645	H	-124	-115	-87	-152	305	T	O	11.7	0.1	1.6	330	.	139	25.0	9.5	COLBERT PLUME
60577	720	H	-87	-152	-124	-115	762	T	O	.	0.0	0.0	73	.	116	22.0	8.0	
60577	750	H	-124	-115	-81	-152	1524	T	O	9.1	0.7	1.3	77	.	239	15.5	10.5	
60577	1125	H	-78	-156	-48	-125	305	T	O	8.7	0.6	2.5	53	.	145	26.0	13.0	
60577	1150	H	-48	-125	-78	-156	762	T	O	9.2	0.6	3.3	62	.	134	21.0	12.0	
60577	1430	H	-78	-156	-15	-123	1219	T	O	10.9	0.4	2.6	52	.	229	18.5	11.5	

TREATS AIRCRAFT FIELD STUDY DATA

DATE	TIME	SHIP	XFROM	YFROM	XTO	YTO	ELEV	STYPE	SCLASS	SO4	NO3	NH4	TS	O3	BSCAT	TEMP	DP	COMMENT
60577	1530	H	-15	-123	-78	-156	610	T	O	10.7	0.6	0.6	.	.	.	.	.	POWER SUPPLY PROBLEMS
60777	1700	A	-78	-156	30	92	1676	T	N	2.1	0.4	0.6	18	122	79	8.0	-2.0	
60777	900	H	-78	-156	-51	-153	610	T	O	1.1	0.1	0.1	35	.	50	10.5	4.0	
60877	635	A	30	92	16	35	305	T	N	1.0	0.3	0.6	49	.	84	16.5	-1.5	
60877	705	A	16	35	19	114	610	T	N	1.2	0.2	0.5	61	.	89	15.5	1.0	VERY ROUGH MELOY TRACE
60877	730	A	19	114	16	35	1067	T	N	.	0.0	0.0	18	.	111	13.0	2.5	
60877	755	A	16	35	19	114	1676	T	N	1.8	0.2	0.0	.	.	111	9.5	3.5	
60877	1020	A	19	114	16	35	305	T	N	0.3	0.3	0.1	36	140	84	18.5	3.5	
60877	1050	A	16	35	19	114	610	T	N	3.1	0.3	1.3	31	155	100	16.0	3.5	
60877	1120	A	19	114	16	40	914	T	N	3.0	0.3	1.1	.	134	105	13.5	4.0	
60877	1150	A	16	35	30	92	1676	T	N	1.6	0.4	1.1	.	107	95	10.5	2.5	
60877	1530	A	30	92	14	62	1372	T	N	3.2	0.4	1.1	.	.	121	13.0	4.5	
60877	1620	H	14	62	-78	-156	1372	T	N	13.8	0.2	2.8	.	.	161	14.0	3.5	
60877	545	H	-78	-156	-30	-162	91	T	H	3.3	0.8	3.9	30	.	79	15.0	6.0	
60877	625	H	-30	-162	-78	-156	1524	T	H	0.3	0.1	0.0	47	.	29	9.0	-14.5	
60877	700	H	-78	-156	-30	-162	457	T	H	3.4	0.6	0.9	86	.	55	15.5	.	
60877	730	H	-30	-162	-78	-156	914	T	H	1.5	0.3	0.4	73	.	50	12.0	-1.5	
60877	1015	H	-78	-156	-45	-189	1524	T	H	0.3	0.1	0.8	44	.	29	10.0	-15.0	
60877	1050	H	-45	-189	-72	-168	1067	T	H	1.5	0.2	0.5	52	.	45	11.5	-2.0	
60877	1120	H	-72	-168	-45	-189	610	T	H	2.0	0.3	0.8	69	.	58	16.0	2.5	
60877	1155	H	-45	-189	-72	-168	305	T	H	2.9	0.6	0.9	72	.	55	19.5	3.0	
60877	1415	H	-92	-153	.	.	91	S	H	4.8	0.2	1.5	41	.	82	17.0	3.0	300' TO 5000'
60877	1445	H	-90	-146	.	.	91	S	H	8.1	0.3	1.0	532	.	116	18.0	3.0	300' TO 5000'
60877	1550	H	-81	-123	.	.	91	S	H	0.9	0.1	1.2	51	.	71	17.5	4.0	300' TO 5000'
60877	1615	H	-81	-123	-78	-156	1524	T	H	5.9	0.5	2.2	143	.	76	17.0	2.5	5000' TO 100'
61377	1115	A	-77	-165	-45	-189	1067	T	I	2.7	0.6	1.9	41	190	171	23.0	15.5	CLOUDS
61377	1145	A	-45	-189	-77	-165	1372	T	I	3.7	0.3	1.4	22	166	171	20.0	13.5	CLOUDS
61377	1215	A	-78	-156	-36	-195	2286	T	I	3.7	0.2	2.2	.	93	229	12.5	9.0	CLOUDS
61377	1250	H	-36	-195	-77	-165	2286	S	I	2.4	0.2	1.2	.	57	89	10.0	8.0	SPIRAL 7500' TO 1050'
61377	1305	A	-77	-165	.	.	1585	S	I	3.9	0.3	1.7	.	180	229	22.7	17.0	SPIRAL 5200' TO 1250'
61377	1230	H	-78	-156	-45	-189	762	T	I	6.4	0.7	1.5	115	.	129	25.5	17.0	
61377	1305	H	-45	-189	-78	-156	305	T	I	5.2	0.6	1.7	205	.	121	30.0	18.0	
61877	645	H	-77	-165	-40	-191	152	T	I	5.4	0.2	0.0	34	160	300	22.5	19.0	UP AND DOWN OF COLBERT
61877	715	A	-40	-191	-78	-165	914	T	I	0.3	0.0	0.1	22	123	229	20.0	17.5	UP AND DOWN OF COLBERT
61877	1155	H	-78	-165	-47	-149	1050	S	N	2.7	0.1	0.6	.	111	79	15.5	7.0	SPIRAL 2500' TO 9400'
61877	1220	A	-47	-149	.	.	1296	S	N	6.9	0.1	2.0	.	132	89	18.5	13.0	SPIRAL 9400' TO 1000'
61877	1310	A	-11	-137	.	.	1296	S	N	3.4	0.3	1.0	.	134	208	16.5	10.5	SPIRAL 1000' TO 9500'
61877	1335	H	-11	-137	-78	-165	1296	T	N	4.0	0.1	2.3	.	105	250	17.0	12.5	TRAVERSE 9500' TO 1000'
61877	625	H	-78	-156	-39	-191	61	T	I	6.7	0.3	2.3	261	.	321	21.0	20.0	UP AND DOWN OF COLBERT
61877	710	H	-39	-191	-78	-156	305	T	I	12.0	0.3	2.5	366	.	266	23.0	19.0	UP AND DOWN OF COLBERT
61877	1220	H	-54	-163	.	.	762	S	I	5.4	0.9	1.8	201	.	171	23.5	20.0	500' TO 3000'
61877	1305	H	-119	-164	.	.	762	S	I	3.7	0.7	1.0	246	.	134	23.5	20.0	500' TO 3000'
61877	1405	H	-77	-165	-83	-152	457	T	I	5.5	0.7	1.6	281	.	.	25.5	20.5	UP AND DOWN OF COLBERT
62477	1110	A	-29	-162	-57	-109	305	T	N	3.5	0.4	0.8	44	189	161	26.0	20.5	UP AND DOWN OF COLBERT
62477	1135	A	-55	-110	-43	-170	914	T	N	2.8	0.3	0.1	27	141	150	23.0	17.0	UP AND DOWN OF COLBERT
62477	1205	A	-42	-171	-61	-126	1524	T	N	1.6	0.3	0.0	.	87	129	17.5	12.5	UP AND DOWN OF COLBERT
62477	1350	A	16	-159	-9	-111	305	T	N	2.5	0.4	0.6	15	148	139	28.5	18.5	UP AND DOWN OF COLBERT
62477	1415	H	-5	-108	16	-159	914	T	N	6.2	0.4	3.8	.	141	139	24.0	17.0	UP AND DOWN OF COLBERT
62477	1440	H	16	-159	-9	-111	1676	T	N	2.1	0.3	0.6	.	96	150	17.5	13.5	UP AND DOWN OF COLBERT
62477	1520	A	51	-84	74	-130	305	T	N	2.5	0.4	0.1	.	132	139	28.0	18.0	UP AND DOWN OF COLBERT
62477	1550	A	74	-130	51	-84	914	T	N	1.5	0.3	0.1	.	132	139	23.0	16.5	UP AND DOWN OF COLBERT
62477	1655	A	51	-84	74	-124	1524	T	N	1.8	0.3	0.1	.	106	134	18.0	11.0	UP AND DOWN OF COLBERT
62477	1725	A	63	-108	.	.	1676	S	N	2.3	0.4	0.0	.	95	126	24.0	13.5	SPIRAL 5500' TO 1500'
62477	1810	A	11	-108	.	.	1676	S	N	2.2	0.3	0.6	.	104	134	23.5	17.0	SPIRAL 5500' TO 1250'

TREATS AIRCRAFT FIELD STUDY DATA

DATE	TIME	SHIP	XFROM	YFROM	XTO	YTO	ELEV	STYPE	SCLASS	SO4	NO3	NH4	TS	O3	BSCAT	TEMP	DP	COMMENT
62477	1115	H	-123	-189	-162	-165	305	T	I	7.1	1.4	0.2	325	.	66	26.0	20.0	UP AND DOWN OF COLBERT
62477	1145	H	-162	-165	-123	-189	914	T	I	2.0	1.5	0.6	310	.	45	22.0	15.5	UP AND DOWN OF COLBERT
62477	1225	H	-125	-192	-179	-210	152	T	I	3.0	1.7	0.6	260	.	61	29.0	20.5	UP AND DOWN OF COLBERT
62477	1345	H	-180	-211	-216	-170	305	T	I	2.3	1.7	0.2	195	.	45	29.5	19.0	UP AND DOWN OF COLBERT
62477	1415	H	-216	-170	-180	-211	914	T	I	2.3	1.6	0.1	193	.	55	23.5	17.0	UP AND DOWN OF COLBERT
62477	1455	H	-189	-198	.	.	1067	S	I	3.4	1.6	0.1	155	.	79	29.0	17.0	3500' TO 100'
62477	1625	H	-161	-179	.	.	1067	S	I	2.5	1.4	0.5	.	.	45	27.5	18.5	3500' TO 100'
62477	1645	H	-161	-179	-102	-161	610	T	I	1.9	1.4	0.4	.	.	42	28.0	18.0	UP AND DOWN OF COLBERT
62777	1715	B	-67	-134	30	92	1676	T	N	1.2	0.5	0.2	.	88.0	139	17.0	7.0	
62877	710	B	30	92	100	55	152	T	O	1.6	0.5	0.2	33	94.0	171	24.0	19.5	PASS THROUGH GALLATIN PLUME
62877	735	B	100	55	30	92	610	T	O	1.6	0.1	0.0	35	126.0	161	22.5	18.0	
62877	955	B	37	84	132	-75	610	T	O	2.3	0.6	0.3	16	122.0	166	23.0	18.0	
62877	1055	B	132	-75	14	62	1067	T	O	1.9	0.5	0.3	.	111.0	171	20.5	17.0	
62877	1320	B	30	92	26	104	305	T	O	4.1	0.9	1.0	16	104.0	211	27.0	20.5	
62877	1350	B	26	104	60	43	914	T	O	4.8	0.4	1.1	.	185.0	221	22.5	17.0	
62877	1000	H	-90	-137	-96	-62	457	T	I	3.4	3.1	0.3	232	.	97	23.0	19.5	
62877	1050	H	-96	-62	-78	-156	762	T	I	3.4	2.8	0.3	242	.	100	21.5	18.5	
62877	1325	H	-84	-134	-123	-66	457	T	I	4.2	3.3	0.6	132	.	66	25.0	19.0	
62877	1405	H	-123	-66	-116	-98	914	T	I	3.6	3.2	0.7	140	.	79	21.0	17.0	
62877	1430	H	-116	-98	-84	-134	914	T	I	3.9	2.7	0.1	133	.	76	21.5	17.5	
62877	1620	H	-84	-134	-105	-114	457	T	I	3.9	2.6	0.4	89	.	61	26.0	18.5	
62877	1650	H	-105	-114	-83	-134	457	T	I	2.6	1.9	0.0	91	.	79	26.0	18.5	
62877	1725	H	-134	-83	-84	-134	914	T	I	3.7	2.5	0.8	98	.	79	22.0	17.0	
63077	640	B	30	92	162	13	152	T	O	3.9	0.4	1.1	28	135.0	171	25.0	21.0	
63077	715	B	162	13	123	72	610	T	O	3.0	0.3	0.7	20	159.0	134	24.0	19.5	
63077	745	B	123	72	12	80	610	T	O	2.5	0.2	0.9	20	157.0	134	24.5	19.0	
63077	1000	B	30	92	53	84	152	T	O	3.6	0.0	0.5	.	221.0	161	26.0	20.5	
63077	1340	B	127	44	157	-73	457	T	O	3.8	0.3	0.7	16	167.0	139	28.5	19.0	
63077	1345	B	157	-73	127	44	914	T	O	2.4	0.2	0.8	19	158.0	150	25.0	18.5	
63077	1420	B	30	92	64	23	610	T	O	0.7	0.6	0.3	17	.	84	21.5	8.5	
63077	1450	B	64	23	30	92	1128	T	O	2.3	0.9	2.8	5	.	95	17.0	7.5	
63077	600	H	-90	-137	-126	-110	152	T	I	2.7	0.4	0.6	80	.	121	23.5	19.0	
63077	625	H	-126	-110	-167	-90	152	T	I	3.2	1.0	0.0	93	.	134	23.5	20.0	
63077	650	H	-167	-90	-126	-110	610	T	I	2.2	1.1	0.5	106	.	95	24.5	19.0	
63077	715	H	-126	-110	-87	-147	610	T	I	2.3	1.2	0.8	104	.	100	24.0	19.0	
63077	950	H	-81	-150	-112	-104	305	T	I	2.2	1.0	0.7	62	.	129	25.0	21.5	
63077	1020	H	-112	-104	-147	-57	305	T	I	3.5	1.5	0.0	70	.	139	25.0	22.0	
63077	1050	H	-147	-57	-111	-101	610	T	I	2.7	1.0	0.7	78	.	150	22.5	20.5	
63077	1115	H	-111	-101	-83	-147	610	T	I	1.5	0.8	0.5	77	.	129	23.0	20.5	
63077	1320	H	-86	-144	-147	-57	762	T	I	3.6	1.7	0.9	56	.	105	23.5	19.5	
63077	1410	H	-147	-57	-86	-144	305	T	I	3.6	0.1	1.1	60	.	89	28.5	21.0	
70177	1145	B	14	62	0	9	305	T	N	1.9	0.2	0.2	.	.	.	25.5	16.5	CLOUDS AND RAIN (BNA PLUME)
70177	1225	B	0	9	17	-145	457	T	N	4.5	0.2	0.6	.	.	.	25.0	18.0	CLOUDS AND RAIN (BNA PLUME)
70177	610	H	-89	-144	-120	-56	152	T	I	3.4	2.1	0.7	53	.	121	25.0	19.5	
70177	650	H	-120	-56	-89	-144	610	T	I	1.9	1.7	0.2	60	.	100	22.5	18.5	
70577	1020	B	-78	-156	-6	-130	610	T	B	13.2	0.4	2.1	43	28.3	.	28.5	21.0	
70577	1045	B	-6	-130	-12	-28	610	T	B	18.6	0.2	2.8	55	338.0	.	26.5	20.5	
70577	1115	B	-12	-28	14	62	610	T	B	11.6	0.4	2.0	55	237.0	.	25.0	18.5	N'VILLE & POSSIBLY GALL. PLUME
70577	1410	B	36	86	119	44	305	T	B	10.6	0.1	1.0	52	284.0	500	28.5	21.0	
70577	1440	B	119	44	195	24	305	T	B	10.7	0.2	0.9	30	199.0	400	26.5	21.0	
70577	1510	B	195	24	119	44	914	T	B	10.1	0.0	0.7	.	176.0	500	22.5	18.5	
70577	1535	B	119	44	36	86	914	T	B	17.4	0.1	1.3	.	193.0	600	21.0	16.5	
70577	1120	H	-84	-152	-107	-123	610	T	B	17.5	0.4	3.1	.	.	316	22.5	17.0	
70577	1200	H	-141	-105	-84	-152	1128	T	B	13.0	0.4	4.4	173	.	311	20.5	15.0	

TREATS AIRCRAFT FIELD STUDY DATA

DATE	TIME	SHIP	XFROM	YFROM	XTO	YTO	ELEV	STYPE	SCLASS	SO4	NO3	NH4	TS	O3	BSCAT	TEMP	DP	COMMENT
70577	1405	R	-81	-150	-107	-123	610	T	R	4.3	0.1	0.5	157	.	337	27.0	17.5	
70577	1430	R	-107	-123	-153	-96	610	T	B	12.0	0.4	2.0	184	.	200	27.0	16.5	
70577	1455	R	-153	-96	-117	-123	1219	T	R	8.6	0.3	1.6	204	.	229	21.5	15.0	
70577	1525	R	-117	-123	-81	-150	1219	T	R	22.7	0.4	2.4	205	.	413	21.5	16.5	
70677	745	B	36	86	119	44	152	T	I	15.5	0.7	1.9	40	231	479	27.0	21.0	
70677	815	B	119	44	46	74	305	T	I	22.2	0.2	2.6	52	246	550	26.5	19.5	K'VILLE & POSSIBLY GALL. PLUME
70677	845	B	46	74	119	44	610	T	I	21.3	0.1	2.6	.	192	550	24.0	18.0	
70677	920	B	128	46	46	74	1981	T	I	0.1	0.2	0.0	.	95	39	19.0	-5.0	
70677	1225	B	-23	129	-81	113	305	T	I	20.8	0.3	1.8	51	151	461	28.5	20.5	
70677	1255	B	-81	113	-4	131	610	T	I	12.5	0.4	2.2	51	137	500	25.5	20.0	
70677	1510	B	33	88	122	31	305	T	I	20.7	0.3	2.9	54	161	600	29.5	19.5	
70677	1540	B	122	31	51	66	610	T	I	26.4	0.1	2.7	.	146	629	26.0	18.5	
70677	1550	B	51	66	36	86	457	T	I	19.9	0.1	2.1	36	158	550	27.5	18.5	
70677	555	R	-86	-144	-126	-110	152	T	O	19.0	0.5	3.1	89	.	403	28.0	19.0	
70677	630	R	-126	-110	-86	-144	457	T	O	14.2	0.2	3.1	105	.	366	26.5	17.5	
70677	705	R	-86	-144	-126	-110	762	T	O	15.8	0.3	2.4	121	.	434	24.0	17.5	
70677	735	R	-126	-110	-86	-144	1067	T	O	9.3	0.3	1.9	122	.	274	22.0	15.0	
70677	1010	R	-81	-150	-159	-117	152	T	O	19.0	0.8	4.8	76	.	432	29.0	20.5	
70677	1050	R	-159	-117	-81	-150	610	T	O	13.2	0.7	4.0	90	.	445	25.5	19.0	
70677	1400	R	-81	-150	-159	-120	305	T	O	15.7	1.2	5.5	63	.	266	30.5	19.5	
70677	1450	R	-159	-120	-81	-150	762	T	O	16.7	1.2	3.1	81	.	197	26.5	18.0	
70777	635	B	24	91	-67	84	152	T	N	14.6	0.4	2.5	39	116	450	28.5	20.0	
70777	710	B	67	84	24	91	457	T	N	14.0	0.2	2.2	41	128	469	27.0	20.0	
70777	735	B	24	91	-67	84	762	T	N	5.1	0.2	0.3	.	86	200	24.5	18.0	
70777	805	B	-67	84	30	92	457	T	N	18.3	0.1	3.9	28	121	489	27.0	20.0	
70777	1050	B	-14	140	-129	90	305	T	N	14.3	0.2	2.3	34	140	521	28.0	22.0	
70777	1140	B	-129	90	-14	140	914	T	N	8.1	0.1	1.9	.	97	289	24.0	17.0	
70777	1450	B	14	62	0	0	610	T	N	17.4	0.4	2.4	.	155	550	28.0	20.0	
70777	1525	B	-3	-12	-52	-103	610	T	N	13.1	0.1	2.8	.	137	450	28.5	19.0	
70777	1550	B	-52	-103	-67	-142	610	T	N	12.3	0.2	2.0	.	131	411	28.5	19.0	
70777	1015	R	-78	-156	-159	-137	305	T	O	.	0.0	0.0	118	.	534	28.5	19.0	
70777	1100	R	-159	-137	-78	-156	610	T	O	13.6	0.5	3.2	114	.	.	23.5	17.5	
70777	1345	R	-79	-156	-30	-162	152	T	O	19.1	0.7	3.2	65	.	.	32.0	20.5	
70777	1415	R	-30	-162	-78	-156	457	T	O	17.2	0.5	3.2	79	.	.	29.5	20.0	
70777	1445	R	-78	-156	-30	-162	762	T	O	19.9	0.5	2.9	88	.	.	26.0	18.5	
70777	1510	R	-30	-162	-78	-156	1067	T	O	12.3	0.4	2.2	87	.	.	23.5	17.5	
70877	915	B	-77	-156	.	.	152	S	N	17.0	0.2	3.2	.	155	421	23.5	15.0	500' TO 6300'
70877	950	B	-77	-156	.	.	2347	S	N	1.5	0.1	0.3	.	64	61	7.0	-6.5	7700'TO 12900'
70877	1030	B	-77	-156	.	.	2652	S	N	11.3	0.1	2.7	.	131	550	20.0	14.0	8700' TO 1000'
121875	832	B	-78	-156	-354	-34	610	T	I	2.3	0.0	0.5	.	.	.	-14.0	.	
121875	1126	B	-354	-34	-239	132	518	T	I	3.6	0.1	0.7	.	.	.	-12.0	.	
121875	1452	B	-354	-34	-348	-179	762	T	I	0.9	0.1	0.2	.	.	.	-10.0	.	
121875	1546	B	-359	-179	.	.	1067	S	N	1.1	0.1	0.3	.	.	.	-8.0	.	SPIRAL SFC 500'-3500'
121975	925	B	-376	-171	.	.	1219	S	I	1.3	0.1	0.4	.	.	.	-0.5	.	SPIRAL-4000'
121975	1027	B	-369	-193	.	.	1219	S	I	1.4	0.1	0.4	.	.	.	-0.5	.	SPIRAL-4000'
121975	1228	B	-360	-184	-263	-220	305	T	I	1.6	0.1	0.4	.	.	.	0.0	.	
121975	1316	B	-262	-220	-360	-184	610	T	I	1.9	0.1	0.3	.	.	.	-2.0	.	
121975	1405	B	-360	-184	-263	-220	914	T	I	0.9	0.0	0.2	.	.	.	2.0	.	
121975	1452	B	-263	-220	-360	-184	1214	T	I	0.6	0.1	0.2	.	.	.	1.5	.	

N=265

APPENDIX C

ALTITUDE CORRECTION, MELOY MODEL SH202 AND SA285 SULFUR ANALYZER

APPENDIX C

ALTITUDE CORRECTION, MELOY MODEL SH202 and SA285 SULFUR ANALYZER

The flame photometric detector (FPD) is noted for its excellent sensitivity to low background levels of sulfur and its linear logarithmic response over several orders of magnitude. Unfortunately, it is also sensitive--in an instrument-specific manner--to ambient pressure, which is a function of altitude. As a result of this altitude sensitivity, a study was conducted to develop altitude corrections for the Meloy model SH202 and SA285 sulfur analyzers used in the TVA TREATS studies.

Both sulfur analyzers were mounted in an aircraft. The analyzers were connected in parallel with a tee connection and through a 4-way valve to three bags. The Teflon bags were filled with zero air, and low and high background concentrations of SO_2. The fourth valve position sampled cabin air.

An initial reference response was obtained from each bag while sitting on the runway at 152 m MSL. Additional responses to the three bagged gases were obtained at 762 and 1370 m MSL. Results from the test are given in Table C.1.

TABLE C.1. MELOY SH202 ALTITUDE TEST

Elevation (m MSL)	Analyzer response (ppb as SO_2)					
	Model SH202[a]			Model 285		
	Zero	Low	High	Zero	Low	High
152	4.4	20.2	127	0	23	125
762	2.3	20.4	116	-5.1	16.5	120
1370	2.6	16.7	110	-0.65	15.8	115

[a] SH202 response based on March 4, 1976, calibration (i.e., $c = 2706A^{0.61134}$).

Modeling Altitude Response

The change in response (parts per billion as SO_2) of the flame photometric detector as pressure drops is characterized by a decrease in baseline current and a reduction in detector sensitivity. For the SH202 FPD, both the zero shift and reduction in sensitivity were significant. These effects were most severe at low concentrations. For the SA285, only the zero shift with altitude was significant.

The corrected SH202 response is well described by the equation,

$$C = C' + 0.46 + 0.000128 (Z - 152) C',$$

where

C' = uncorrected response, ppb,
C = altitude corrected response, ppb, and
Z = elevation, m MSL.

This model explains 98 percent of the altitude variation, and has a standard error of 1.2 ppb. This is well within the accuracy of the instrument and usual calibration procedures.

The corrected SA285 response is well described by the equation,

$$C = C' - 0.6 + 0.00716 (Z - 152),$$

where

C' = uncorrected response, ppb,
C = altitude corrected response, ppb, and
Z = elevation, m MSL.

This model explains 95 percent of the altitude variation, again well within the accuracy of the instrument and usual calibration procedures.

All total sulfur readings were corrected with these models.

APPENDIX D

TABULATION OF TREATS 1976 AND 1977 HIGH-VOLUME FIELD STUDY DATA

ABBREVIATIONS AND UNITS FOR APPENDIX D

DATE	Date of sample, month of year
STATION	Name of station
LOCATION	Classification, I (inflow), O (outflow), N (neither I nor O)
X,Y*	Coordinate location of high-volume sampler, km
TSP	Total suspended particulate concentration, μg m^{-3}
$SO_4^=$	Suspended water-soluble sulfates, μg m^{-3}
N	Number of samples averaged for station
DURATION	Average duration of sample, h

---

*The origin of the coordinate system is Nashville, Tennessee. The Y-axis is rotated 1.8 degrees east of north.

TREATS 1976 & 1977 HIGH-VOLUME FIELD STUDY DATA

DATE	STATION	LOCATION	X	Y	TSP	SO4	N	DURATION
21076	LBL	O	-118	71	18.0	9.0	1	9.0
21076	JOHNSONVILLE	N	-105	-18	33.5	7.5	2	9.0
21076	CUMBERLAND	N	-83	24	36.5	7.5	2	9.0
21076	PARADISE	O	-30	114	29.5	7.5	2	9.0
21076	GALLATIN	N	27	24	39.0	8.5	2	9.0
21076	WIDOWS CREEK	O	90	-144	30.5	10.5	2	9.0
21976	LBL	O	-118	71	41.0	5.0	1	24.0
21976	JOHNSONVILLE	N	-105	-18	76.0	15.0	1	24.0
21976	COLBERT	I	-99	-159	37.5	3.0	2	24.0
21976	CUMBERLAND	N	-83	24	61.5	3.0	2	24.0
21976	GILES	N	-24	-108	54.0	4.0	1	24.0
21976	GALLATIN	O	27	24	53.0	2.5	2	24.0
21976	WIDOWS CREEK	N	90	-144	50.5	3.0	2	24.0
22076	LBL	O	-118	71	50.0	8.0	1	9.0
22076	JOHNSONVILLE	N	-105	-18	39.0	5.0	1	9.0
22076	COLBERT	I	-99	-159	44.5	7.0	2	9.0
22076	CUMBERLAND	N	-83	24	45.0	6.0	2	9.0
22076	PARADISE	O	-30	114	77.5	6.5	2	9.0
22076	GILES	N	-24	-108	34.0	13.0	1	9.0
22076	GALLATIN	N	27	24	49.0	6.0	1	9.0
22076	WIDOWS CREEK	I	90	-144	38.0	9.0	2	9.0
22476	LBL	N	-118	71	23.0	2.0	1	24.0
22476	JOHNSONVILLE	N	-105	-18	24.0	3.0	2	24.0
22476	COLBERT	I	-99	-159	19.0	2.5	2	24.0
22476	CUMBERLAND	N	-83	24	30.0	2.5	2	24.0
22476	PARADISE	O	-30	114	87.0	4.0	2	24.0
22476	GILES	N	-24	-108	32.0	4.0	1	24.0
22476	GALLATIN	N	27	24	34.0	4.0	2	24.0
22476	WIDOWS CREEK	N	90	-144	29.5	3.5	2	24.0
31176	LBL	N	-118	71	14.0	5.0	1	9.0
31176	JOHNSONVILLE	N	-105	-18	27.5	8.5	2	9.0
31176	COLBERT	I	-99	-159	28.0	5.5	2	9.0
31176	CUMBERLAND	N	-93	24	38.5	9.0	2	9.0
31176	PARADISE	O	-30	114	63.5	13.0	2	9.0
31176	GILES	N	-24	-108	12.0	4.0	1	9.0
31176	GALLATIN	N	27	24	47.0	12.0	2	9.0
31176	WIDOWS CREEK	O	90	-144	189.5	12.5	2	9.0
31876	LBL	N	-118	71	33.0	3.0	1	24.0
31876	JOHNSONVILLE	N	-105	-18	48.0	5.5	2	24.0
31876	COLBERT	I	-99	-159	35.5	5.5	2	24.0
31876	CUMBERLAND	N	-83	24	43.0	5.0	2	24.0
31876	PARADISE	O	-30	114	70.0	5.5	2	24.0
31876	GILES	N	-24	-108	37.0	6.0	1	24.0
31876	GALLATIN	N	27	24	72.0	5.0	1	24.0
31876	WIDOWS CREEK	O	90	-144	43.0	6.5	2	24.0
31976	LBL	O	-118	71	24.0	6.0	1	9.0
31976	JOHNSONVILLE	N	-105	-18	68.5	9.5	2	4.5
31976	COLBERT	I	-99	-159	24.5	5.5	2	9.0
31976	CUMBERLAND	N	-83	24	67.0	9.0	1	9.0
31976	PARADISE	O	-30	114	60.5	9.5	2	9.0
31976	GILES	N	-24	-108	47.0	11.0	1	9.0
31976	GALLATIN	N	27	24	55.5	11.0	2	4.5
31976	WIDOWS CREEK	I	90	-144	11.0	5.0	1	9.0
32376	LBL	O	-118	71	30.0	10.0	1	9.0

TREATS 1976 & 1977 HIGH-VOLUME FIELD STUDY DATA

DATE	STATION	LOCATION	X	Y	TSP	SO4	N	DURATION
32376	JOHNSONVILLE	N	-105	-18	29.5	4.5	2	9.0
32376	COLBERT	I	-99	-159	74.0	7.0	2	9.0
32376	CUMBERLAND	N	-83	24	31.0	4.0	2	9.0
32376	PARADISE	O	-30	114	50.0	4.0	2	9.0
32376	GILES	N	-24	-108	29.0	7.0	1	9.0
32376	GALLATIN	N	27	24	50.0	6.5	2	9.0
32376	WIDOWS CREEK	I	90	-144	87.0	9.0	2	9.0
32476	LBL	O	-118	71	35.0	4.0	1	24.0
32476	JOHNSONVILLE	N	-105	-18	42.0	6.0	2	24.0
32476	COLBERT	I	-99	-159	43.5	7.0	2	24.0
32476	CUMBERLAND	N	-83	24	41.5	5.0	2	24.0
32476	PARADISE	O	-30	114	66.0	6.0	1	24.0
32476	GILES	N	-24	-108	50.0	5.0	1	24.0
32476	GALLATIN	N	27	24	53.0	5.5	2	24.0
32476	WIDOWS CREEK	I	90	-144	37.0	5.5	2	24.0
60277	SHAWNEE	I	-176	101	77.5	9.0	2	9.0
60277	JOHNSONVILLE	N	-105	-18	58.5	10.0	2	9.0
60277	COLBERT	O	-99	-159	57.0	12.0	2	9.0
60277	CUMBERLD.	N	-83	24	27.0	5.5	2	9.0
60277	HENDERSON		-72	186	58.0	1.0	1	8.0
60277	OWENSBORO		-36	176	118.0	9.0	1	6.8
60277	BOWLING GREEN		29	92	46.0	6.0	1	8.0
60277	WIDOWS CREEK	O	90	-144	53.5	6.0	2	9.0
60277	KINGSTON	O	203	-26	40.0	8.5	2	9.0
60377	SHAWNEE	O	-176	101	81.0	10.5	2	9.0
60377	JOHNSONVILLE	N	-105	-18	61.5	8.0	2	9.0
60377	COLBERT	O	-99	-159	75.5	17.0	2	9.0
60377	CUMBERLD.	N	-83	24	60.0	9.0	2	9.0
60377	HENDERSON	I	-72	186	0.0	0.0	1	8.0
60377	OWENSBORO	I	-36	176	117.0	11.0	1	9.3
60377	PARADISE	I	-30	114	69.0	3.0	2	8.7
60377	GILES COUNTY	O	-24	-108	49.0	13.0	1	9.0
60377	BOWLING GREEN	I	29	92	45.0	1.0	1	8.0
60377	WIDOWS CREEK	O	90	-144	109.0	11.0	2	9.0
60377	KINGSTON	N	203	-26	82.5	11.0	2	9.0
60477	SHAWNEE	N	-176	101	114.5	18.5	2	9.0
60477	JOHNSONVILLE	N	-105	-18	77.0	19.5	2	9.0
60477	COLBERT	O	-99	-159	75.0	12.0	2	9.0
60477	CUMBERLD.	N	-83	24	64.0	12.0	2	9.0
60477	PARADISE	I	-30	114	97.0	14.5	2	9.0
60477	GILES COUNTY	N	-24	-108	18.0	4.0	1	9.0
60477	WIDOWS CREEK	O	90	-144	96.0	14.0	2	9.0
60477	KINGSTON	N	203	-26	76.5	10.5	2	9.0
60577	SHAWNEE	I	-176	101	94.0	11.5	2	9.0
60577	JOHNSONVILLE	N	-105	-18	71.5	12.5	2	9.0
60577	COLBERT	N	-99	-159	103.5	17.0	2	9.0
60577	CUMBERLD.	N	-83	24	77.0	8.5	2	9.0
60577	PARADISE	N	-30	114	98.0	9.5	2	9.0
60577	GILES COUNTY	O	-24	-108	63.0	18.0	1	9.0
60577	WIDOWS CREEK	O	90	-144	205.5	23.0	2	9.0
60577	KINGSTON	O	203	-26	65.0	14.0	1	9.0
60877	SHAWNEE	I	-176	101	165.5	7.5	2	9.0
60877	JOHNSONVILLE	I	-105	-18	54.5	6.0	2	9.0
60877	COLBERT	B	-99	-159	50.5	9.0	2	9.0

TREATS 1976 & 1977 HIGH-VOLUME FIELD STUDY DATA

DATE	STATION	LOCATION	X	Y	TSP	SO4	N	DURATION
60877	CUMBERLD.	I	-83	24	85.0	7.5	2	9.0
60877	HENDERSON	N	-72	186	97.0	5.0	1	8.0
60877	OWENSBORO	N	-36	176	163.0	2.0	1	8.7
60877	PARADISE	N	-30	114	115.0	8.5	2	9.0
60877	GILES COUNTY	N	-24	-108	62.0	11.0	1	9.0
60877	BOWLING GREEN	N	29	92	110.0	4.0	1	8.0
60877	WIDOWS CREEK	B	90	-144	130.5	14.5	2	9.0
60877	KINGSTON	O	203	-26	38.5	7.0	2	9.0
61377	HENDERSON	I	-72	186	69.0	10.0	1	24.0
61377	OWENSBORO	I	-36	176	118.0	31.0	1	9.3
61377	BOWLING GREEN	I	29	92	408.0	5.0	1	8.0
61777	SHAWNEE	N	-176	101	31.5	6.5	2	9.3
61777	JOHNSONVILLE	N	-105	-18	20.0	7.5	2	9.0
61777	CUMBERLD.	I	-83	24	22.0	6.5	2	9.0
61777	HENDERSON	O	-72	186	78.0	2.0	1	8.2
61777	OWENSBORO	O	-36	176	140.0	3.0	1	9.0
61777	PARADISE	O	-30	114	39.0	11.5	2	8.9
61777	GILES COUNTY	O	-24	-108	29.0	7.0	1	9.0
61777	BOWLING GREEN	O	29	92	66.0	6.0	1	8.0
61777	WIDOWS CREEK	N	90	-144	32.0	9.5	2	8.8
61777	KINGSTON	O	203	-26	51.5	14.0	2	9.0
61877	SHAWNEE	I	-176	101	65.3	8.6	4	24.0
61877	LBL	I	-118	71	39.0	7.9	1	24.0
61877	JOHNSONVILLE	I	-105	-18	30.2	8.7	5	24.0
61877	COLBERT	I	-99	-159	33.0	8.4	4	24.0
61877	CUMBERLAND	I	-83	24	45.3	10.6	6	24.0
61877	DACD	N	-81	-156	36.0	9.3	2	24.0
61877	PARADISE	O	-30	114	63.3	13.3	6	24.0
61877	GILES	N	-24	-108	35.0	10.6	1	24.0
61877	GALLATIN	O	27	24	32.3	9.8	4	24.0
61877	HYTOP	N	63	-138	35.0	10.2	1	24.0
61877	WIDOWS CREEK	O	90	-144	60.2	14.1	6	24.0
61877	KINGSTON	O	203	-26	55.5	17.1	2	24.0
62477	SHAWNEE	I	-176	101	50.5	6.2	4	24.0
62477	LBL	I	-118	71	40.0	4.5	1	24.0
62477	JOHNSONVILLE	I	-105	-18	44.2	7.1	5	24.0
62477	COLBERT	I	-99	-159	63.4	4.5	5	24.0
62477	CUMBERLAND	I	-83	24	64.0	6.0	7	24.0
62477	DACD	N	-81	-156	96.0	5.8	2	24.0
62477	HENDERSON	O	-72	186	41.0	7.0	1	8.5
62477	OWENSBORO	O	-36	176	163.0	4.0	1	9.1
62477	PARADISE	O	-30	114	42.0	6.8	5	24.0
62477	GILES	N	-24	-108	82.0	6.8	1	24.0
62477	GALLATIN	O	27	24	63.8	8.7	4	24.0
62477	BOWLING GREEN	O	29	92	71.0	12.0	1	8.0
62477	HYTOP	N	63	-138	89.0	4.6	1	24.0
62477	WIDOWS CREEK	O	90	-144	100.7	9.4	6	24.0
62477	KINGSTON	O	203	-26	36.0	9.8	4	24.0
62877	SHAWNEE	N	-176	101	120.0	8.5	2	9.0
62877	JOHNSONVILLE	N	-105	-18	126.0	6.0	2	9.0
62877	COLBERT	O	-99	-159	127.0	20.0	2	9.0
62877	CUMBERLD.	N	-83	24	144.0	8.5	2	9.0
62877	HENDERSON	I	-72	186	125.0	12.0	1	8.8
62877	OWENSBORO	I	-36	176	259.0	6.0	1	8.3

TREATS 1976 & 1977 HIGH-VOLUME FIELD STUDY DATA

DATE	STATION	LOCATION	X	Y	TSP	SO4	N	DURATION
62877	PARADISE	I	-30	114	151.5	7.5	2	9.0
62877	GILES COUNTY	N	-24	-108	136.0	15.0	1	9.0
62877	BOWLING GREEN	I	29	92	69.0	2.0	1	8.0
62877	WIDOWS CREEK	N	90	-144	120.5	7.0	2	9.0
62877	KINGSTON	N	203	-26	71.0	6.0	2	9.0
63077	SHAWNEE	I	-176	101	59.5	7.1	4	24.0
63077	LBL	I	-118	71	46.0	3.7	1	24.0
63077	JOHNSONVILLE	I	-105	-18	45.5	7.6	6	24.0
63077	COLBERT	I	-99	-159	63.6	5.3	5	24.0
63077	CUMBERLAND	I	-83	24	39.4	6.9	7	24.0
63077	OACD	N	-81	-156	64.5	4.7	2	24.0
63077	HENDERSON	O	-72	186	110.0	13.0	1	8.2
63077	OWENSBORO	O	-36	176	200.0	4.0	1	9.0
63077	PARADISE	O	-30	114	65.0	10.2	5	24.0
63077	GILES	N	-24	-108	44.0	8.4	1	24.0
63077	GALLATIN	O	27	24	58.5	10.0	4	24.0
63077	BOWLING GREEN	O	29	92	76.0	2.0	1	8.0
63077	HYTOP	N	63	-138	39.0	5.0	1	24.0
63077	WIDOWS CREEK	O	90	-144	63.8	9.4	5	24.0
63077	KINGSTON	O	203	-26	60.8	12.7	4	24.0
70577	SHAWNEE	O	-176	101	92.0	19.0	2	9.0
70577	JOHNSONVILLE	N	-105	-18	90.0	30.0	2	9.0
70577	COLBERT	I	-99	-159	116.5	25.0	2	9.0
70577	CUMBERLD.	N	-83	24	91.5	27.5	2	9.0
70577	PARADISE	O	-30	114	132.5	29.5	2	6.9
70577	GILES COUNTY	I	-24	-108	97.0	29.0	1	9.0
70577	WIDOWS CREEK	I	90	-144	123.0	24.0	2	9.0
70577	KINGSTON	N	203	-26	88.5	25.0	2	9.0
70677	SHAWNEE	I	-176	101	101.5	25.9	4	24.0
70677	JOHNSONVILLE	N	-105	-18	131.7	38.2	6	24.0
70677	COLBERT	O	-99	-159	101.8	27.6	5	24.0
70677	CUMBERLAND	N	-83	24	123.4	32.6	5	24.0
70677	OACD	O	-81	-156	108.0	29.8	1	24.0
70677	PARADISE	I	-30	114	129.8	25.2	5	24.0
70677	GILES	O	-24	-108	88.0	27.6	1	24.0
70677	GALLATIN	N	27	24	99.3	29.0	3	24.0
70677	HYTOP	O	63	-138	66.0	17.9	1	24.0
70677	WIDOWS CREEK	O	90	-144	97.5	27.8	6	24.0
70677	KINGSTON	N	203	-26	103.3	26.8	4	24.0
70777	SHAWNEE	I	-176	101	80.7	13.3	3	9.0
70777	JOHNSONVILLE	N	-105	-18	90.0	28.0	2	9.0
70777	COLBERT	O	-99	-159	134.5	25.5	2	9.0
70777	CUMBERLD.	N	-83	24	116.5	29.5	2	9.0
70777	PARADISE	N	-30	114	141.0	25.0	2	9.0
70777	GILES COUNTY	N	-24	-108	146.0	42.0	1	9.0
70777	WIDOWS CREEK	O	90	-144	207.0	33.5	2	9.0
70777	KINGSTON	O	203	-26	91.5	29.5	2	9.0

N=209

APPENDIX E

INVERSION HEIGHTS AND AVERAGE WIND VELOCITIES FOR LAGRANGIAN AND EULERIAN DAYS

ABBREVIATIONS AND UNITS FOR APPENDIX E

Sampling class: I = inflow, 0 = outflow

Inversion type: R = radiation; S = subsidence

Station : BNA = Nashville, TN (NWS)
JSV = Johnsonville Steam Plant, New Johnsonville, TN
KIN = Kingston Steam Plant, Kingston, TN
COL = Colbert Steam Plant, Pride, AL
PAR = Paradise Steam Plant, Drakesboro, KY
GAL = Gallatin Steam Plant, Gallatin, TN
WID = Widows Creek Steam Plant, Bridgeport, AL

Wind velocity : Angle defines average direction from which wind is blowing. Directions in degrees from true north, speed in meters per second. Numbers in parentheses are the resultant wind through the transport layer.

TABLE E.1 INVERSION HEIGHTS AND AVERAGE WIND VELOCITIES FOR LAGRANGIAN AND EULERIAN DAYS

Date	Sampling class	Time (L)	Upper air station	Inversion height (type) (m AGL)	Wind velocity (m s^{-1})	Layer (m)
2/10/76	I	0515	BNA	626 (S)	(219/14.0)	SFC-626
	O	1345	JSV	915 (S)		SFC-915
	O	1715	BNA		(215/13.2)	SFC-915
2/19/76	I	0810	COL	244 (R)		
	I	0930	JSV		237/4.7	SFC-244
	I	0810	COL	1829 (S)		
	I	0930	JSV		278/13.8	245-1829
	I	0930	JSV		(276/12.4)	SFC-1829
	O	1643(avg)	BNA & WID	1900 (S)	(269/6.9)	SFC-1900
3/11/76	I	0815	COL	366 (R)		
	I	0830	COL		232/2.0	SFC-366
	I	1015	JSV	1829 (S)	235/2.7	367-1829
	I	0923(avg)	COL & JSV		(235/2.6)	SFC-1829
	O	1530(avg)	JSV & BNA	1250 (S)	(183/5.2)	SFC-1250
3/18/76	I	0655	WID & COL	519 (R)	230/8.4	SFC-519
	I	0815	COL	1524 (S)		
	I	0655(avg)	WID & COL		249/10.3	520-1524
	I	0655(avg)	WID & COL		(243/9.5)	SFC-1524
	O	1340	JSV	1372 (S)		
	O	1700	BNA		(212/12.2)	SFC-1372
3/23/76	I	0815	COL	305 (R)		
	I	0810			086/2.1	SFC-305
	I	0815	COL	1219 (S)		
	I	0810			021/1.3	306-1219
	I	0810	COL		(043/1.3)	SFC-1219
	O	1705	BNA	1767 (S)		
	O	1415	JSV		(213/6.6)	SFC-1767

TABLE E.1 (continued)

Date	Sampling class	Time (L)	Upper air station	Inversion height (type) (m AGL)	Wind velocity (m s^{-1})	Layer (m)
3/24/76	I	0655(avg)	COL & WID	564 (R)		
	I	0825(avg)	COL & WID		192/6.9	SFC-564
	I	0655(avg)	COL & WID	1752 (S)	197/9.9	565-1752
	I	0655(avg)	COL & WID		(196/8.9)	SFC-1752
	O	1332	JSV	1829 (S)		
	O	1315(avg)	JSV & KIN		(201/10.6)	SFC-1829
6/03/77	I	0640(avg)	PAR & BNA	305 (R)	061/6.0	SFC-305
	I	0615	PAR	1646 (S)	348/6.3	306-1676
	I	0630(avg)	PAR & BNA		(358/5.6)	SFC-1676
	I	0950	JSV	1646 (S)		
	I	0805	JSV		(064/3.9)	SFC-1646
	I	1600(avg)	JSV & BNA	1524 (S)		
	I	1605	JSV		(046/2.2)	SFC-1524
	O	0845	COL	366 (R)		
	O	1110	COL		068/2.7	SFC-366
	O	0845	COL	1645 (S)		
	O	1110	COL		009/5.2	SFC-1645
	O	1110	COL		(016/4.4)	SFC-1645
	O	0950	JSV	1646 (S)		
	O	1110	COL		(016/4.4)	SFC-1646
	O	1400	JSV	1524 (S)		
	O	1510	COL		(009/2.8)	SFC-1524
6/04/77	I	0650	GAL	457 (R)		
	I	0630	GAL		125/2.9	SFC-457
	I	0650	GAL	1219 (S)		
	I	0630	GAL		145/1.0	458-1219
	I	0630	GAL		(132/1.7)	SFC-1219
	I	1015	JSV	1128 (S)		
	I	1200	JSV		(020/1.4)	SFC-1128
	I	1435(avg)	JSV, COL, & BNA	1433 (S)		
	I	1325	JSV		(349/2.3)	SFC-1433

TABLE E.1 (continued)

Date	Sampling class	Time (L)	Upper air station	Inversion height (type) (m AGL)	Wind velocity (m s^{-1})	Layer (m)
6/04/77 (Cont.)	O	0845	COL	366 (R)		
	O	0725	COL		(124/2.6)	SFC-366
	O	0610(avg)	COL (2)	1280 (S)		
	O	0725	COL		315/2.7	367-1280
	O	0725	COL		(322/1.2)	SFC-1200
	O	1235	COL	1524 (S)		
	O	1510	COL		(005/2.9)	SFC-1524
6/28/77	I	0940(avg)	COL & JSV	1524 (S)		
	I	1110	COL		(239/9.0)	SFC-1372
	I	1400	JSV	1372 (S)		
	I	1510	JSV		(232/8.1)	SFC-1372
	O	0700	GAL	365 (R)	244/10.6	SFC-365
	O	0620	JSV	1524 (S)		
	O	0700	GAL		266/11.8	366-1524
	O	0700			(262/10.8)	SFC-1524
	O	1040(avg)	KIN & JSV	1372 (S)		
	O	1140(avg)	KIN, WID & JSV		(237/9.0)	SFC-1372
6/30/77	I	0430	COL	366 (R)		
	I	0710	COL		234/7.9	SFC-366
	I	0430	COL	1220 (S)		
	I	0710	COL		240/9.8	367-1220
	I	0710			(238/9.2)	SFC-1220
	I	1220	COL	1524 (S)		
	I	1140(avg)	COL & JSV		(234/9.8)	SFC-1524
	I	1650(avg)	COL	1524 (S)		
	I	1445(avg)	JSV & COL		(233/10.0)	SFC-1524
	O	0650	GAL	548 (R)		
	O	0655(avg)	GAL, PAR, & KIN		223/8.5	SFC-548
	O	0650	GAL	1220 (S)		
	O	0655(avg)	GAL, PAR, & KIN		240/9.3	549-1220
	O	0655(avg)	GAL, PAR, & KIN		(233/8.8)	SFC-1220

TABLE E.1 (continued)

Date	Sampling class	Time (L)	Upper air station	Inversion height (type) (m AGL)	Wind velocity (m s^{-1})	Layer (m)
6/30/77	0	1145	KIN	1220 (S)		
	0	1155(avg)	KIN & JSV		(234/8.5)	SFC-1220
	0	1510	KIN	1829 (S)		
	0	1420	JSV		(230/12.0)	SFC-1829
7/06/77	I	0810	GAL	365 (R)		
	I	0800	GAL		057/0.6	SFC-365
	I	0800(avg)	PAR & GAL	990 (S)		
	I	0750	PAR		014/0.9	366-990
	I	0755(avg)	PAR & GAL		(026/0.7)	SFC-990
	I	1005	JSV	1067 (S)		
	I	1415	JSV		(333/1.9)	SFC-1067
	0	0820	COL	366 (R)		
	0	0715	COL		082/2.9	SFC-366
	0	0820	COL	1372 (S)		
	0	0715	COL		012/4.6	367-1372
	0	0715	COL		(024/3.8)	SFC-1372
	0	1230	COL	1372 (S)		
	0	1110	COL		(020/2.2)	SFC-1372
	0	1700(avg)	COL (2)	1036 (S)		
	0	1510	COL		(355/3.2)	SFC-1036

APPENDIX F

SYNOPTIC METEOROLOGICAL SUMMARIES FOR LAGRANGIAN AND EULERIAN DAYS

APPENDIX F

SYNOPTIC METEOROLOGICAL SUMMARIES FOR LAGRANGIAN AND EULERIAN DAYS

Meteorology for the two field studies is analyzed for the Lagrangian and Eulerian measurement days shown in Table 6. Thus, six days were analyzed for the 1976 spring study and eight for the 1977 summer study. The following analyses describe by study and date the most significant meteorological parameters.

1976 STUDY

In the Tennessee Valley region, February and especially March are typically characterized by spring type weather; that is, frequent frontal passages are the rule, with good ventilation (wind speed times mixing height) and rapidly changing airmass characteristics. Typical inversion heights and wind speeds are about 600 m and 5.5 m s^{-1} in the morning and 1800 m and 7 m s^{-1} in the afternoon. Typical daily maximum temperatures average 15°C, whereas daily minimum temperatures average around 3°C. Surface wind speeds average 5 m s^{-1}; this represents the strongest average flow for any period during the year. Precipitation typically occurs on one out of every three days, and mean cloud cover averages 65 percent. Analysis of weather types (see the Meteorological Characterization subsection of Section 3) indicates that the spring season has similar characteristics to the annual average weather. High-pressure systems occur most frequently (27 percent), with the centers of these systems typically located northeast and east of Nashville. Maritime tropical and modified polar airmasses occur equally during this time of the year and account for 80 percent of all airmass types.

February 10, 1976

As noted previously, February (and March) weather is typified by strong ventilation and frequent frontal passages. This is exemplified by the weather pattern of February 10, 1976. On the morning of February 10, 1976, a developing low-pressure center and associated cold front were located in the Great Plains area of Iowa and Kansas, while at the same time, a large modified continental polar airmass was centered over central Florida. The combined effect of these two systems produced an influx of maritime tropical air, with accompanying clouds. Early-morning inflow ceilings (near Muscle Shoals, Alabama) were around 1000 m AGL, but gradually rose above 1500 m AGL at the afternoon outflow boundary (near Bowling Green, Kentucky). No significant rainfall occurred during the sampling day, and the maximum average surface temperature was 20°C (68°F). Temperature soundings showed that warm air advection produced a morning mixing layer (~600 m AGL) nearly equal to the climatological average, whereas the afternoon mixing height (~900 m AGL) was significantly below the afternoon climatological average. As might be expected, winds under this pressure configuration were southwesterly and strong; Valley-wide mixing-layer wind velocity averaged 215 degrees at 13 m s^{-1} throughout the sampling period. The average of the surface and 850-mb 24-h back-trajectory for February 10, 1976, showed that the airmass originated along the Louisiana-Texas border area (Figure F.1).

February 19, 1976

The weather pattern on this date was characterized by a weak surface frontal passage through the study area during the daylight hours, which caused little change in the prevailing modified maritime polar airmass weather characteristics. Generally, fair skies with southwesterly surface winds early in the morning and westerly winds by midday characterized the prevailing weather conditions. Areawide temperatures were warm, with highs generally around 20°C (68°F). Winds aloft were westerly from near surface to 1800 m AGL, the top of the afternoon mixed layer. The morning radiation inversion was about 300 m AGL. The 24-h back-trajectory for February 19, 1976, indicated the source region to be eastern Kansas (Figure F.2).

March 11, 1976

The synoptic weather pattern for March 11, 1976, was predominantly influenced by an east-west-oriented stationary front located through central Kentucky and a high-pressure center located along the Georgia-South Carolina border. This combination produced high cloud ceilings over the field study area and an influx of maritime tropical air. Winds, both surface and aloft, were southwesterly during the morning hours, whereas a gradual backing produced a more southerly component by afternoon. The morning radiation inversion height was about 400 m AGL, and the morning subsidence inversion height was about 1800 m AGL. Due to warm air advection, the afternoon inversion height decreased by about 500 m. No precipitation occurred during the measurement period, and high temperatures were again around 20°C. Also, the 24-h back-trajectory indicated that the airmass originated in central Mississippi (Figure F.3).

March 18, 1976

Somewhat similar to the weather of March 11, 1976, a high-pressure center was located along the Georgia-South Carolina border, with a warm front through northern Kentucky. Again, southwesterly flow of maritime tropical air occurred across the study area. Partly cloudy skies prevailed, with temperatures again reaching 20°C. The morning radiation and subsidence inversions were about 500 and 1500 m AGL respectively.

By afternoon, the subsidence inversion had decreased to about 1400 m AGL due, again, to warm air advection. The 24-h trajectory analysis indicated that the source region included southern Louisiana and Mississippi (Figure F.4).

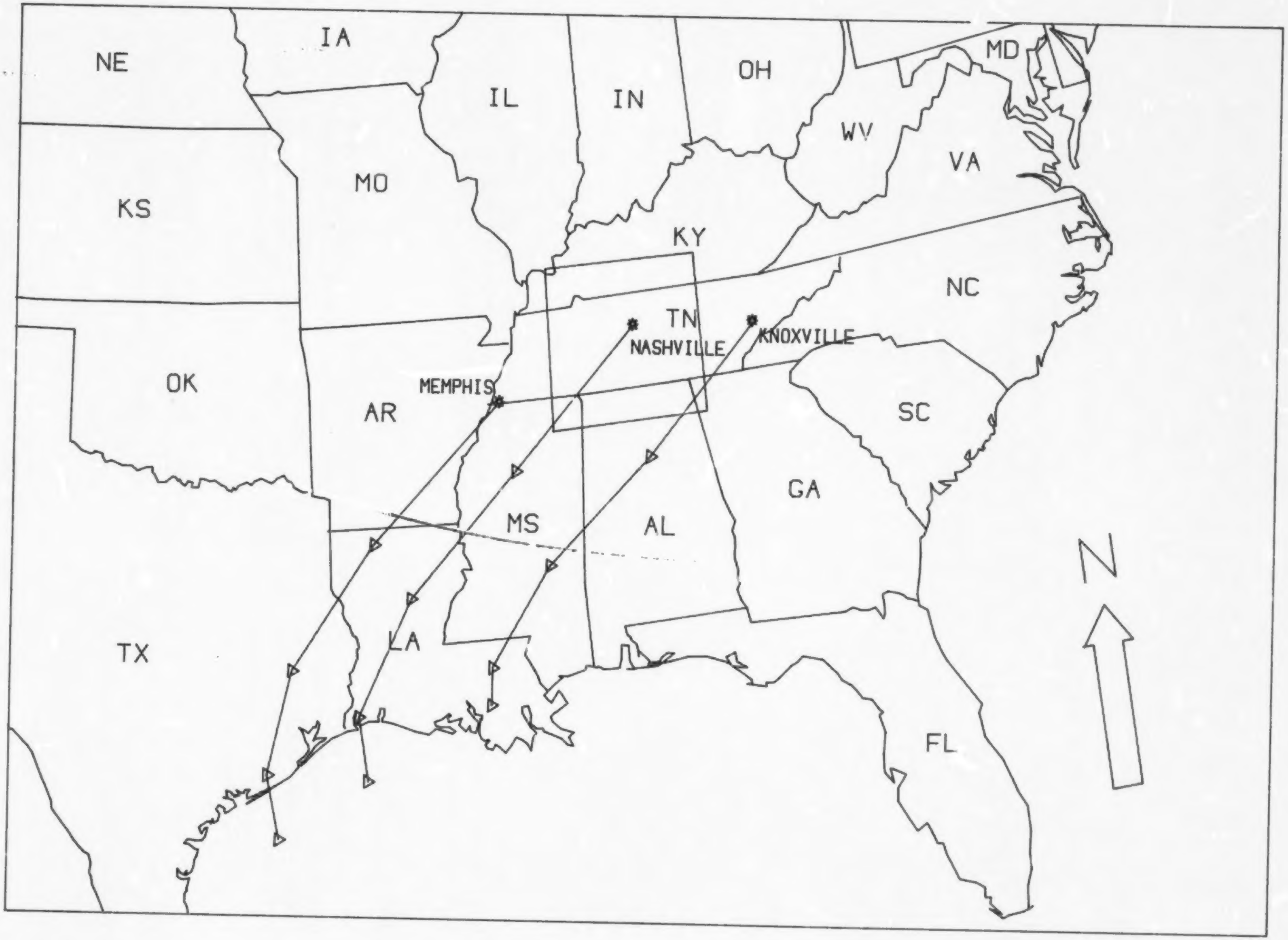
NE
IA
IL
IN
OH
MD
WV
VA
KS
MO
KY
NC
TN
NASHVILLE
KNOXVILLE
OK
MEMPHIS
AR
SC
GA
MS
AL
N
TX
LA
FL

Figure F.1. The 24-h boundary-layer back-trajectories for 1800 h CST, February 10, 1976.

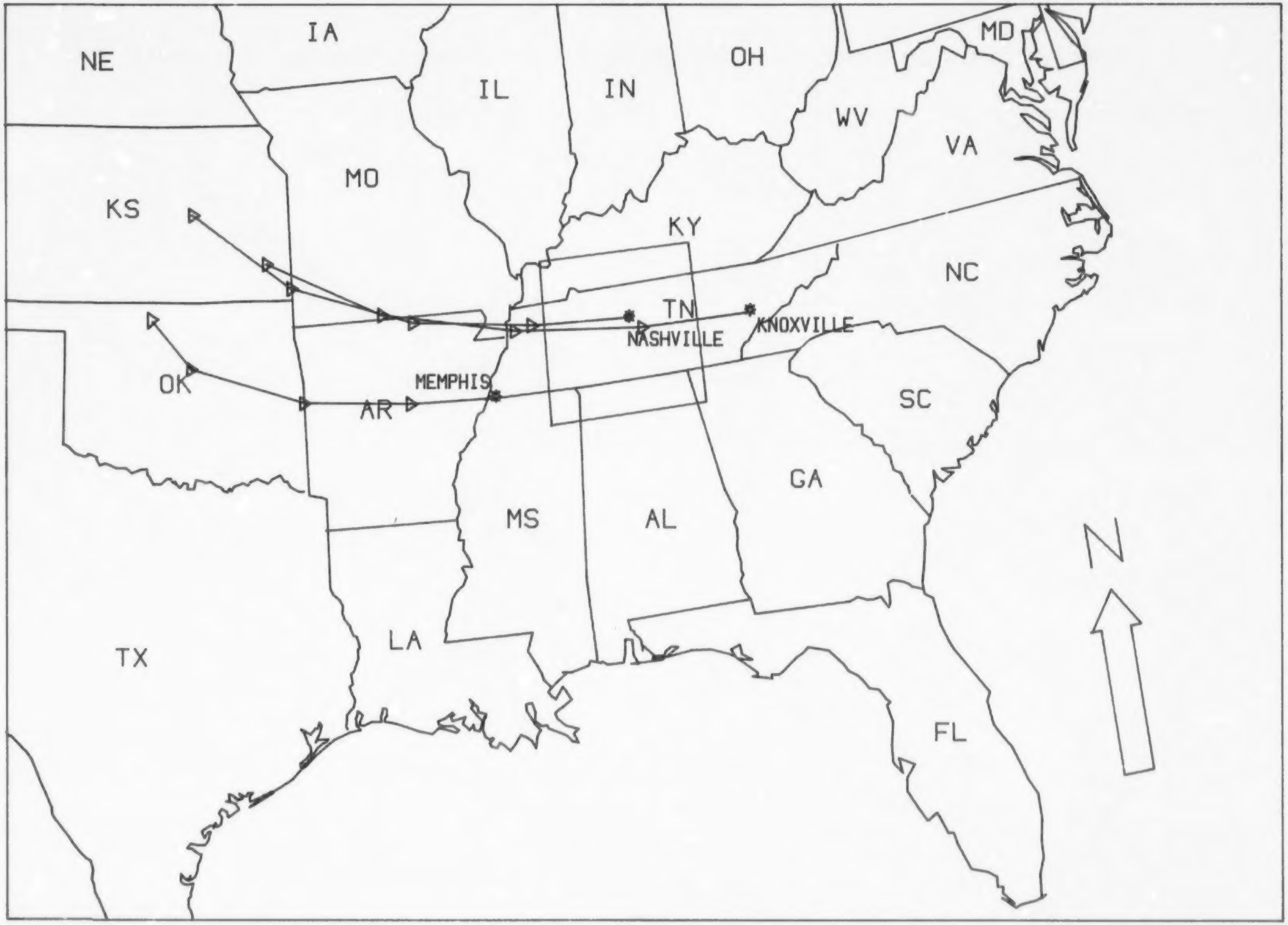
NE
IA
IL
IN
OH
MD
WV
VA
KS
MO
KY
NC
TN
NASHVILLE
KNOXVILLE
OK
MEMPHIS
AR
SC
GA
MS
AL
TX
LA
FL
N

Figure F.2. The 24-h boundary-layer back-trajectories for 0600 h CST, February 19, 1976.

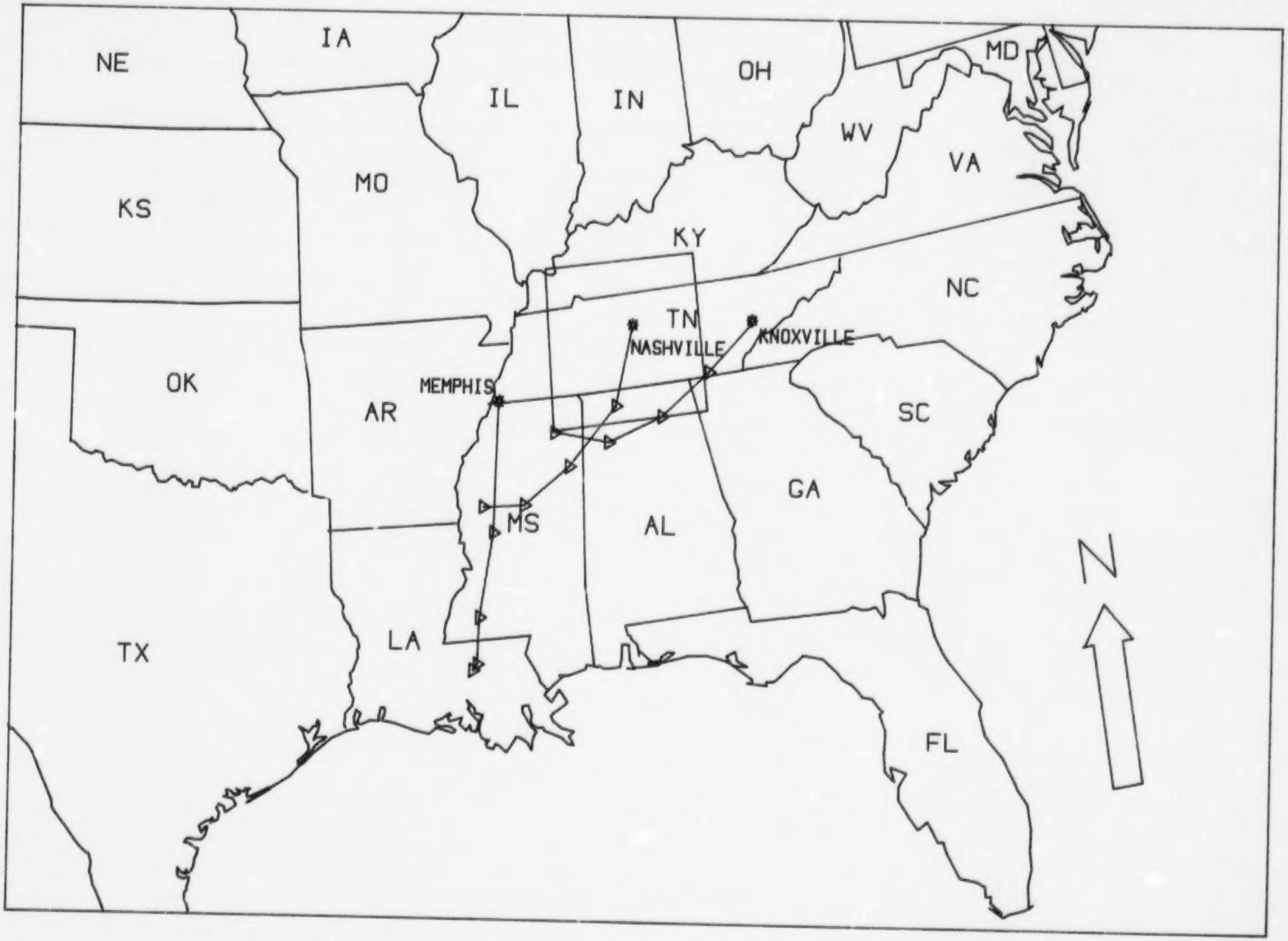
NE
IA
IL
IN
OH
MD
WV
VA
KS
MO
KY
NC
TN
NASHVILLE
KNOXVILLE
OK
MEMPHIS
AR
SC
GA
MS
AL
TX
LA
FL
N

Figure F.3. The 24-h boundary-layer back-trajectories for 1800 h CST, March 11, 1976.

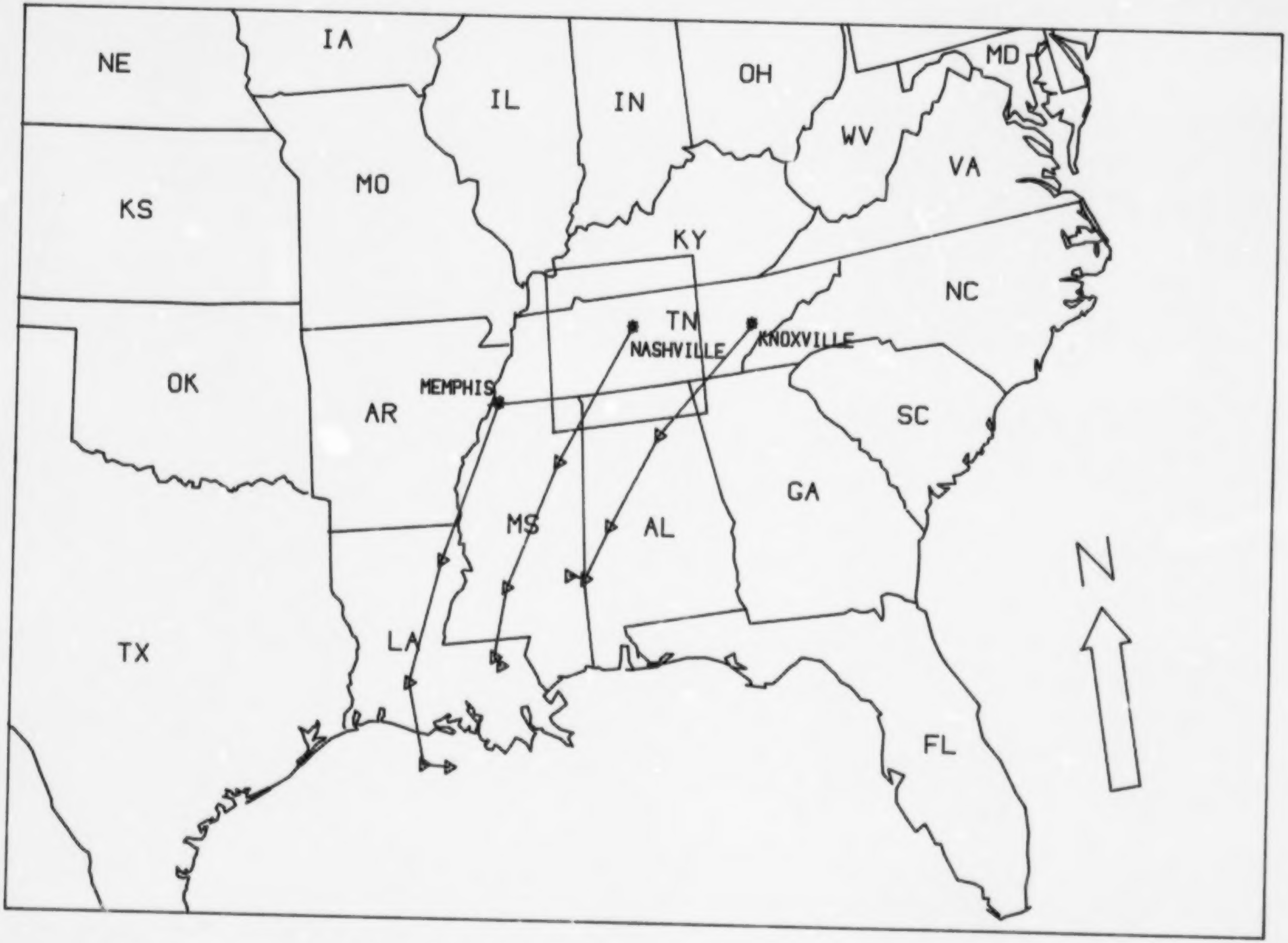
NE
IA
IL
IN
OH
MD
WV
VA
KS
MO
KY
NC
OK
TN
NASHVILLE
KNOXVILLE
MEMPHIS
AR
SC
GA
MS
AL
N
TX
LA
FL

Figure F.4. The 24-h boundary-layer back-trajectories for 1800 h CST, March 18, 1976.

March 23, 1976

A meteorological pattern different from the previous two occurred on this date. A modified continental high-pressure airmass was centered over the Chesapeake Bay area, with a very weak pressure gradient over the study area. Boundary-layer winds were light and northeasterly early in the morning, but became stronger and southwesterly by afternoon. Skies were generally clear throughout the sampling period, with the area temperature again peaking around 20°C. Morning radiation and subsidence inversion heights averaged 300 and 1200 m AGL, respectively, whereas the afternoon subsidence inversion height rose to about 1800 m AGL. The 24-h back-trajectory shows a complex trajectory path resulting from the changing nature of the high-pressure center's location (Figure F.5).

March 24, 1976

The high-pressure center of the previous day was well off the eastern seaboard by the morning of March 24, 1976. An approaching cold front with a pressure-frontal orientation similar to that described on February 10, 1976, caused an influx of warm, moist tropical air. Middle and high cloud cover increased throughout the day; however, rainfall did not occur in the study area until after dark. Morning radiation and subsidence inversion heights were about 600 and 1750 m AGL respectively, with the afternoon subsidence inversion height rising slightly to about 1800 m AGL. The 24-h trajectory shows that once again the source region was southern Louisiana and Mississippi (Figure F.6).

1977 STUDY

Summertime (June and July) weather in the Tennessee Valley region, as in most of the eastern United States, is typified by infrequent frontal passages and slow-moving high-pressure systems. Due to increased solar insolation, vertical mixing is usually good, with climatological morning and afternoon averages being about 450 and 1900 m AGL respectively. However, total ventilation is significantly less, on the average, than the spring season due to reduced wind speeds. Transport layer speeds average only 3.5 $m\ s^{-1}$ in the morning and 5 $m\ s^{-1}$ in the afternoon. The average daily maximum temperature is 31°C (twice the daily springtime average maximum), whereas the daily minimum averages 20°C. Typical surface wind speeds average 3 $m\ s^{-1}$, the slowest average wind speed of any season. Precipitation occurs on an average of one third of the days, and mean cloud cover averages about 55 percent. Analysis of weather typing indicates that stationary fronts and high-pressure centers without associated frontal systems predominate. Most pressure centers fall within a 300- to 399-km radius of Nashville or are greater than 500 km and favor the 45- through 134-degree sector (northeast through southeast of Nashville). Maritime tropical airmasses cover the area 75 percent of the time and either one or more of the four Tennessee weather stations record measurable precipitation 60 percent of the time.

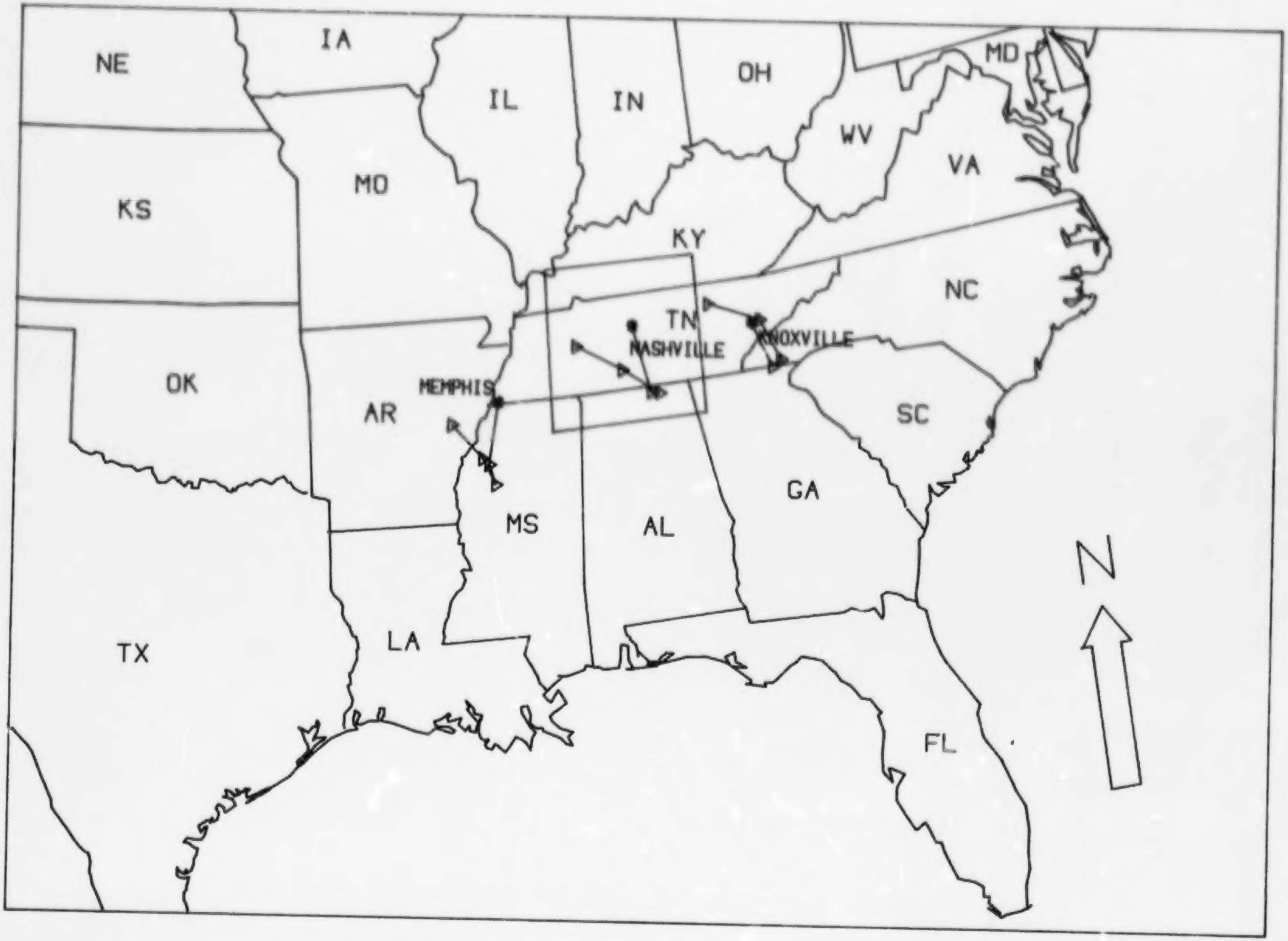
NE
IA
IL
IN
OH
MD
KS
MO
WV
VA
KY
NC
TN
NASHVILLE
KNOXVILLE
OK
MEMPHIS
AR
SC
GA
MS
AL
N
TX
LA
FL

Figure F.5. The 24-h boundary-layer back-trajectories for 1800 h CST, March 23, 1976.

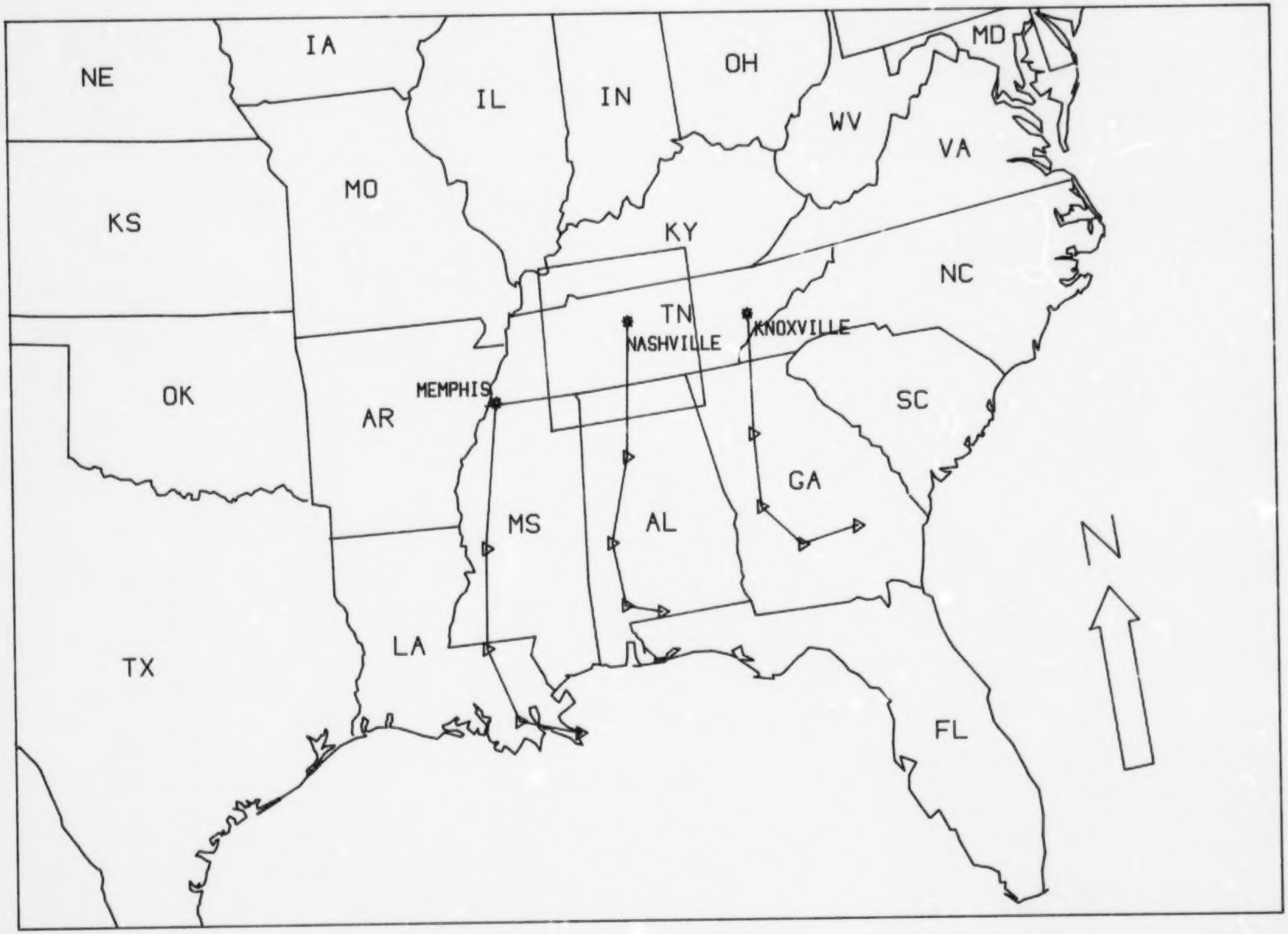
NE
IA
IL
IN
OH
MD
WV
VA
KS
MO
KY
NC
TN
NASHVILLE
KNOXVILLE
OK
AR
MEMPHIS
SC
GA
MS
AL
N
LA
TX
FL

Figure F.6. The 24-h boundary-layer back-trajectories for 1800 h CST, March 24, 1976.

June 3, 1977

Early in the morning of June 3, 1977, a weak continental polar front lay east-west across northern Alabama and Georgia. Behind it, to the north, was a modified continental airmass centered over central Michigan. This high-pressure system produced northerly winds, no precipitation, and morning radiation and subsidence inversion heights that averaged about 350 and 1650 m AGL respectively. The average field study afternoon inversion level decreased to about 1500 m due to subsidence of superior air. The average maximum temperature was 30°C, with mostly sunny skies prevailing. The 24-h trajectory data showed that the source region was in southern Indiana and Illinois (Figure F.7).

June 4, 1977

The high-pressure center of the previous day moved southeastward and was centered over West Virginia on the morning of June 4, 1977. Again, airflow was light and from a northerly direction. Average morning radiation and subsidence inversion heights were 400 and 1250 m AGL respectively. The afternoon inversion height rose to around 1400 m AGL. Again, no significant cloud cover was present over the study area, and the average maximum temperature was 31°C. The trajectory data indicated that the airmass originated along the Ohio River Valley area (Figure F.8).

June 5, 1977

By the morning of June 5, 1977, the high-pressure center of the previous two days dissipated and began merging with the Bermuda high. Winds were west-northwesterly throughout the boundary layer. Inversions averaged 350 and 1400 m AGL during the morning hours and 1750 m AGL during the afternoon. Again, no significant cloud cover was present and the average high temperature reached 33°C. The 24-h trajectory data indicated that the airmass originated along the Mississippi River west of the study region (Figure F.9).

June 8, 1977

A modified continental high-pressure airmass was centered over northern Alabama on June 8, 1977. Morning radiation and subsidence inversion heights averaged 300 and 1600 m AGL respectively. By afternoon, the subsidence inversion rose to about 1800 m AGL. Boundary-layer winds were light and variable over northern Alabama and west-northwesterly over the northern half of the field study area. Trajectory analysis shows that the 24-h airmass source region was in central Indiana and Illinois (Figure F.10). Temperatures rose to around 27°C under fair skies.

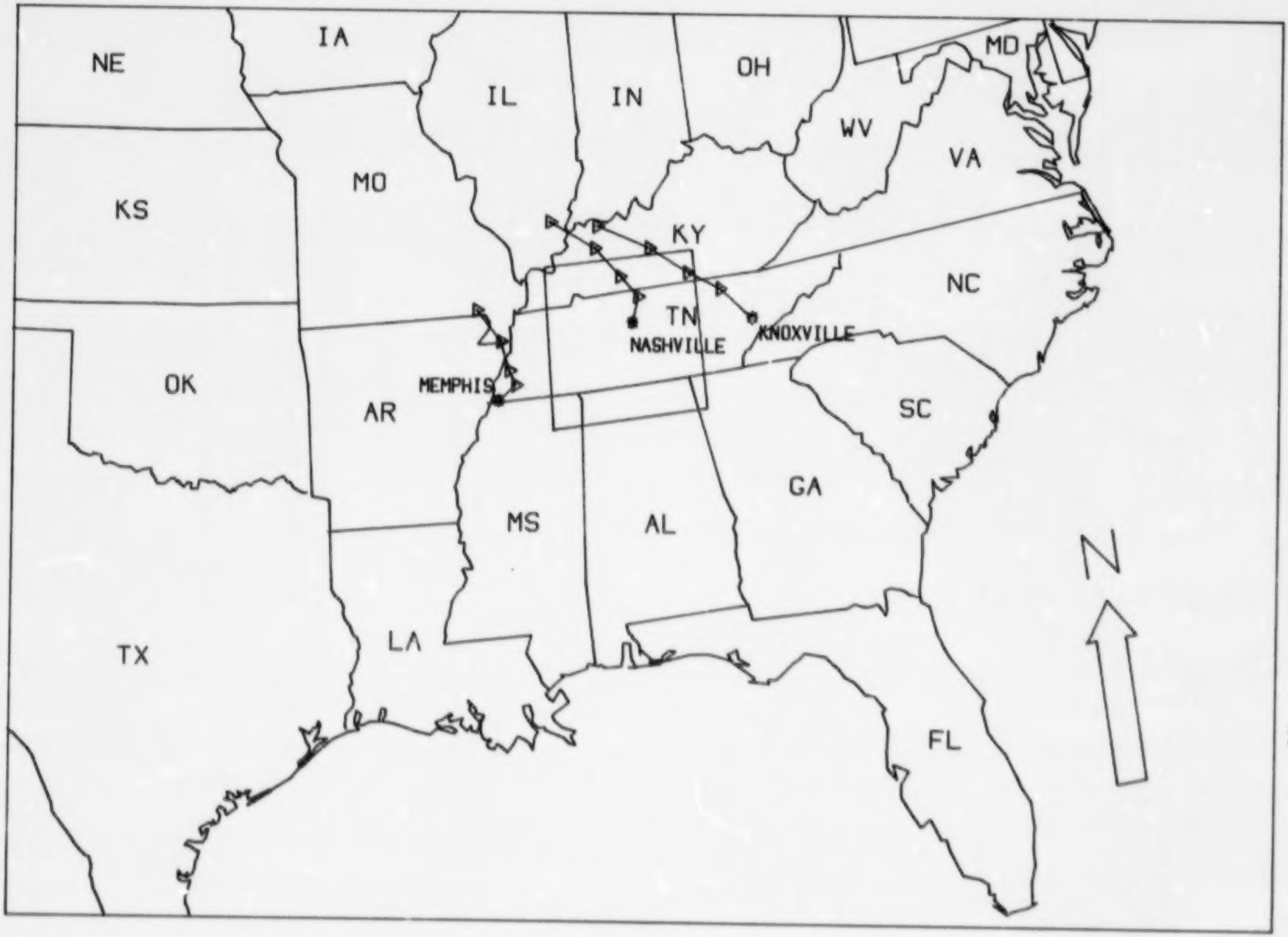
NE
IA
IL
IN
OH
MD
WV
VA
KS
MO
KY
NC
TN
NASHVILLE
KNOXVILLE
OK
MEMPHIS
AR
SC
GA
MS
AL
TX
LA
FL
N

Figure F.7. The 24-h boundary-layer back-trajectories for 0600 h CST, June 3, 1977.

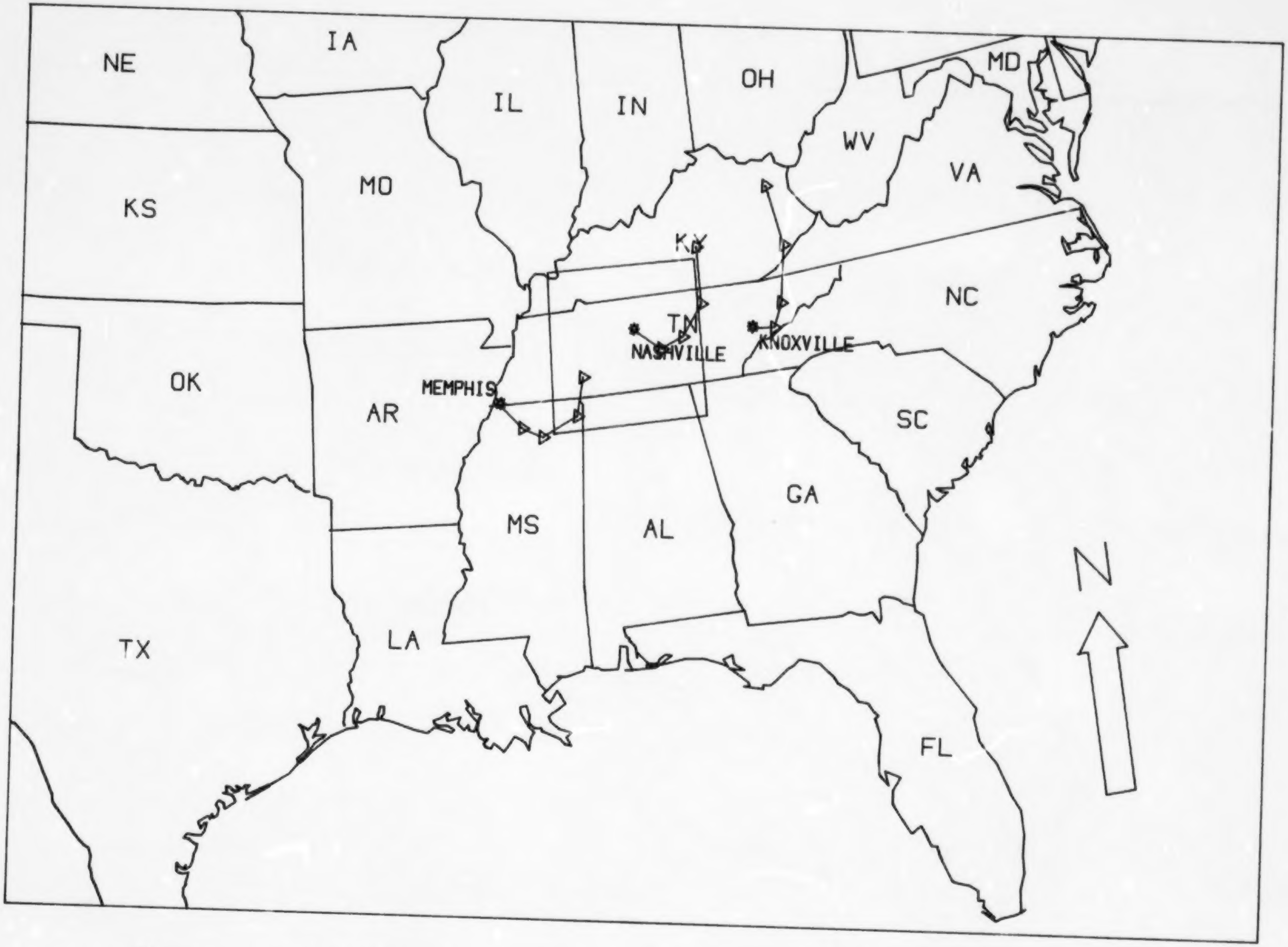
NE
IA
IL
IN
OH
MD
WV
VA
KS
MO
KY
NC
OK
AR
TN
MEMPHIS
NASHVILLE
KNOXVILLE
SC
MS
AL
GA
TX
LA
FL
N

Figure F.8. The 24-h boundary-layer back-trajectories for 0600 h CST, June 4, 1977.

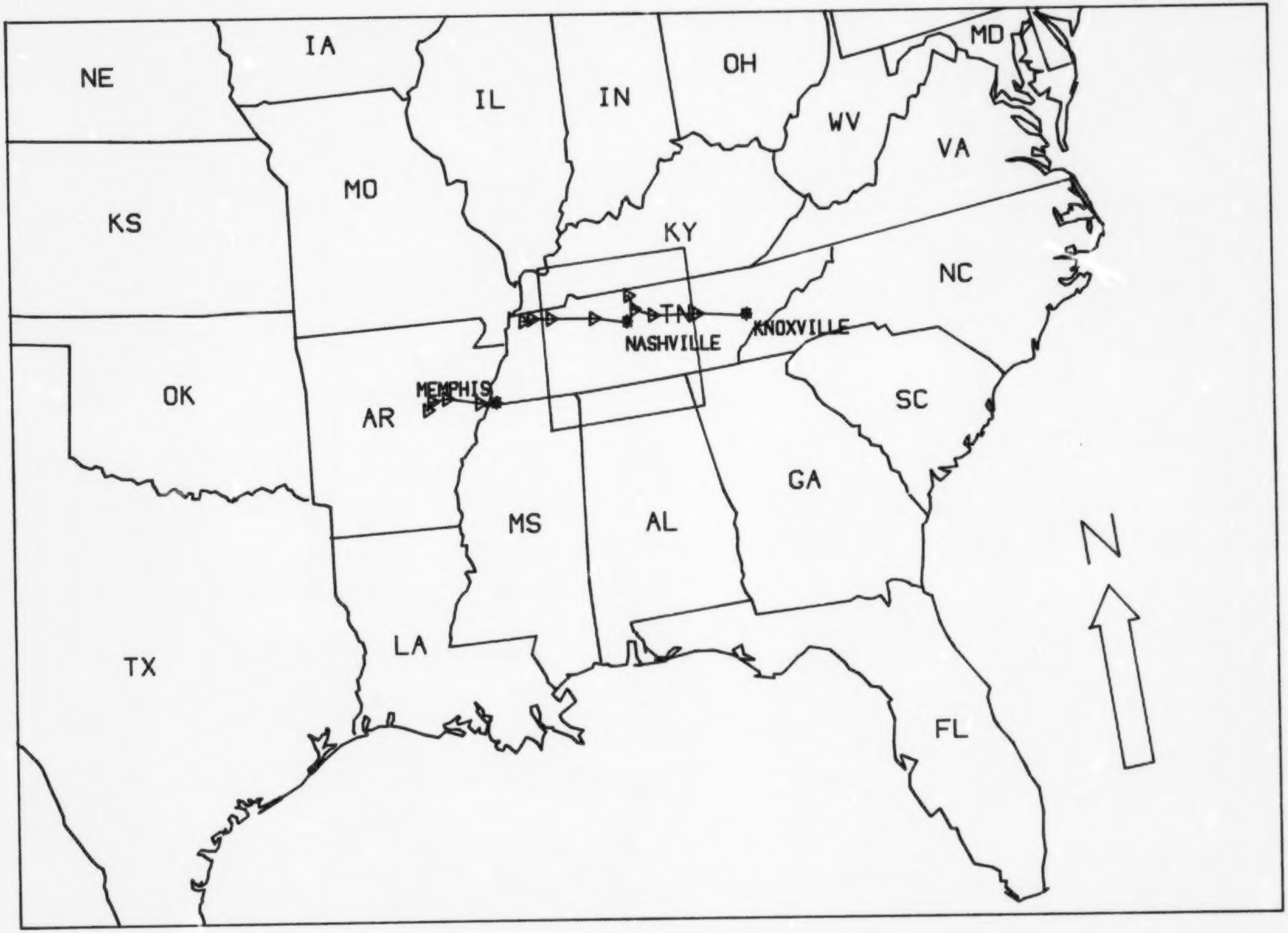
NE
IA
IL
IN
OH
MD
WV
VA
KS
MO
KY
NC
TN
KNOXVILLE
NASHVILLE
OK
MEMPHIS
AR
SC
GA
MS
AL
N
LA
TX
FL

Figure F.9. The 24-h boundary-layer back-trajectories for 1800 h CST, June 5, 1977.

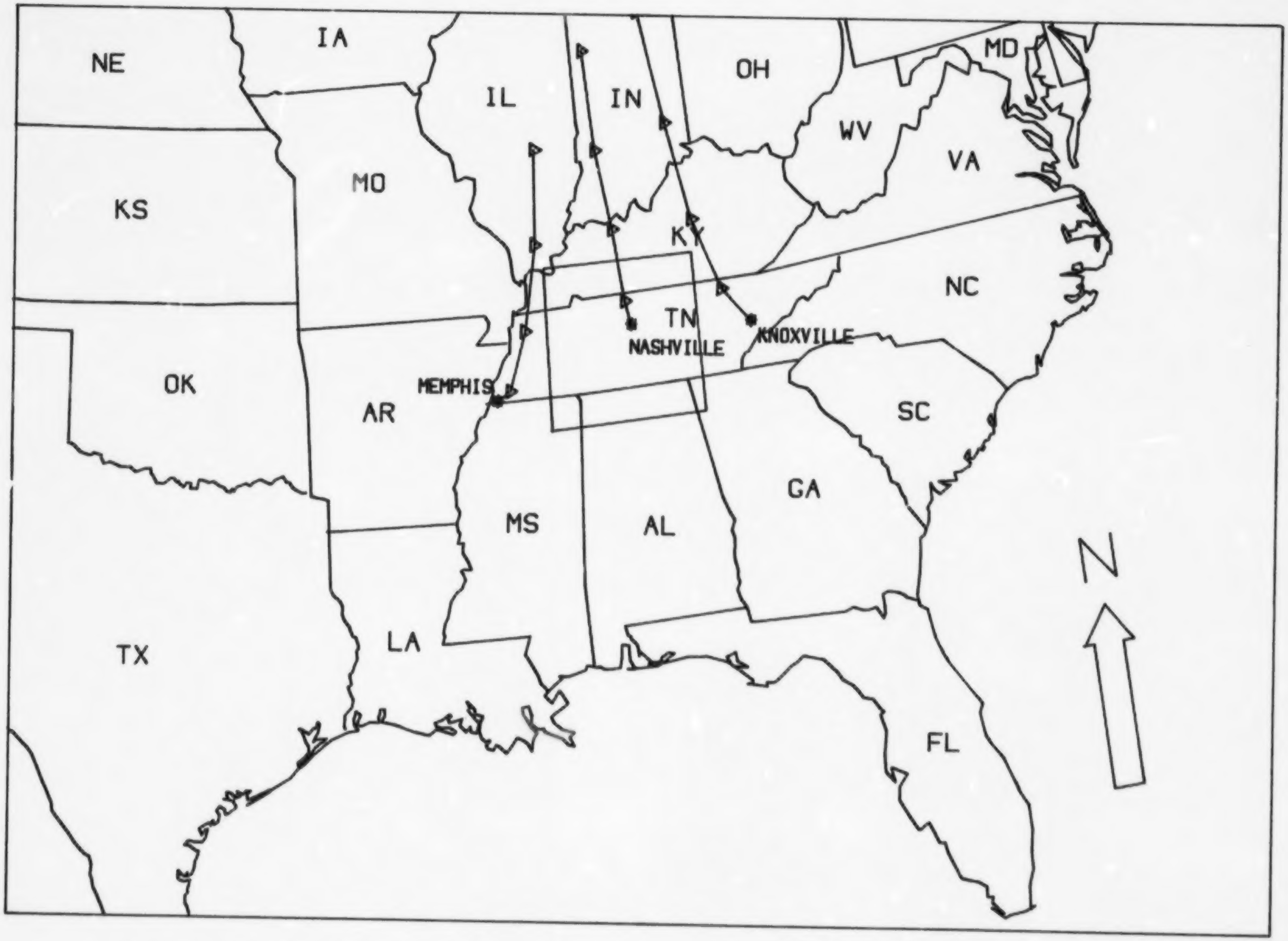
NE
IA
IL
IN
OH
MD
WV
VA
KS
MO
KY
NC
TN
NASHVILLE
KNOXVILLE
OK
MEMPHIS
AR
SC
GA
MS
AL
N
TX
LA
FL

Figure F.10. The 24-h boundary-layer back-trajectories for 0600 h CST, June 8, 1977.

June 28, 1977

A significant departure from the earlier June northerly wind flow regime was evident during the last one third of the month. On June 28, 1977, an approaching cold front located in the Great Plains combined with the Bermuda high to produce steady southwesterly flow of maritime tropical air. Boundary-layer winds throughout the study area were southwesterly and relatively strong (7 to 10 m s^{-1}). Morning radiation and subsidence inversion heights averaged about 400 and 1500 m AGL, respectively, whereas afternoon inversion heights were around 1400 m AGL. Despite the approaching frontal system, only mid-level small cumulus and altocumulus clouds were evident. Average high temperatures reached 32°C. Significant rainfall did not materialize until after sunset, and most of that was confined to the western part of the field study area. The 24-h trajectory data indicated that airmass source regions included the Gulf Coast area of eastern Texas and southern Louisiana (Figure F.11).

June 30, 1977

By the morning of June 30, 1977, the southward moving cold front of June 28, 1977, was located over Kentucky and had begun moving northward as a warm front in response to the approach of a second maritime polar airmass. This new frontal system was situated through central Iowa, then southwestward to southern Colorado. Again, warm moist tropical air accompanied relatively strong (8 to 11 m s^{-1}) southwesterly winds. Morning radiation and subsidence inversion heights averaged 450 and 1200 m AGL, respectively, with the afternoon subsidence inversion rising to about 1650 m AGL. Hazy but fair skies were prevalent in the morning; however, by midafternoon isolated cumulus congestus and cumulonimbus clouds produced shower activity near the northern study area boundary. Maximum temperatures were around 35°C. The 24-h trajectories indicated that the airmass originated in the northern Louisiana area (Figure F.12).

July 6, 1977

Weather conditions within the Tennessee Valley area and, in fact, across most of the eastern United States were dominated by a large, sprawling high-pressure system on July 6, 1977. The surface center of this maritime tropical airmass was located over southern Louisiana, whereas the upper-level core was located over the bootheel area of Missouri. Boundary-layer winds were light (<4 m s^{-1}) and northerly. Morning radiation and subsidence inversions were relatively low, with values averaging 350 and 1100 m AGL, respectively, whereas afternoon subsidence inversion levels remained relatively stable. Maximum temperatures peaked around 35°C while subsiding air effectively eliminated cloud cover. Trajectory data indicated that the little air movement present came from the northwest (Figure F.13).

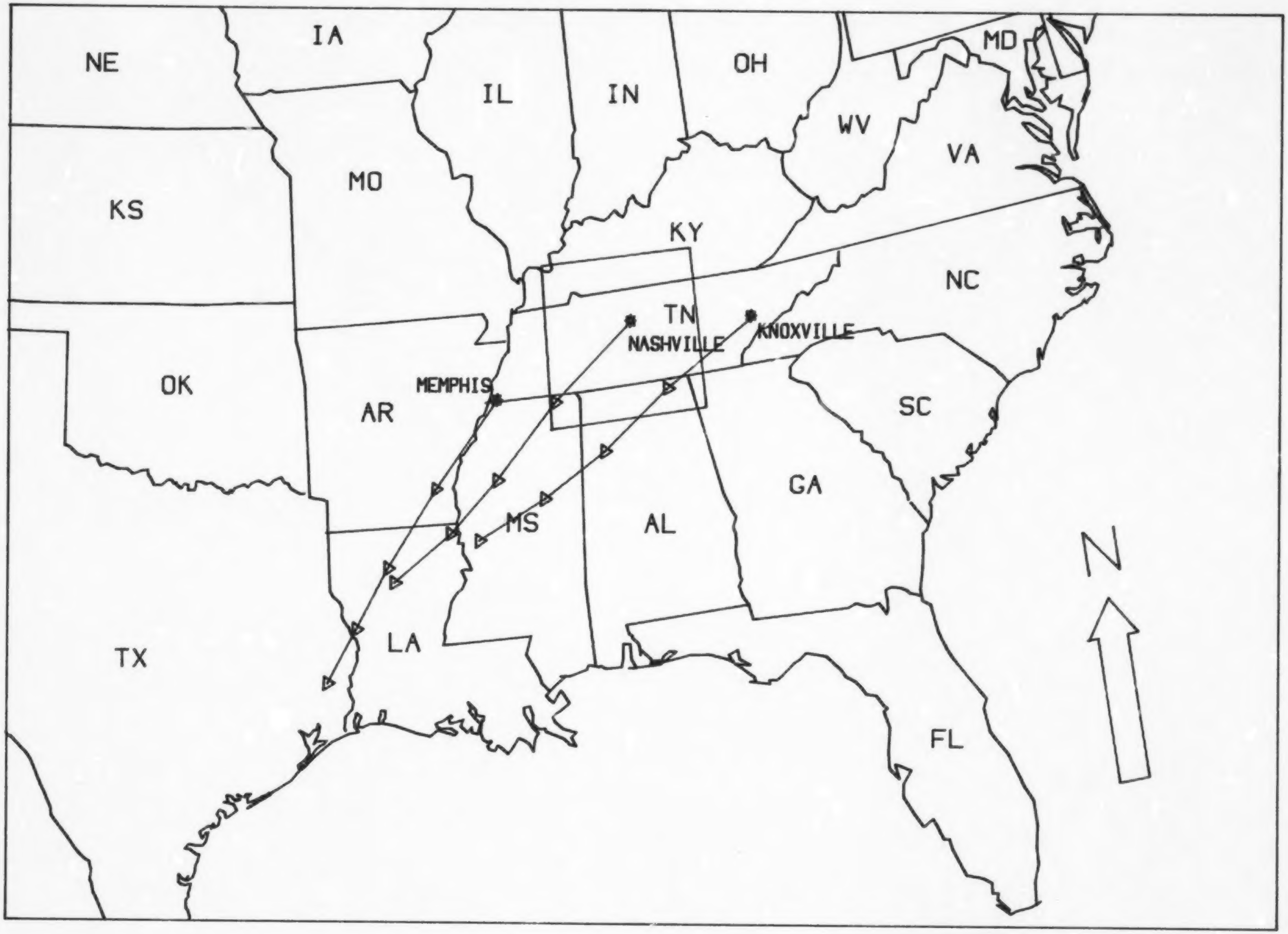
NE
IA
IL
IN
OH
MD
WV
VA
KS
MO
KY
NC
TN
KNOXVILLE
NASHVILLE
OK
MEMPHIS
AR
SC
GA
MS
AL
TX
LA
FL
N

Figure F.11. The 24-h boundary-layer back-trajectories for 0600 h CST, June 28, 1977.

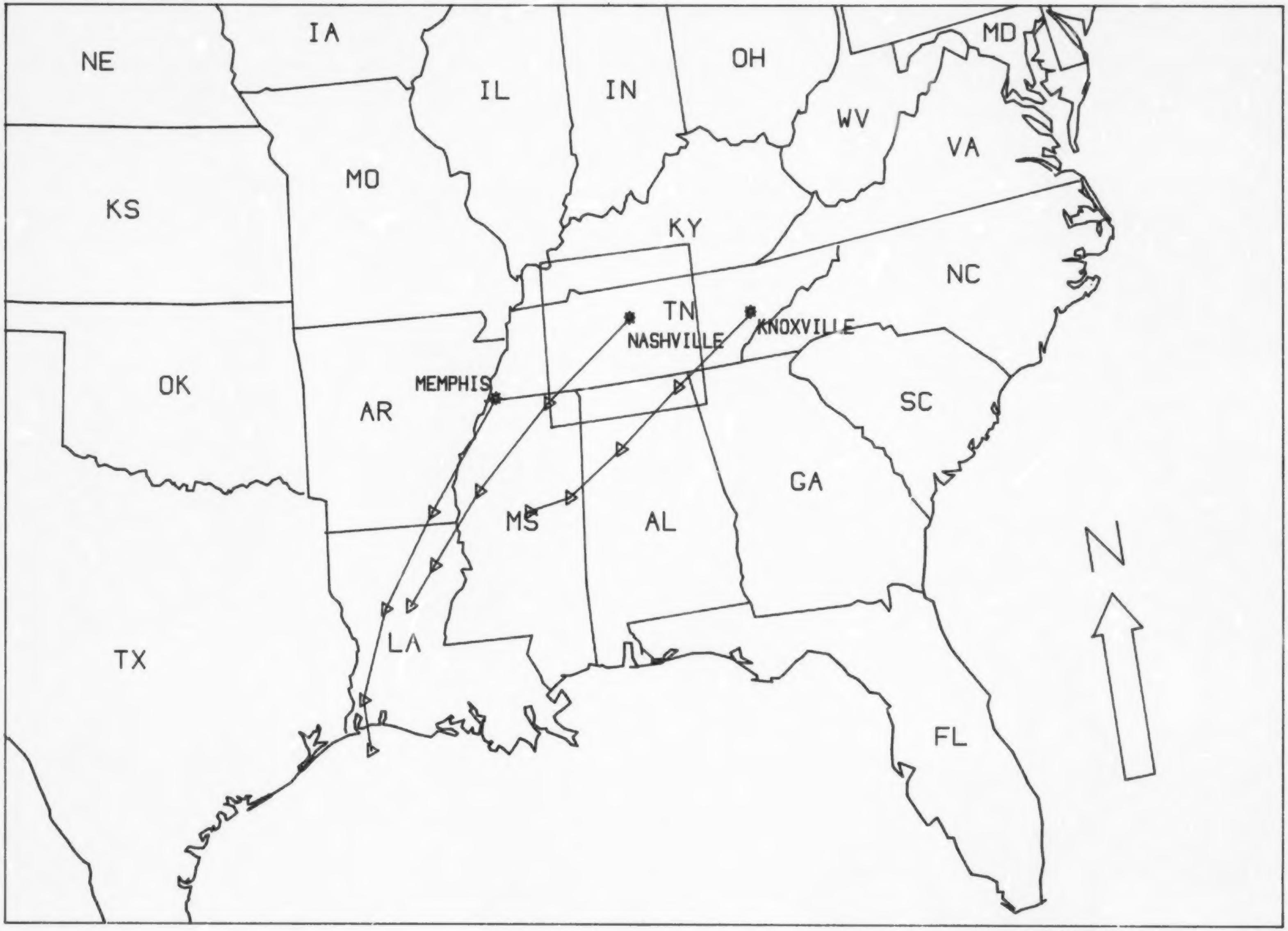
NE
IA
IL
IN
OH
MD
WV
VA
KS
MO
KY
NC
TN
KNOXVILLE
NASHVILLE
MEMPHIS
OK
AR
SC
GA
MS
AL
N
TX
LA
FL

Figure F.12. The 24-h boundary-layer back-trajectories for 1800 h CST, June 30, 1977.

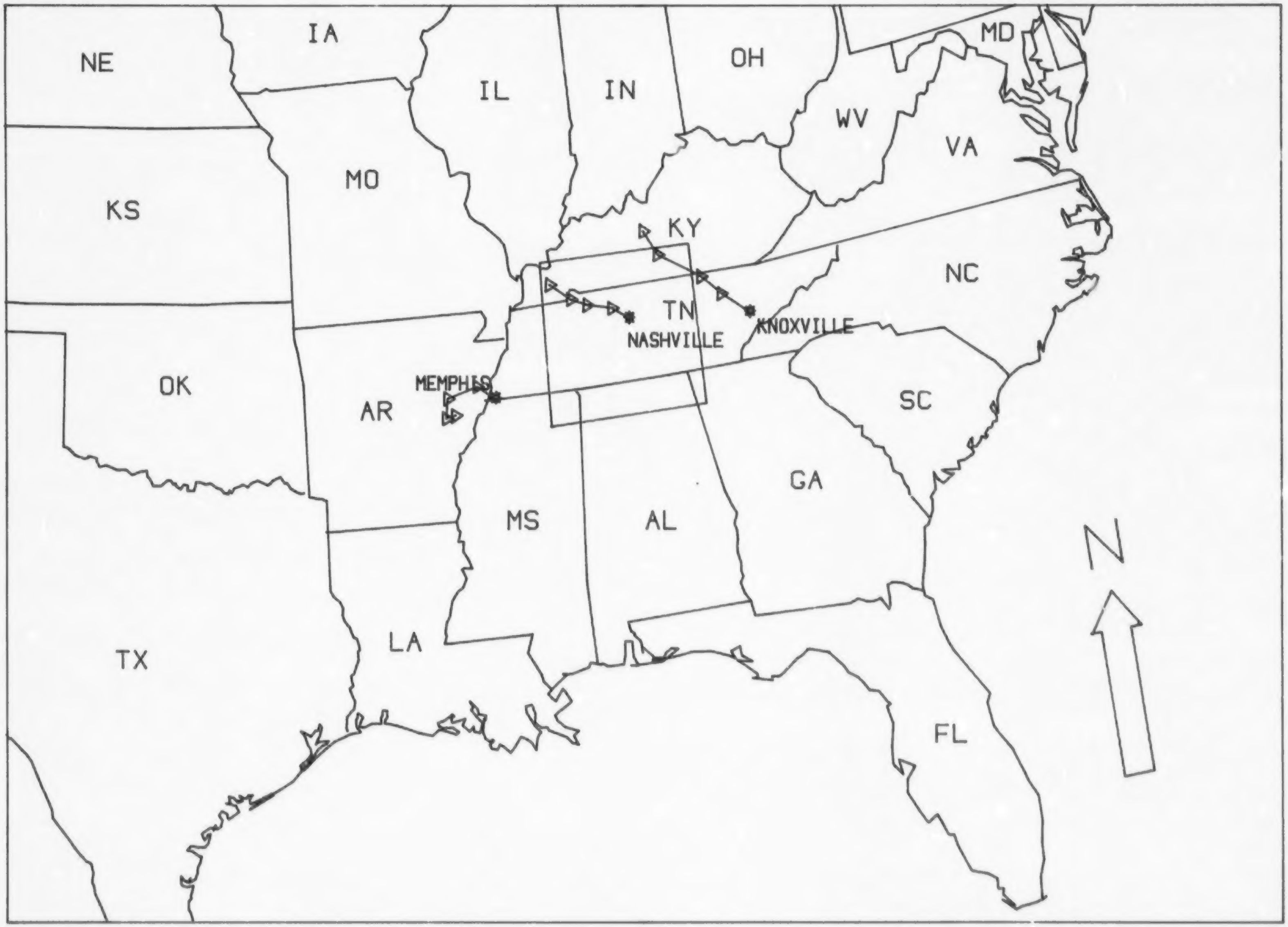
NE
IA
IL
IN
OH
MD
WV
VA
KS
MO
KY
NC
TN
NASHVILLE
KNOXVILLE
OK
MEMPHIS
AR
SC
GA
MS
AL
N
LA
TX
FL

Figure F.13. The 24-h boundary-layer back-trajectories for 0600 h CST, July 6, 1977.

July 7, 1977

Similar to July 6, 1977, this day's weather was characterized by a continuation of the Bermuda high-pressure system over much of the eastern United States. The upper-level high-pressure cell was centered over the study area. Maritime tropical air continued to pervade the area. Boundary-layer winds were again light (<5 m s^{-1}) and generally from the WNW. Morning radiation and subsidence inversion heights averaged 200 and 1700 m AGL. Skies were generally fair, and average maximum surface temperatures once again reached 35°C. The 24-h trajectories indicated that the airmass affecting the study area once again originated near the Mississippi River (Figure F.14).

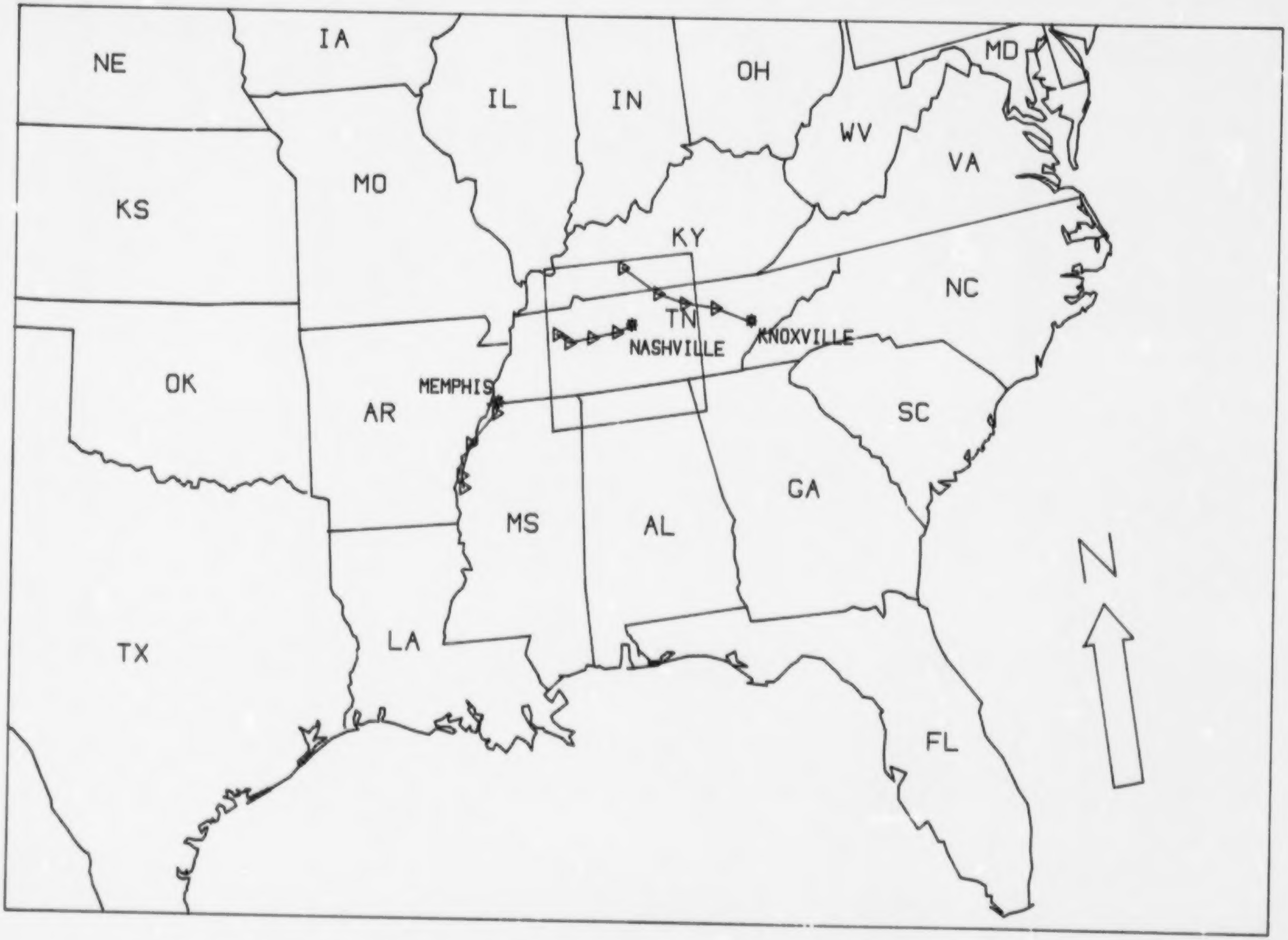
NE
IA
IL
IN
OH
MD
KS
MO
WV
VA
KY
NC
TN
NASHVILLE
KNOXVILLE
OK
MEMPHIS
AR
SC
GA
MS
AL
TX
LA
FL
N

Figure F.14. The 24-h boundary-layer back-trajectories for 0600 h CST, July 7, 1977.